DEVELOPMENT OF MICROBIAL FUEL CELL BASED SENSOR FOR ON-LINE MEASUREMENT OF BOD IN WASTEWATER

SHAILESH KHARKWAL

(M. Tech, IIT Kharagpur, India)

A THESIS SUBMITTED

FOR THE DEGREE OF DOCTOR OF PHILOSOPHY

NUS GRADUATE SCHOOL FOR INTEGRATIVE SCIENCES AND ENGINEERING

NATIONAL UNIVERSITY OF SINGAPORE

2014

Declaration

I hereby declare that this thesis is my original work and it has been written by me in its entirety. I have duly acknowledged all the sources of information which have been used in the thesis.

This thesis has also not been submitted for any degree in any university previously.

Shailesh Kharkwal

23 January 2014

Acknowledgments

First and foremost, I would like to express my sincere gratitude to my supervisor, A/P Ng How Yong, for his continuous support, valuable guidance and constant encouragement throughout the period of this research. His generous attitude towards students always helps them to groom more independently. He not only mentored and encouraged me throughout my Ph.D. study and research, but also advised me genuinely in my personal development. I really appreciate his down-to-earth nature and scientific attitude towards applied research.

I would like to equally acknowledge my co-supervisor Prof Li Fong Yau for his immense support and guidance during my research work. I really admire his polite and supporting nature.

I extend my sincere thanks to the members of the thesis advisory committee for their continuous guidance during my research work and the examination committee for reviewing this thesis.

I want to express my deep appreciation to all the staff of the Water Science and Technology Laboratory in the Department of Civil and Environmental Engineering, especially Mr. Chandrasegaran, Ms. Lee Leng Leng, and Ms. Tan Xiaolan, for their assistance in reactor setup and instrument usage. I extend my sincere thanks to members of the MFC group, Dr. Lefebvre Olivier, Ms. Shen Yujia, Ms. Nichanan, Mr. Tan Zi and Mr. Mohammad for their help and guidance in planning my experiments. Contributions by final year students, Mr. Soon Huat Won, Mr. Tan Yi Chao and Mr. Lim Kok Hau are gratefully acknowledged. I also thank my seniors and lab mates, Dr Parida, Mr. Melvin, Mr. Shi Xue Qing, Ms. Low Siok Ling, Ms. Xiaodi, Dr. Ng Kok Kwang and Mr. Fu Chen for their support.

I would like to thank NUS Graduate School for Integrative Sciences and Engineering for giving me an opportunity to pursue my Ph.D.

Heartfelt thanks to my family for their constant encouragement, patience and strength without which this research and thesis writing journey would have been difficult. Lastly, but most importantly, I am deeply grateful to the almighty God for giving me the strength and confidence to move on during the toughest obstacles and showing me the way through.

Table of Content

Summary

To ensure the efficient operation of wastewater treatment processes, continuous monitoring of biochemical oxygen demand (BOD) of the treated effluent is essential. The standard 5-day BOD (BOD_5) method has been widely used to determine the BOD concentration in wastewater. The major drawback of the standard method is the 5-day measurement time, which obviates any real-time water quality monitoring. Therefore, a bio-sensor-based method is needed for rapid and accurate measurement of BOD in wastewater. In this study, microbial fuel cell (MFC) was developed as an alternative BOD sensing device for on-line measurement of BOD in wastewater. MFC is a device that uses microorganisms to generate an electric signal (voltage or current) through the oxidation of bio-convertible organic matter present in wastewater. The calibration between the voltage (or current) and BOD concentration allows MFC for use as a sensor for on-line BOD measurement.

A single-chambered MFC was designed and constructed using MnO_2 (α, β, and γ-MnO_2) catalyst in place of expensive Pt catalyst. Considering the lower cost of catalyst MnO_2 and the comparable performance, the β-MnO_2 and γ-MnO_2-based MFC were further explored as MFC-BOD sensor. The performance of the MFC-BOD sensor was investigated in terms of various parameters such as BOD measurement range, response time, sensitivity and long-term stability. The β-MnO_2-MFC-BOD sensor was found superior over the γ-MnO_2-MFC-BOD sensors in terms of sensitivity and stability over time.

With a view to implement MFC-BOD sensor in wastewater treatment plants, a sequential optimization strategy was applied to lower the response time and

increase the sensitivity of the MFC-BOD sensor. Sequential optimization of the MFC-BOD sensor was completed in five steps – HRT optimization, volume optimization, choice of PEM, cathode catalyst and anode material. As a result of sequential optimization, the optimized MFC-BOD sensor was determined to be with a volume of 12.6 ml, HRT of 2 min, Nafion membrane as PEM, Pt as cathode catalyst and graphite as an anode material. The optimized MFC-BOD sensor showed excellent performance with faster response time (120 min), best linearity (R^2=0.93) and highest sensitivity (± 0.2%). The excellent compliance of the BOD_5 values as predicted by the optimized MFC-BOD sensor (BODp) with conventional BOD_5 was determined (slight variation of ±2-6%).

To get a better understanding of the mechanism of the MFC-BOD sensor, the behaviour of the electrochemically-active biofilm of MFC-BOD sensor was studied. A proportion of live and dead cells in the biofilm of different ages were estimated and a decrease in the number of live cells (92 to 44%) in the period of 1 month to 1 year was observed. The role of the thickness and density of anodic biofilm in the performance of the MFC-BOD sensor was investigated. It was observed that MFC-BOD sensor with bigger volume could produce an anodic biofilm that was less thick, more highly dense, less porous, and displayed lower sensitivity to BOD concentrations. Finally, the performance of the MFC-BOD sensor was evaluated at different environmental conditions such as, operating temperature, anodic pH and conductivity.

The results of this study suggest the potential of MFC-BOD sensor in on-line measurement of BOD in wastewater, considering the advantages of quick response time, high sensitivity, good measurement range, long-term stability and simple in design.

List of Tables

List of Figures

Abbreviations

AEM	Anion exchange membrane
APHA	American Public Health Association
ASP	Activated Sludge Process
AWW	Artificial wastewater
BES	Bioelectrochemical systems
BOD	Biochemical oxygen demand
CE	Coulombic efficiency
CEM	Cation exchange membrane
COD	Chemical oxygen demand
CV	Cyclic voltammetry
DGGE	Denaturing gradient gel electrophoresis
DL	Diffusion layer
DO	Dissolved oxygen
DWW	Domestic wastewater
EA	Elemental analysis
E^0_{an}	The maximum potential obtained at the anode
E^0_{cell}	Theoretical cell voltage
E^0_{cat}	The maximum potential obtained at the cathode
E_{emf}	Electromotive force
E_{thermo}	Thermodynamically predicted voltage
F	Faraday's constant
FCM	Flow cytometry
FISH	Fluorescent in situ hybridization
GC	Gas chromatography

HRT	Hydraulic retention time
I	Current
IC	Ion chromatography
MEA	Membrane electrode assembly
MFC	Microbial fuel cell
OCV	Open circuit voltage
ORR	Oxidation reduction reaction
P	Power
PBS	Phosphate buffered saline
PC	Polarization curve
PEM	Proton exchange membrane
P_{max}	Maximum power density
PTFE	Poly tetra fluro ethylene
R_{ext}	External resistance
R_{int}	Internal resistance
SCMFC	Single chamber microbial fuel cell
SEM	Scanning electron microscope
T	Absolute temperature (K)
TDS	Total dissolved solid
TSS	Total suspended solid
UF	Ultrafiltration
V_{cell}	Voltage output
VSS	volatile suspended solids
WRP	Water reclamation plant
η_{act}	Activation loss

η_{conc}	Concentration loss
η_{ohmic}	Ohmic loss

Publications

Journal Articles

1. **Kharkwal, S.**, Lu, M., Lefebvre, O., Ng, H. Y., Li, S. F. Y. Development and long-term stability of a novel microbial fuel cell BOD sensor with MnO_2 catalyst. (In preparation).
2. **Kharkwal, S.**, Lefebvre, O., Ng, H. Y., Li, S. F. Y. An Insight into microbial fuel cell-type BOD sensors. (In preparation).
3. **Kharkwal, S.**, Lefebvre, O., Lu M., Ng, H. Y., Li, S. F. Y. Optimized microbial fuel cell BOD sensor for improved dynamic response. (In preparation).
4. Lu, M., Guo, L., **Kharkwal, S.**, Wu, H., Ng, H. Y., Li, S. F. Y. Manganese–polypyrrole–carbon nanotube, a new oxygen reduction catalyst for air-cathode microbial fuel cells. 2013. J Power Sources, 221 (1), 381-386.
5. Lefebvre, O., Tan, Z., **Kharkwal, S.**, Ng, H.Y. Effect of increasing anodic NaCl concentration on microbial fuel cell performance. Bioresour. Technol. 2012. 112, 336-340.
6. Lu, M., **Kharkwal, S.**, Ng, H. Y., Li, S. F. Y. Carbon nanotube supported MnO_2 catalysts for oxygen reduction reaction and their applications in microbial fuel cells. Biosens. Bioelectron. 2011. 26 (12), 4728-4732.

Conference Oral Presentation

1. **Kharkwal, S.**, Lu, M., Lefebvre, O., Ng, H. Y., Li, S. F. Y. "Development and long-term stability of a novel microbial fuel cell BOD sensor with MnO_2 catalyst", 4th International MFC conference, Cairns, Australia, 1-4 September 2013.
2. **Kharkwal, S.**, Lu, M., Huat, S., Ng, H. Y., Li, S. F. Y. "Microbial fuel cell based biosensor for on-line measurement of BOD in wastewater", IWA World Water Congress & Exhibition, Busan, South Korea, 16-18 September 2012.
3. **Kharkwal, S.**, Lu, M., Huat, S., Ng, H. Y., Li S. F. Y., "Microbial fuel cell based bio-sensor for continuous measurement of BOD (Biochemical Oxygen Demand) in Wastewater", 11th AIChE Annual Meeting, USA, 16-21 October 2011.
4. **Kharkwal, S.**, Ng H.Y., Li S. F. Y., "Development of MnO_2-cathode-catalyst based MFC-BOD sensor", 21st Joint KAIST-KU-NTU-NUS Symposium on Environmental Engineering, Malaysia, 15-16 Jul, 2012.
5. **Kharkwal, S.,** Lu, M., Ng, H. Y., Li, S. F. Y. "Exploring microbial fuel cell as BOD sensing device". Young water Talent Symposium at Singapore International Water Week, Singapore. 1 July 2012.

Awards

1. Silver Award in SPORE (Singapore Peking Oxford Research Enterprise) Scientific Challenge 2012 (SSC2012).

2. Gold Award in SPORE (Singapore Peking Oxford Research Enterprise) Scientific Challenge 2011 (SSC2011).

.

1. Introduction

1.1 Background

Water is one of nature's most important gifts to mankind and it should be protected and preserved well to save our environment and civilization. Since water is a finite resource, water scarcity is a major problem that is being encountered all across the globe. At present only 3-4 % of the wastewater in the world is recycled and that leaves a huge potential for recycle or reuse to solve a water scarcity problem. Under these circumstances, treatment of used water coming from different sources like households, industries, educational institutes, restaurants, business offices, urban runoff, reservoirs, etc. become essential. The major aim of wastewater treatment processes is to reduce or remove organic matter, nutrients, and suspended solids before effluent is discharged back to the environment. However, most wastewater treatment systems are dynamic in nature. They constantly undergo changes because of seasonal variations in water chemistry, varying plant operating conditions, new environmental laws, and other factors. Because of this, proper monitoring of parameters which can affect the treatment process is essential.

Conventional wastewater treatment consists of a combination of physical, chemical, and biological processes and operations to remove solids, organic matter and, sometimes, nutrients from wastewater. General terms used to describe different degrees of treatment, in order of increasing treatment level, are preliminary, primary, secondary, and tertiary and/or advanced wastewater treatment. In some countries, disinfection to remove pathogens sometimes follows

the last treatment step. A generalized wastewater treatment diagram is shown in Figure 1.1.

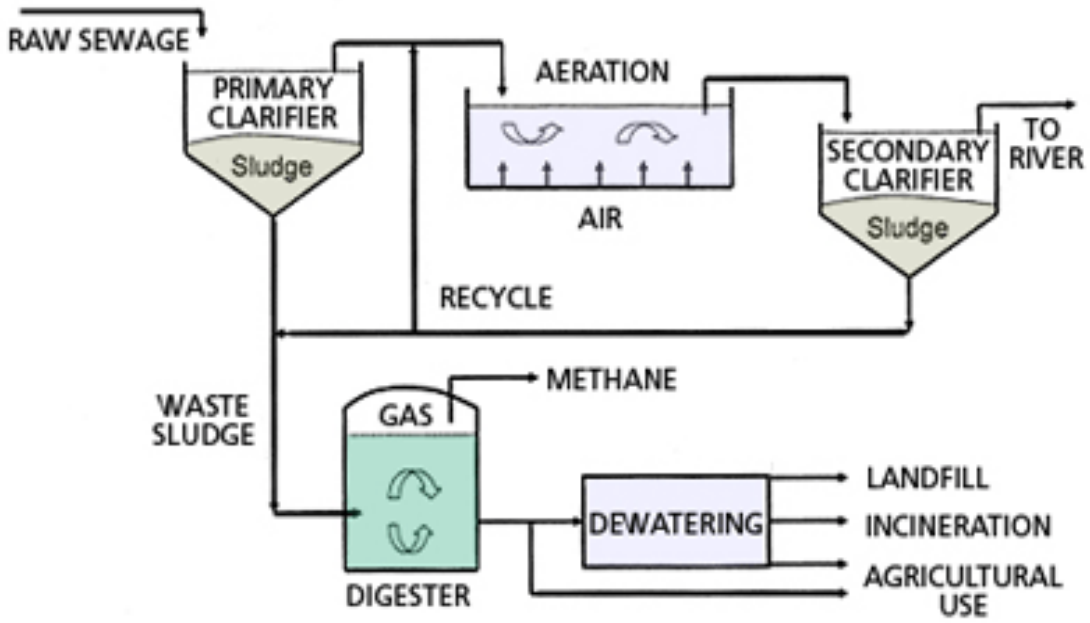

Figure 1.1: A typical flow diagram of a conventional wastewater treatment process.

Biological wastewater treatment processes use microorganisms, mostly bacteria, in the biochemical decomposition of wastewaters to stable end products. More microorganisms, or activated sludge, are formed and a portion of the waste is converted to carbon dioxide, methane, water and other end products. Generally, biological treatment methods can be divided into aerobic and anaerobic methods, based on availability of dissolved oxygen. Therefore, to ensure efficient operation of any biological wastewater treatment process, the quality of influent and effluent water is usually monitored by biochemical oxygen demand (BOD). BOD can be described as a quantitative measure of the dissolved oxygen needed by bacteria

and microorganisms for the biological oxidation of organic wastes in a unit volume of waste water at certain temperature over a specific time period (Clair 2003). The BOD measurement has its widest application in measuring waste loading to biological wastewater treatment plants and in evaluating the BOD removal efficiency of such treatment systems (APHA 2005).

1.2 Conventional BOD measurement method

BOD has been determined conventionally by taking a sample of water, aerating it well, placing it in a sealed bottle (standard size of 300 ml volume), incubating for a standard period of time at $20^{o}C$ in the dark, and determining the oxygen consumption in the water at the end of incubation (Madigan 1997). According to the Standard Methods the incubation time is 5 days and the BOD values based on this standard are called BOD_5 in short (APHA 2005), whereas the incubation time is 7 days in the Swedish standard and the abbreviation is BOD_7 (Sverige 1979). The conventional BOD test has certain benefits such as being a universal method of measuring most wastewater samples, and furthermore, no expensive equipment is needed. It has, however, the limitation of being time consuming, and consequently it is not suitable for on-line process monitoring. Thus, it is necessary to develop an alternative method that could circumvent the weakness of the conventional BOD test described above. In this case, the use of biosensor, if suitably calibrated to read BOD_5, can reduce the measurement time to the order of minutes. Keeping this in mind, several studies have been switched towards developing alternative methods or devices that could give rapid and stable measurements of BOD in the water treatment processes. In this regard, various BOD sensors have been reported considering their interest in reducing batch

retention time and continuous treatment process with in-situ BOD monitoring and control help sustain the research and development of BOD biosensors.

1.3 Existing microbial BOD bio-sensors

1.3.1 Single-microbial-culture-based sensors

Since 1977, when Karube et al (1997) reported first ever microbial cell sensor using single culture as a sensing device based on its features to bio-oxidise organic substrate, several other microbial cell based sensors have been developed and reported. In general practice, single microbial culture based sensors are constructed from the pure culture of cells, which can be immobilized by polyacrylamide gel or fixed to a glass cell (Karube et al. 1977a, Karube et al. 1977b), or sandwiched between a porous cellulose membranes. The response can also be measured in the form of different microbial responses, such as DO consumption (Hikuma et al. 1979, Yang et al. 1997), emission of light (Hyun et al. 1993), electric signals (Kim et al. 2003), etc. In the literature different immobilized sensors were reported using single microorganism such as *Clostridium butyricum, Trichosporon cutaneum* (Yang et al. 1997, Yang et al. 1996), Thermophiles (Karube and Yokoyama 1993), *Pseudomonas putida* (Chee et al. 1999, 2000, 2001), etc. , which were entrapped inside cellulose membranes or hydrogel by using an aqueous solution of polyvinylalcohol (PVA) (Riedel 1998, Tan and Wu 1999) or poly(-carbamoyl) sulphonate (PCS) (Chan et al. 1999, Tan et al. 1993). In general, single-culture-BOD-sensors have an advantage in a stable sensor performance over a desired period, but the detection will be limited by the narrow substrate spectrum of the single strain. Figure 1.2 shows different features of conventional BOD method and bio-assay indicators based on single culture

species. The category of single culture based sensor can further be divided into other sub-categories, based on their design and measuring principle.

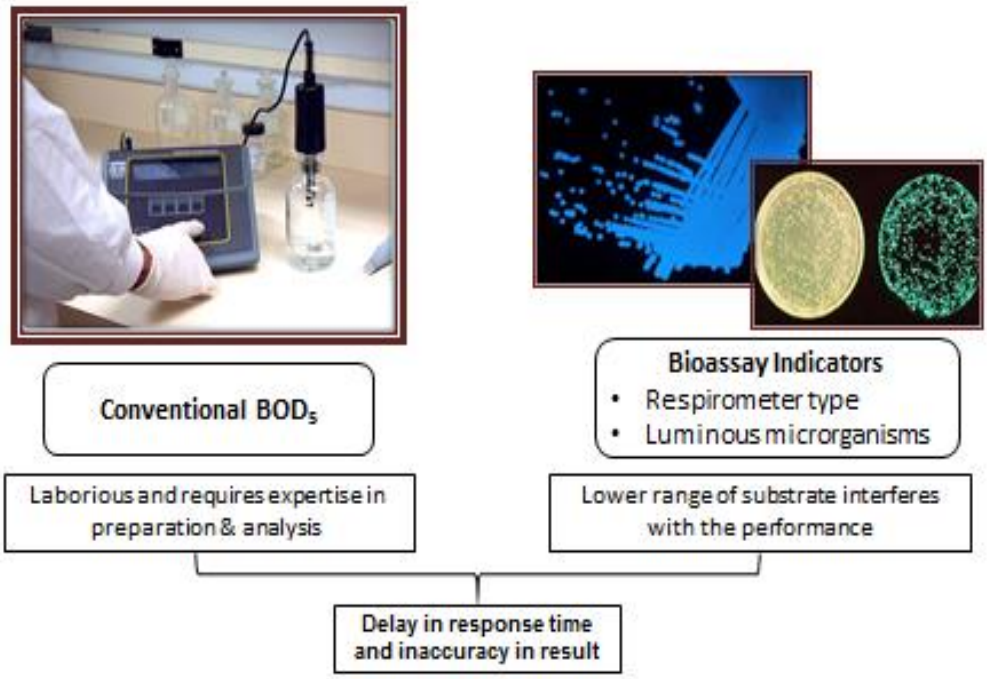

Figure 1.2: Flow diagram for the comparison of conventional BOD mehod and bioassay indicators.

1.3.1.1 Respirometer-type sensor

Respirometer-type sensor generally works with the principle of change in the pressure drop in the head space of a closed sample vessel due to oxygen uptake (respiration) by the microorganisms, which are in contact with the sample. Respirometric BOD sensor has mainly reported the use of *Bacillus subtilis* (Riedel et al. 1988), *Arxula ardeninivorans* (Riedel 1998), and *Trichospora Cutaneum* (Yang et al. 1996), etc. The main advantage of this kind of sensor is its simple design and construction process, which allows the change of attached transducer

without affecting the immobilized cells. Additionally, these biosensor take advantage of the high reaction rates of microorganisms interfaced to electrodes to measure the DO consumption. However, the presence of toxic compounds, such as heavy metals, volatile organic compounds (VOC), high salt concentration, pesticides, and herbicides in the wastewater sample can severely inhibit microbial respiration and consequently, affect the sensor performance. Moreover, low substrate versatility, short-term stability of probe and lysis of immobilized microbial strains are other limitations (Bourgeois et al. 2001, Vanrolleghem et al. 2003) .

1.3.1.2 Optical biosensors

Luminous bacteria like *Photobacterium phosphoreum* have been incorporated into BOD sensor (Hyun et al. 1993). Concept involves the use of luminous bacteria, isolated from marine sources; it emits light at a constant rate in proportion to the amount of assimilable organic compounds in wastewater. The intensity of the luminescence can be measured using a photodiode (Karube and Yokoyama 1993). These biosensors have advantages of giving rapid response and good sensitivity. Reynolds and Ahmad (1997) also reported a technique to analyse the fluorescent intensities of microbial communities growing in wastewater excited by UV at 340 nm (Reynolds and Ahmad 1997). However, being made up of single microbial species; optical biosensors are not able to consume broad substrate range. Moreover, some other unconsumed compounds can also interfere with the performance of the sensor.

1.3.2 Existing commercialized bio-sensors

In 1983, Nisshin Denki (Electric) C. Ltd launched the first reported commercialized microbial bio-sensor to asses BOD in a measuring range of 0-100

and 0-200 mg/L. Since then, several more BOD biosensors have been commercialized by DKK Corporation, Japan (measuring range 0-60 mg/L); Autoteam FmbH, Germany (measuring range 5-500 mg/L); Prufgeratewerk Medingen GmbH, Germany (measuring range 0-60 mg/L); Dr. Lange GmbH, Germany (measuring range 0-22 or 2-33 mg/L); STIP Isco GmbH, Germany (measuring range 5-1500, 20-1500, and 20-100000 mg/L); Kelma, Belgium (measuring range 0-500000 mg/L); LARAnalytik and Umweltmesstechnik GmbH, Germany (measuring range 0-5 and 0-200000 mg/L); Bioscience, Inc., USA (measuring range 0.5-300 mg/L); USFilter, USA (measuring range 100-4000 mg/L) (D'Souza 2001, Mattiasson 2002). These bio-sensors were reported for their commercial use; however, in-depth details and working principles were not publically available.

1.4 MFC-BOD bio-sensors

MFC-BOD bio-sensors share the same working principle as of MFC, which is based on the conversion of chemical energy into electrical energy by the means of metabolic activity of microorganisms (Rabaey and Verstraete 2005). Figure 1.3 depicts the basic concept behind the working of MFC-BOD sensors. Organic concentration present in wastewater can be inducted by the BOD concentration, which serves as food for microbial growth on the anode in the anodic chamber. Microorganisms excrete electrons, and by the means of their travel in a closed electrical circuit, voltage and current is generated, termed as signal response. Finally, the calibration between the produced voltage (or current) and BOD concentration allows MFC for use as a sensor for continuous BOD measurement.

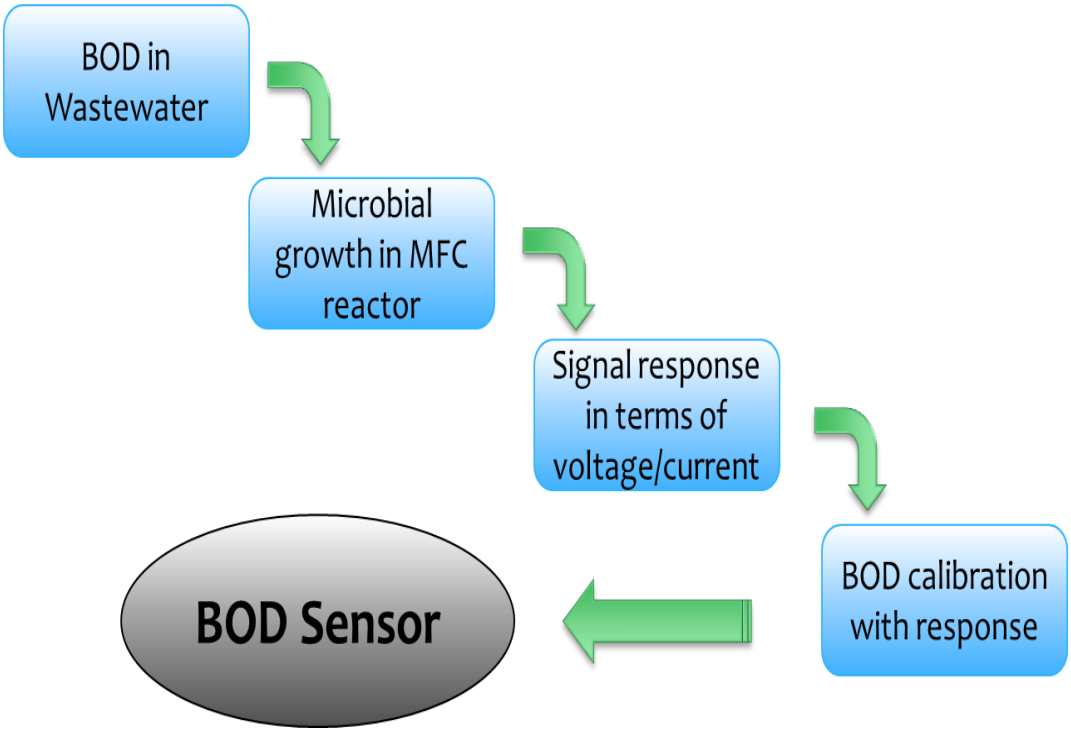

Figure 1.3: Basic concept behind the use of MFC as BOD sensing device.

MFC-BOD sensors have been studied as a BOD sensor for a long time. First, Karube et al. (1977) developed a BOD sensor based on an MFC using the hydrogen produced by *Clostridium butyricum* immobilized on the electrode. MFCs with electron-mediators have also been studied as BOD sensors (Bennetto et al. 1985, Moon et al. 2004, Thurston et al. 1985), where the mediators are used to facilitate electron transfer from the microbial cells to the electrode. In the recent years, MFC has been examined as an alternative BOD sensing device (Gil et al. 2003). MFC-based BOD sensors are quick, portable, and also contain a mixed population of microorganisms capable to oxidize a wide range of substrates (Kim et al. 2003). Yet the design and operation conditions as reported in the literature are suboptimal, consisting of two-chambered MFC systems (Moon et al. 2004, Kumlanghan et al. 2007) functioning in batch mode (Chang et al. 2004, Chang et al. 2005, Pandit et al. 2011). For the operator of a wastewater treatment plant, to

continuously monitor the evolution of BOD in effluent samples, a continuous "on-line' system is needed. Furthermore, the use of single-chambered MFCs should be preferred as these are easier and cheaper to operate than their two-chambered counterparts, mostly because the cathode can directly be exposed to ambient air as a free and sustainable source of oxygen. Other aspects for improvement of MFC sensors are in the area of better sensitivity and quicker response time. Additionally, with a view to implement BOD sensor in wastewater treatment plants, the performance stability of the sensor must be evaluated over a longer period of time.

1.5 Research objectives

The ultimate objective of this research is to develop an efficient, economic, and stable MFC BOD sensor for on-line detection of BOD. In order to attain this goal, this study focuses on the following specific sub-objectives.

1. To design, construct and develop a MFC reactor system, which generates stable voltage over a long time period and has small internal resistance.

2. To explore MFCs for on-line detection of BOD under ambient temperature and pH conditions. Analyse the performance of BOD sensor in terms of various parameters such as flow rate, detection range, response time, result reproducibility and operational stability.

3. To improve the performance of BOD sensor by optimizing different parameters and MFC constituents such as HRT, anode volume, PEM, cathode catalyst, etc.

4. To understand the role of anode biofilm in sensor sensitivity and long-term stability, and to analyse the effects of different environmental conditions (i.e., conductivity, pH and temperature) on the sensor performance.

1.6 Thesis organization

This dissertation is organized into a total of seven chapters including this introduction chapter. It comprises literature review (chapter 2), materials and methods (chapter 3), results and discussions (Chapter 4, 5 and 6), and finally conclusion and recommendations (chapter 7), summarizing the major findings of this research along with recommendations for future research. Figure 1.4 gives the overview of every chapter.

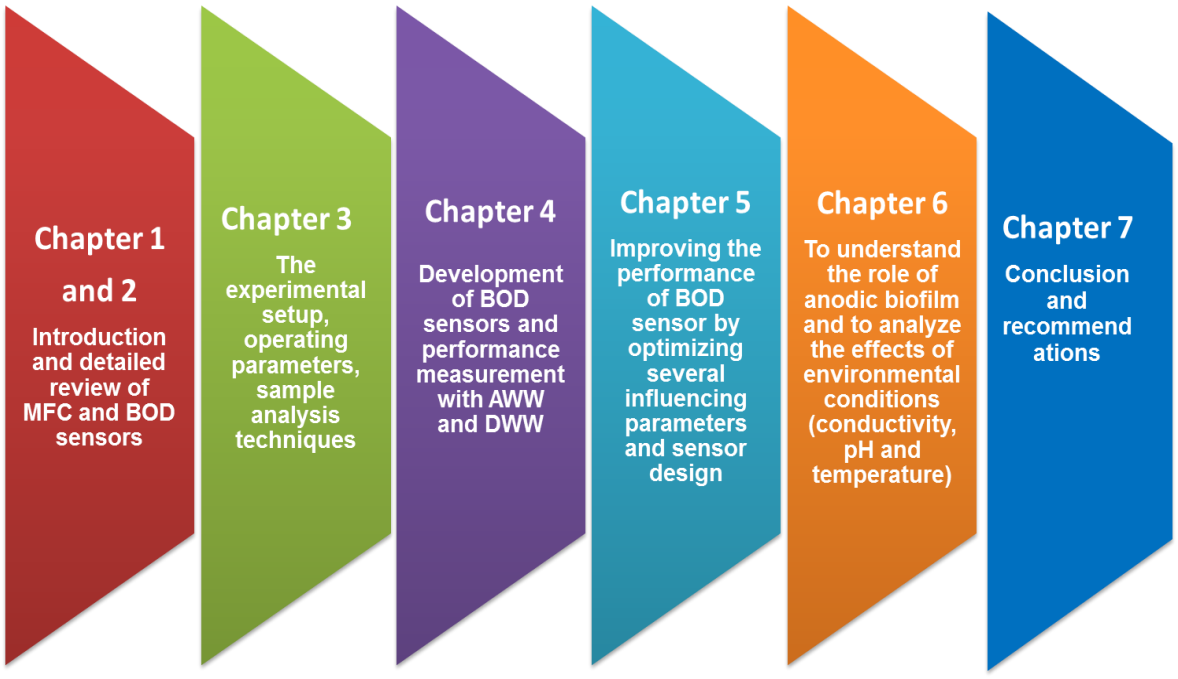

Figure 1.4: Overview of the thesis.

In chapter 4, the development of MFC-BOD sensor using MnO_2-catalyst cathode and its performance in both AWW and DWW for a long time period of more than

1.5 years are discussed. MFC-BOD sensor was calibrated by investigating a linear relationship between BOD and the produced voltage.

Chapter 5 focusses on the improvement of the performance of MFC-BOD sensor by optimizing several parameters and MFC constituents such as HRT, anode volume, PEM, cathode catalyst, etc.

In chapter 6, biological characteristics of the MFC-BOD sensor were investigated to get a better understanding of the mechanism of the MFC-BOD sensor. In addition to this, the effect of environmental conditions such as conductivity, pH and temperature was examined.

Finally, major findings of this research are summarized along with recommendations for future research in Chapter 7.

2. Literature Review

2.1 Working principle and mechanism of MFC

MFC is a device that uses microorganisms to generate an electric current through the oxidation of bio-convertible organic matter (e.g., glucose, acetate) present in the wastewater (Grzebyk and Poźniak 2005, Logan et al. 2006). This oxidation process causes the generation of electrons and protons in the anaerobic compartment. The electrons produced are transferred to the anode (negative terminal in anaerobic compartment) either via membrane-associated components or soluble electron shuttles, and flowed to the cathode (positive terminal in aerobic compartment) through an external resistor. At the same time, protons migrate to the cathode through a proton exchange membrane (PEM). At the cathode, the migrated electrons and protons produce water in the presence of oxygen. The reactions occur in the anode and cathode compartments are listed as follows:

Anode: $C_6H_{12}O_6 + 6H_2O \rightarrow 6CO_2 + 24H^+ + 24e^-$ (2.1)

Cathode: $24H^+ + 6O_2 + 4e^- \rightarrow 12H_2O$ (2.2)

In order to be a preferred electron acceptor, the anode should be available with a higher (more positive) potential than other possible electron acceptors in waste stream, such as sulphate or iron, so that the energetic gain will be higher for bacteria that can deliver the electrons to the anode (Logan and Regan 2006). On the other hand, if the anode potential is too low, electricity generation will cease

and fermentation will start. Due to its high potential, oxygen should be avoided in the vicinity of the anode. At the cathode, an electron acceptor is chemically reduced. Ideally, oxygen is reduced to water. Incomplete reduction of oxygen leads to low energy conversion efficiency and produces reactive intermediates such as H_2O_2 (He and Angenent 2006):

$$2O_2 + 4e^- + 4H^+ \rightarrow \ 2H_2O_2 \ \ (E^{o'} = 0.295\ V) \qquad (2.3)$$

The larger the difference between the reduction potentials, the more energy is released. The total energy released during a reaction can be calculated as according to Eq. 2.4.

$$\Delta G = -nF\Delta E \qquad (2.4)$$

where ΔG = total energy (J/mol)

n = the number of electrons involved

F = Faraday's constant (96,485 J/V/mol)

ΔE = difference between the reduction potentials of the electron acceptor and donor

Using Eq. 2.4, the theoretical potential difference of an MFC when electrons are transferred from acetate to oxygen is approximately 1.1 V (ΔE = (+0.82V)-(-0.32V)), leading to an energy gain of 847.60 kJ/mol of acetate. However, the measured MFC voltage is considerably lower due to a number of losses.

Overall reactions of MFC (Eqs. 2.1 and 2.2) show the production of carbon dioxide as an oxidation product. However, the amount of net carbon emission is much lower in comparison to fossil fuel combustion and other wastewater

treatment technologies. Especially, in plant-MFC fixed carbon dioxide is released as small molecular weight carbohydrates by the plant roots and can be utilized by microorganisms yielding carbon dioxide, protons and electrons. The carbon dioxide is then returned into the atmosphere, so the process becomes carbon neutral.

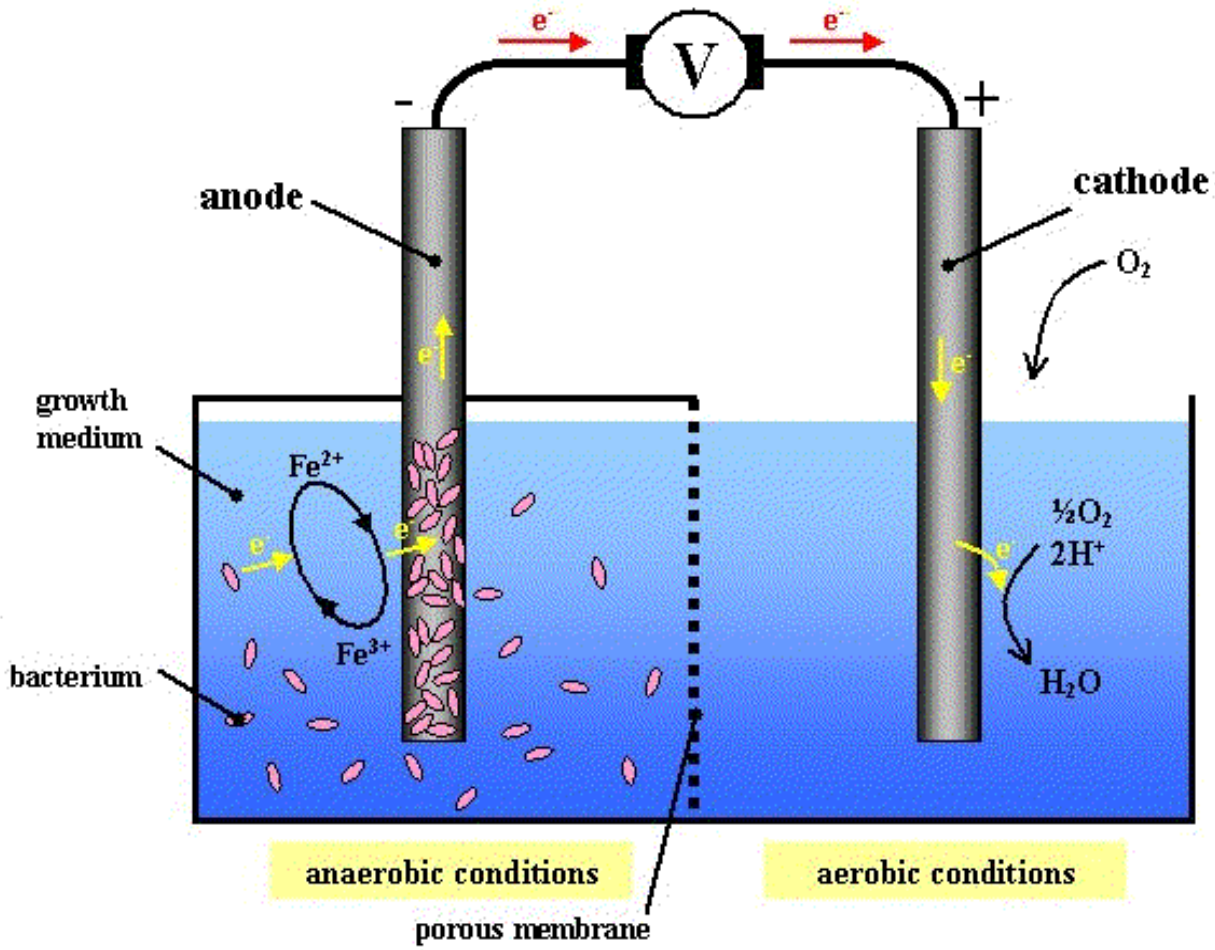

Figure 2.1: Schematic diagram of microbial fuel cell system (Chaudhuri and Lovley 2003).

An MFC converts energy, available in a bio-convertible substrate, directly into electricity. This can be achieved when bacteria switch from the natural electron acceptor, such as oxygen or nitrate, to an insoluble acceptor, such as the MFC anode (Fig. 2.1). This transfer occurs by the electrons low through a resistor to a cathode, at which the electron acceptor is reduced. In contrast to anaerobic

digestion, an MFC creates electrical current and an off-gas containing mainly carbon dioxide.

2.2 Microorganisms in MFC: Exoelectrogens

Anodic biofilm contains a variety of microorganisms; however, only some microorganisms among them are really able to transfer electrons outside their cell surface, called exoelectrogens. “Exo” comes for exocellular and “electrogens” is termed for their ability to directly transfer electrons to a chemical or material that is not the immediate electron acceptor (Logan 2008). Many anaerobes can only transfer electrons to soluble compounds such as nitrate or sulfate (not cell synthesized) that can diffuse across the cell membrane and into the cell. Exoelectrogenic bacteria are distinguished from these anaerobes by their ability to directly transport electrons outside of the cell which permits them to function in an MFC. A list of main exoelecterogenic microorganisms is presented in Table 2.1 together with their substrates. Generally, marine sediment, soil, wastewater, fresh water sediment and activated sludge are all rich sources for these microorganisms (Niessen et al. 2004a, Zhang et al. 2006). Recently, community analysis of electrochemically active biofilms in MFCs suggests a far greater diversity of exoelectrogens. Mainly exoelctrogens come in two dissimilatory metal reducing genera (*Shewanella* and *Geobacter*) (Bond and Lovley 2003, Kim et al. 2002); however, the exact mechanism of electron transfer to extracellular electron acceptors is still poorly understood. Moreover, the path of electron flow from cell membrane to the anode surface is still in debate among researcher (Beliaev et al. 2001, Myers and Myers 2001).

Table 2.1: Exoelectrons present inside anodic biofilm.

Microbes	Substrate	Applications
Actinobacillus succinogenes	Glucose	Neutral red or thionin as electron mediator (Park and Zeikus 1999, 2000)
Aeromonas hydrophila	Acetate	Mediator-less MFC (Pham et al. 2003)
Alcaligenes faecalis, Enterococcus gallinarum, Pseudomonas aeruginosa	Glucose	Self-mediate consortia isolated from MFC with a maximal level of 4.31 Wm^{-2}. (Rabaey et al. 2004)
Clostridium beijerinckii	Starch, glucose, lactate, molasses	Fermentative bacterium (Niessen et al. 2004b)
Clostridium butyricum	Starch, glucose, lactate, molasses	Fermentative bacterium (Niessen et al. 2004a, Park et al. 2001)
Desulfovibrio desulfuricans	Sucrose	Sulphate/sulphide as mediator (Ieropoulos et al. 2005, Park et al. 1997)
Geobacter metallireducens	Acetate	Mediator-less MFC (Min et al. 2005)
Geobacter sulfurreducens	Acetate	Mediator-less MFC (Bond and Lovley 2003, Bond et al. 2002)
Shewanella putrefaciens	Lactate, pyruvate, acetate, glucose	Mediator-less MFC (Chaudhuri and Lovley 2003, Liu et al. 2006)
Shewanella oneidensis	Lactate	Anthraquinone-2,6-disulfonate (AQDS) as mediator (Ringeisen et al. 2006)
Pseudomonas aeruginosa	Glucose	Pyocyanin and phenazine-1-carboxamide as mediator (Rabaey et al. 2004, Rabaey et al. 2005a)
Klebsiella pneumoniae	Glucose	HNQ as mediator biomineralized manganese as electron acceptor (Menicucci et al. 2006, Rhoads et al. 2005))

2.3 Voltage/power generation by MFC

The theoretical voltage of MFC (E^0_{cell}) is calculated by the potential difference between the anode (E^0_{an}) and the cathode (E^0_{cat}), and can be described as

$$E^0_{cell} = E^0_{cat} - E^0_{an} \quad (2.5)$$

$$V_{op} = E_{thermo} - [(\eta_{act} + \eta_{ohmic} + \eta_{conc})\, cathode + (\eta_{act} + \eta_{ohmic} + \eta_{conc})\, anode] \quad (2.6)$$

where E_{thermo} is thermodynamically predicted voltage, η_{act} is the activation loss due to reaction kinetics, η_{ohmic} is the ohmic loss from ionic and electronic resistances, and η_{conc} is the concentration loss due to mass transport limitations.

Usually, a maximum working voltage of 0.30–0.70 V is commonly achieved in an MFC (Logan 2008). The voltage is a function of the external resistance (R_{ex}), or load on the circuit, and the current, I. The relationship between these variables is the following well-known Eq. 2.7

$$V = I R_{ex} \quad (2.7)$$

Where V is the cell potential.

The current produced from a single MFC is typically small. Therefore, the produced current is normally not measured, but instead is calculated from the measured voltage drop across the resistor as $I = V / R_{ex}$. The highest voltage generated in an MFC is the open circuit voltage, *OCV*, which can be measured while the circuit is disconnected (infinite resistance, zero current). As the resistance is decreased, the voltage decreases. In order to estimate the maximum

power generated by an MFC, electromotive force, and internal resistance of MFC are calculated by plotting a polarization curve over a range of external resistance and over a period of time (Fig. 2.2). The electromotive force is estimated as the intercept of the regression with the Y-axis, whereas the internal resistance is the opposite of its slope. In this case, the maximum power generated by the MFC can be calculated according to following equations.

$$P_{max} = \frac{E_{emf}^2}{4R_{int}} \quad (2.8)$$

$$E_{emf} = E^0 - \frac{RT}{\eta F}\ln(\frac{[red]^\gamma}{[ox]^\beta}) \quad (2.9)$$

In these equations, E_{emf} is the electromotive force in voltage, E^0 is the standard free energy at pH = 7 in voltage, R_{int} is the internal resistance of the MFC and P_{max} is the maximum power generated by the MFC. R is the universal gas constant (8.314 J/mol K), T is the operation temperature (K), n is the number of electrons transferred, F is the Faraday constant (96,485 Coulombs/mol), [ox] and [red] are the concentrations of the oxidized and reduced compounds, respectively, and γ and β are their corresponding stoichiometric coefficients.

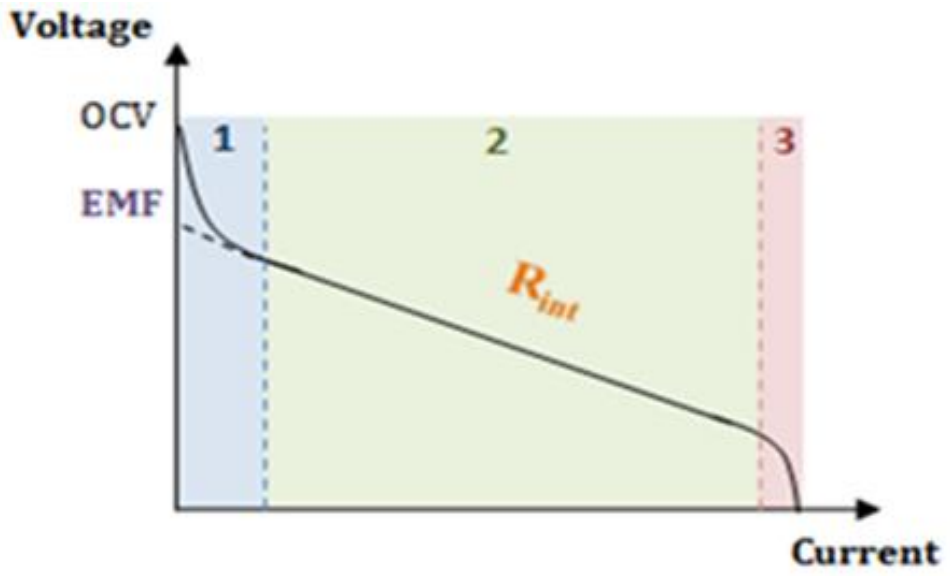

Figure 2.2: Polarization curve of an MFC.

2.3 Parameters influencing the performance of MFC

There are several parameters, which may influence the performance of MFCs either independently or cumulatively.

2.3.1 Substrate

The substrate used is able to influence the MFC performance including the power density and the Coulombic efficiency. It serves as a carbon source for microbial metabolism. The efficiency and economic viability of converting organic wastes to bioenergy depend on the characteristics and components of the waste material. Various studies have been conducted to investigate the performance of the MFC with the usage of synthetic wastewater (Gurung et al. 2012, Pant et al. 2010, Rezaei et al. 2007). Acetate is most commonly studied, as it is able to increase the ionic strength and hence decrease the internal resistance (Thygesen et al. 2009).

However, MFCs have been operated using a wide variety of other substrates such as glucose, butyrate (Liu et al. 2005a), cysteine (Logan et al. 2005), proteins (Heilmann and Logan 2006), lignocellulose (Rismani-Yazdi et al. 2005), as well as complex substrates such as domestic wastewater (Cheng et al. 2006a). Table 2.2 presents a comprehensive list of substrates that have been used in MFC studies and the respective produced current density.

Table 2.2: Commonly used substrates in MFCs for higher current density.

Type of substrate	Concentration	Source	Current density (mA/cm^2) at maximum power	Reference
Acetate	1 (g/L)	Pre-acclimated bacteria from MFC	0.8	Logan et al. (2007)
Arabitol	1.22 (g/L)	Pre-acclimated bacteria from MFC	0.68	Catal et al. (2008b)
Galacitol	1.22 (g/L)	Pre-acclimated bacteria from MFC	0.78	Catal et al. (2008b)
Glucose	6.7 mM	Mixed bacterial culture maintained on sodium acetate for 1 year (*Rhodococcus* and *Paracoccus*)	0.70	Catal et al. (2008a)
Glucuronic acid	6.7 mM	Mixed bacterial culture	1.18	Catal et al. (2008a)
Mannitol	1.22 (g/L)	Pre-acclimated bacteria from MFC	0.58	Catal et al. (2008b)
Ribitol	1.22 (g/L)	Pre-acclimated bacteria from MFC	0.73	Catal et al. (2008b)
Sodium fumarate	20 mM	Anaerobic digested fluid from a sewage treatment plant	0.22	Ha et al. (2008)
Sorbitol	1.22 (g/L)	Pre-acclimated bacteria from MFC	0.62	Catal et al. (2008b)
Starch	10 (g/L)	Pure culture of	1.3	Niessen

		Clostridium butyricum		et al. (2004)
Sucrose	2.67 (g/L)	Anaerobic sludge from septic tank	0.19	Behera and Ghangrekar (2009)
Xylitol	1.22 (g/L)	Pre-acclimated bacteria from MFC	0.71	Catal et al. (2008b)
Xylose	6.7 mM	Mixed bacterial culture	0.74	Catal et al. (2008a)

2.3.2 Membrane

Proton exchange membrane can affect MFC system's internal resistance and concentration polarization loss, hence in this way it may influence the power output of the MFC. Nafion (DuPont, Wilmington, Delaware) is most popular because of its highly selective permeability of protons and high conductivity to various cations (Oh and Logan 2006). However, side effect of other cations transport is unavoidable during the MFC operation even with Nafion. Therefore, there are several attempts done by researchers to look for less expensive and more durable substitutes which also exhibit comparable cation conductivity such as selemion, Ultrex CMI 7000, etc. (Pandit et al. 2011, Rozendal et al. 2007).

2.3.3 External resistance

The external resistance can affect the potential of the anode and thus the microbial activity of the MFC. Large differences in external resistance result in differences both in power production and microbial community structure (Lyon et al. 2010). One way to improve the MFC performance is to operate the MFC under optimal conditions for power production at an optimal external resistance (Clauwaert et al. 2008). The optimal external resistance usually correlates to the internal resistance

of the MFC (Logan and Regan 2006), following electrochemical theory and as supported by biological investigations.

2.3.4 Internal resistance

Internal resistance, including anode resistance, cathode resistance, electrolyte resistance and membrane resistance (if any), limits the power output of an MFC. The internal resistance can be reduced by increasing the anode surface area, the cathode surface area, the surface area of the PEM, the ionic strength of the electrolyte or the pH. Identification of the limiting factor of an MFC requires quantification of the contribution of each component of an MFC to the internal resistance (Ieropoulos et al. 2010, Logan et al. 2007). Like any electrochemical cell, the internal resistance of an MFC can also be classified as ohmic resistance, charge-transfer resistance and diffusion resistance (Kim et al. 2004). There are several different methods to evaluate the internal resistance of an MFC. These include polarization slope, power density peak, electrochemical impedance spectroscopy (EIS) using a Nyquist plot and current interrupt methods. The first two methods are very easily done, and provide quick methods for estimating the internal resistance.

2.3.5 Cathode catalyst

The use of catalysts on the cathode surface can lower the cathodic activation overpotential and increase the current output of MFCs. Such catalysts considerably decrease the activation energy barrier and improve the kinetics of oxygen reduction at the electrode surface (Barbir 2013). Different chemical and biological catalysts have been tested in efforts to improve the MFC performance. Among different metal-based catalysts, platinum (Pt) has been widely used as the

catalyst in cathode materials of MFCs because it has a favorably low over-potential for oxygen reduction. (Logan et al. 2005). However, considering the high cost and low durability of platinum due to corrosion and degradation of catalytic activity over time (Shao et al. 2009), several researches are exploring other metal-based catalyst, such as indium/tin (Chhina et al. 2006), cobalt (Lefebvre et al. 2009), titanium (Ekström et al. 2007), tungsten (Maiyalagan and Viswanathan 2008) and manganese (Lu et al. 2011).

2.3.6 Design of MFC

Several researcher focused their study toward developing an MFC design that will not only produce high power and Coulombic efficiency, but one that is also economical with respect to the materials used and manufacturing process being practical to implement on a large scale. The MFC reactor design that should ultimately prove to meet the requirements of power, efficiency, stability and longevity is still a challenge. Table 2.3 summarizes some of the most commonly used MFC designs. The most basic type is a two-chambered MFC where the anode and cathode compartments are separated by an ion-selective membrane, allowing protons to transfer from the anode to the cathode and preventing oxygen diffusion into the anode chamber. Later, a single-chambered MFC with air exposed cathode side was developed by the Logan's group of Pennsylvania State University. In a single-chambered MFC, the cathode is exposed directly to the air and the oxidation reaction occurs at the surface of the air cathode. A single-chambered air-cathode system without a PEM was also designed, and it was found that protons could be brought directly by the water to the cathode (Liu et al. 2005b) which decreased the internal resistance drastically. In order to decrease the internal resistance and thus increase the power generation in an MFC, the distance

between the anode and cathode should not be too large (Pham et al. 2005). Liu et al. (2005a) observed the increase in maximum power density after decreasing the electrode space from 4 to 2 cm. Small distance between electrodes, decreased the internal resistance and increase power density. Keeping this in mind, the membrane electrode assembly, state-of-the-art was brought into the MFCs (Hays et al. 2011). The MFC with a membrane-electrode assembly (MEA) generated a higher current with an increased coulomb yield when compared to an MFC with a separate cathode. Less oxygen was diffused through an MEA than through a Nafion membrane. Besides these, other MFC designs that have been explored include stacked MFC, up-flow mode MFC, etc. (He et al. 2005, Rabaey et al. 2005b).

Table 2.3: Different design of MFCs with their main features.

MFC design	Main features	Reference/ research group
	Conventional two-chamber microbial fuel cell. Both chambers are gas sparged: anode with nitrogen to maintain anaerobic conditions and cathode with air to provide oxygen in solution	(Logan 2008)
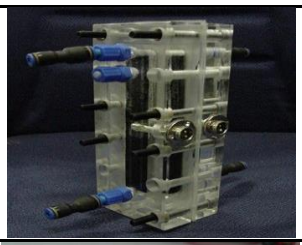	A miniaturized continuous MFC for sensor applications	Gwangju Institute of Science and Technology (Korea) - The Energy and Biotechnology Laboratory (EBL)
	A single chambered MFC using brewery wastewater, sewage wastewater	Harbin Institute of Technology (HIT, China)

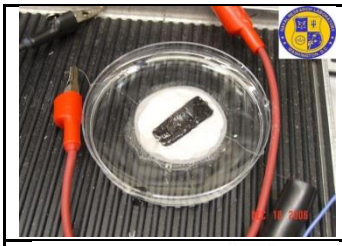	Passive Diffusion Microbial Fuel Cell with a Polycarbonate Membrane and Graphite Felt Electrodes	The Ringeisen Group US Naval Research Laboratory - Washington, D.C. (USA)
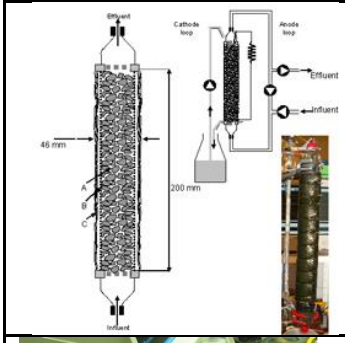	Upflow, tubular type MFC with inner graphite bed anode and outer cathode.	(Rabaey et al. 2005b)
	Single Chamber Microbial Fuel Cell (SCMFC)	(Liu and Logan 2004)

2.4 Limitations of MFC for power generation

The power generation by MFC suffers several limitations such as higher internal resistance, overpotential of electrodes, membrane performance, substrate conversion rate, etc., which make it less efficient and suitable as compared to the other technologies such as fermentation based bioethanol synthesis and anaerobic digestion for methane production (Cheng et al. 2006b). A major limitation to the MFC system is the reduction of molecular oxygen by the cathode. Various metals have typically been used to catalyze the cathodic reaction (Nevin et al. 2009, Zhao et al. 2005) but reduction of oxygen at the cathode is currently an important limiting factor in a MFC. To reduce these cathodic limitations, researchers have increased the cathode to anode ratio (Rabaey et al. 2008) and used biological catalysts (Torres et al. 2008), but still the power generation could not be increased much. Another major problem in the MFC is proton accumulation within the

biofilm. A decrease in the pH of the bulk fluid of an MFC has been shown to decrease power production (Matsunaga et al. 1980).

2.4.1 Cathode limitations

In practice, the actual voltage output of an MFC is less than the predicted thermodynamic ideal voltage due to irreversible losses called overpotentials. The three major irreversibilities that affect MFC performance are: activation losses, ohmic losses and mass transport losses. These losses represent the voltage required to compensate for the current lost due to charge transport, mass transfer processes and electrochemical reactions that take place in both the anode and cathode compartments (O'Hayre 2005).

2.4.1.1 Activation Losses

Reduction kinetics taking place at the cathode affects greatly the current production in an MFC. The reaction kinetics is limited by an activation energy barrier which impedes the conversion of the oxidant into a reduced form. A portion of cathode potential is lost to overcome this energy barrier when current is being drawn from the fuel. This potential loss due to activation is called cathodic activation loss or activation overpotential (Larminie and Dicks. 2003).

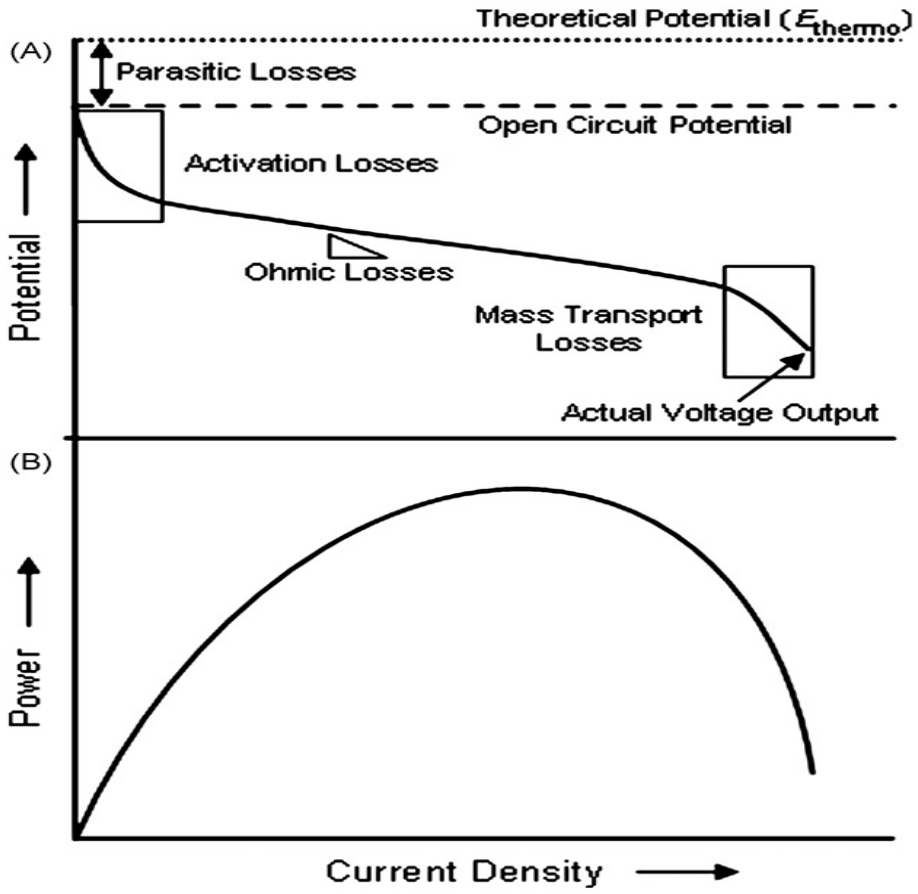

Figure 2.3: (A) Schematic potential losses for a cathodic reaction displaying activation, ohmic, mass transport and parasitic regions. (B) A typical power–current curve.

Activation losses result in a characteristic, exponentially formed loss on the current–voltage curve at low current densities. As more current is taken from the MFC, the activation loss increases and results in a lower cell potential (Larminie and Dicks 2003). The magnitude of activation potential is dependent on the reduction kinetics of the system. The cathodic activation loss usually forms the main contribution to the performance of MFCs (Gil et al. 2003). Kinetic performance can be improved by decreasing the activation barrier and increasing the reaction interface area, temperature or oxidant concentration.

2.4.1.2 Ohmic loss

These losses are the most important losses to be overcome for optimum design of the MFC architecture. These losses arise from resistance of ion (proton)

conduction due to the solution and (if present) the membrane, the flow of electrons through the electrode to the contact point (i.e., where the electrodes connect to a wire) and any relevant internal connections. Ohmic losses can be limited by reducing electrode spacing, choosing membranes or electrode coatings with low resistances (if present), ensuring good contacts between the circuit and electrodes, and increasing solution conductivity and buffering capacity. The ohmic losses due to the solution conductivity between a reference electrode and a bipolar membrane were calculated as (Ter Heijne et al. 2006) -

$$\Delta V_{\Omega} = \frac{\delta_w I}{\sigma} \tag{2.10}$$

Where ΔV_{Ω} is the ohmic voltage drop, δ_w is the distance in the water (cm), I the current density (A/cm^2) and σ is the solution conductivity (S/cm).

2.4.1.3 Mass transport

The transport of substrate to the anodic biofilm and the transfer of products outside of the biofilm will result in concentration or mass transfer losses. Inefficient mass transfer through diffusion and convection of substrate or removal of products may limit the maximal current production at an electrode (Clauwaert et al. 2008).

2.5 Several other applications of MFC

2.5.1 Wastewater treatment

MFCs have several advantages in wastewater treatment when compared to other biological treatment processes. They include high theoretical energy conversion rate, less sludge and no gas processing (Zhou et al. 2011). From conventional standalone MFC systems for domestic wastewater treatment, researchers have

attempted to explore different ways of integrating MFC technology with existing technologies to enhance wastewater treatment process. These include integrating MFC with the activated sludge process (Cha et al. 2010; Liu et al. 2011) and the membrane bioreactor (MBR) (Liu et al. 2013; Wang et al. 2012). There has also been increasing interest to treat streams with higher organic content. An experiment has been carried out on high strength wastewater of total COD of up to 9,978 mg/L (Sevda et al. 2013). These studies showed the potential of MFCs in wastewater treatment processes.

2.5.2 Chemical production

In single-chambered air cathode MFCs, oxygen is reduced to form water at the cathode. However, oxygen could also be reduced to hydrogen peroxide, given in the reduction reaction below:

$$8H^+ + 4O_2 + 4H_2O \rightarrow 2HCO_3^- + H^+ + 4H_2O_2 \quad (2.11)$$

However, the concentration of hydrogen peroxide that can be produced is only 0.13±0.01 wt% (Rozendal et al. 2007). There are also studies done to couple MFCs with bipolar membrane electrodialysis to produce alkali and other side products (Chen et al. 2013, Chen et al. 2012, Rabaey et al. 2010).

2.5.3 Bio-hydrogen production

MFCs can be readily modified to produce hydrogen instead of electricity. Under normal operating conditions, protons released by the anodic reaction migrate to the cathode to combine with oxygen to form water. Hydrogen generation from the protons and the electrons produced by the metabolism of microbes in an MFC is thermodynamically unfavourable. Liu et al. (2005c) applied an external potential to increase the cathode potential in a MFC circuit and thus overcame the

thermodynamic barrier. In this mode, protons and electrons produced by the anodic reaction are combined at the cathode to form hydrogen. However, using a coupled system of microbial electrolytic cells (MEC) and MFC, the requirement external electric supply can be avoided (Sun et al. 2008).

2.5.4 Bio-sensor

Besides, the use of MFCs for abovementioned applications, it has also been explored as on-line sensing device, mainly for the continuous measurement of BOD and toxicity (heavy metals and volatile organic compounds). A number of studies have been reported recently, directed towards the development of MFCs as toxicity sensors by relating the drop in microbial metabolism (in terms of voltage or current) with toxicants present in wastewater (Davila et al. 2011, Kim et al. 2006, Pasco et al. 2011, Shen et al. 2013, Shen et al. 2012, Stein et al. 2012a, b). A more recent development is the use of MFC sensors for the detection of different VFAs present in water (Kaur et al. 2013). These developed sensors are able to respond very quickly (in a range of few minutes) when exposed to different heavy metals, such as Hg, Pb, Cd, Ni, etc.; however, the measurement was quantitative but not qualitative.

2.6 Bio-assay of BOD

2.6.1 Use of immobilized microorganisms

The use of immobilized microorganisms for biosensor application has been adopted for a long time (Mulchandani and Kim 1998, Tumer et al. 1992). Microorganisms can be immobilized on a transducer or support matrices by chemical or physical methods. The fabrication of a microbial biosensor requires immobilization of microorganisms on a transducer in order to facilitate their close

contact with the transducer. The choice of immobilization techniques is a critical parameter which influences the response, operational stability and long-term use. Microorganisms are mainly immobilized chemically or physically. Chemical methods of microbial immobilization include covalent binding and cross-linking (D'Souza 2001, Blum and Coultet 1991, Mikkelsen and Corton 2004). Covalent binding methods rely on the formation of a stable covalent bond between functional groups of the microorganisms' cell wall components such as amine, carboxylic or sulphydryl and the transducer such as amine, carboxylic, epoxy or tosyl. On the other hand, physical method includes adsorption and entrapment for immobilization. In adsorption, a microbial suspension is incubated with an electrode or an immobilization matrix, such as alumina and glass bead, followed by rinsing with buffer to remove unadsorbed cells. In entrapment, dialysis or filter membrane, and polymer gels are generally used for the retention of cells (Mulchandani and Kim 1998).

2.6.2 Optical microbial bio-sensors

Optical properties of some microorganisms, such as *Photobacterium phosphoreum, Ralstonia eutropha, and Cyanobacteria spp,* etc., allow them to emits light at a constant rate in proportion to the amount of assimilable organic compounds in the wastewater (Hyun et al. 1993 , Tibazarwa et al. 2001, Schreiter et al. 2001) . The modulation in optical properties such as UV–vis absorption, bio- and chemi-luminescence, reflectance and fluorescence brought by the interaction of these microorganisms with the target organic concentration is the basis for optical microbial biosensors. The intensity of the luminescence can be measured using a photodiode (Karube and Yokoyama 1993). These biosensors have advantages of giving rapid response and good sensitivity. Reynolds and Ahmad

(1997) reported a technique to analyse the fluorescent intensities of microbial communities growing in wastewater excited by UV at 340 nm.

2.6.3 Electrochemical microbial bio-sensors

Recently, the uses of electrochemical microbial biosensors have emerged as an excellent choice for biosensor applications due to their low cost, miniaturization and potential portability (Obuchowska 2008, Shabani et al. 2008, Susmel et al. 2003). In general, they require simpler equipment, are more easily integrated with electronic readout devices, and are less susceptible to environmental effects and contaminants than other analytical techniques (Palchetti and Mascini 2008). Traditional electrochemistry is performed in solution in a three-electrode electrochemical cell. In this system, the working electrode is the site at which current is measured. A potential is applied to this electrode relative to a second reference electrode, which is also in contact with the test solution. The counter electrode is part of a feedback system that supplies current to the test solution whenever necessary in order to maintain the correct potential at the working electrode-solution interface (Daniels and Pourmand 2007). Cyclic voltammetry is a common electrochemical measurement technique in which a cycling electric potential is applied between the electrodes and the resulting current flow is measured. Electrochemical microbial biosensors can be classified into two main categories - pure microbial cell based biosensors (such as amperometric and potentiometric) and mixed microbial cells based (such as MFC) biosensors.

Amperometric microbial biosensor operates at a fixed potential with respect to a reference electrode, and involves the detection of the current generated by the oxidation or reduction of species at the surface of the electrode. The microbial strains used as biological sensing element include *Torulopsis candida* (Sangeetha

et al. 1996), *Trichosporon cutaneum* (Marty et al. 1997, Yang et al. 1996), *Klebsiella oxytoca* (Ohki et al. 1994), *Bacillus subtilis* (Riedel 1998, Riedel et al. 1988), *Arxula adeninivorans* (Tag et al. 2000), *Serratia marcescens* (Kim and Kwon 1999), etc. Besides their use as a BOD biosensor, amperometric microbial biosensors have also been applied in other fields, such as fermentation industry and clinical toxicology (D'Souza 2001, Reshetilov et al. 2001). On the other hand, conventional potentiometric microbial biosensors consist of ion-selective electrodes, such as ammonium, chloride, phosphate, etc. Potentiometric biosensors measure the difference between a working electrode and a reference electrode, and the signal is correlated to the concentration of organics (Mulchandani and Kim 1998). Microorganisms that have been explored as potentiometric biosensors include *Flavobacterium sp.* (Gaberlein et al. 2000) which used pH electrode as transducer, *Psuedomonas aeruginosa* (Han et al. 2002, Han et al. 2001) which used chloride ion selective electrode as transducer, *Bacillus sp.* (Verma and Singh 2003) which used NH_4^+ ion selective electrode as transducer, etc. for the measurement of organophosphates, trichloroethylene, and urea, respectively.

2.7 Criteria for a good BOD sensor

In order to use BOD sensor as an on-line sensing device, there are several restrictions needs to be resolved. It should match certain norms before it is ready for commercial use. This section will mainly focus on the main criteria for a commercially fit BOD sensor (Fig. 2.4).

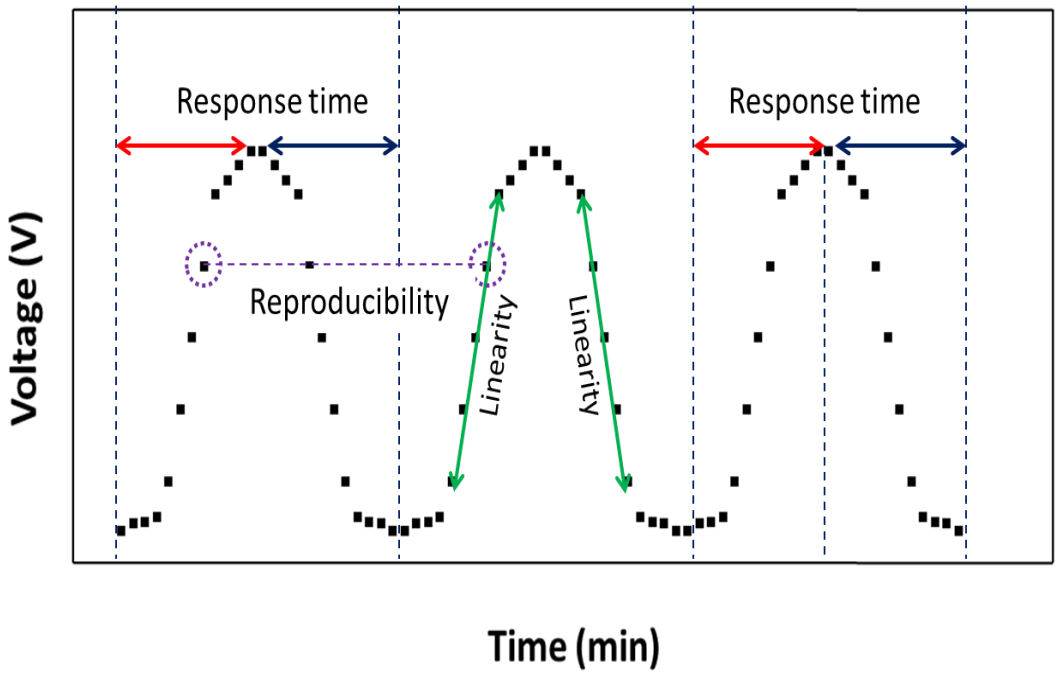

Figure 2.4: Different parameters defining BOD sensor performance.

2.7.1 Response time

In practice, the response time of any sensor can be defined as the time taken by a sensor to approach its true output when subjected to an input. In most of the cases, a sensor does not have any specific response time, but within a range. The response time of a BOD sensor depends on the metabolic recovery of the bacteria after starvation and if we decrease this recovery time, response time can be decreased significantly. It has been observed so far that BOD sensors may be a potential alternative of conventional BOD_5 method and because of its ability to estimate the concentration of rapidly biodegradable organic matter in wastewaters rapidly. Short response time also allows them to work as an on-line monitoring system in any wastewater treatment plant. However, the response time varies with different sensor designs. Liu and Mattison (2002) summarized response time of different type of biofilm-type BOD sensors. It ranged from 0.25 min (measured in initial-rate mode) *by B. subtilis+B. licheniformis* and *Rhodococcus*

erythropolis+Issatchenkia orientalis based biofilm-type BOD sensor (Riedel 1998, Tan et al. 1993) to 60 min (measured in steady-state mode) by multi-species culture (BIOSEED) based sensor (Tan and Wu 1999). In the case of a single-culture based BOD sensor, since there is no competition for substrate by other species, its response time is generally shorter, while multi-species based BOD sensor has longer response time. In the steady-state mode, the time taken to reach a new steady state also depends on the substrate concentration in the sample. In other words, more time will be required for analysing a sample with a higher concentration of substrate.

2.7.2 Precision

Precision can be defined as a degree of repeatability of a measurement. For example, if exactly the same sample at similar operating conditions is to be measured for a number of times, an ideal sensor would output similar value every time. However, a real sensor outputs a range of values distributed in some manner relative to the actual correct value. Sometimes, precision can be easily misunderstood with accuracy. However, precision as a function of both repeatability and reproducibility, whereas accuracy of a sensor is the maximum difference that will exist between an actual value and an indicated value at the output of the sensor. Liu and Mattiason (2002) defined repeatability as a standard deviation of sensor measurement by one operator in the same operating conditions, while reproducibility can be referred as a standard deviation of a series of tested measurement by more than one operator under different operating conditions. The precision of 5-day BOD test is generally poor, especially at lower organic concentrations. According to the APHA standard for 5-day BOD test, the acceptable bias limit is normally ± 15% standard deviation (APHA 2005). The

repeatability of biofilm-type BOD sensors based on amperometric oxygen probe and respirometric measuring principle ranges from ±1.3 to ±20%; however, the operational stability of sensors is not similar (Liu and Mattiasson 2002). Precision (in terms of both repeatability and reproducibility) can be affected by durability of membrane, oxygen probe, presence of toxic material and sensor design. More study is needed in order to incorporate these parameters for the real estimation of precision of any BOD sensor.

2.7.3 Detection limit

Detection limit of any BOD sensor can be defined as the smallest detectable incremental change of input parameter (i.e., BOD) that can be detected in the output signal (Fig. 2.5). Detection limit can be expressed either in absolute terms or in a range. It is largely affected by the nature of the biological entity present inside the sensor. For any single-culture based BOD sensor, detection limit is narrow due to limited substrate consumption, while BOD sensors using microbial consortia in the form of biofilm or activated sludge were found to have broader detection limit (Tan and Wu 1999, Karube et al. 1977a, Liu et al. 2000). The detection limits of immobilized-microorganisms-based BOD sensors differ a lot; however, generally, it ranges between 1-100 mg/L (Riedel et al. 1988, Hikuma et al. 1979, Li and Chu 1991, Riedel et al. 1990).

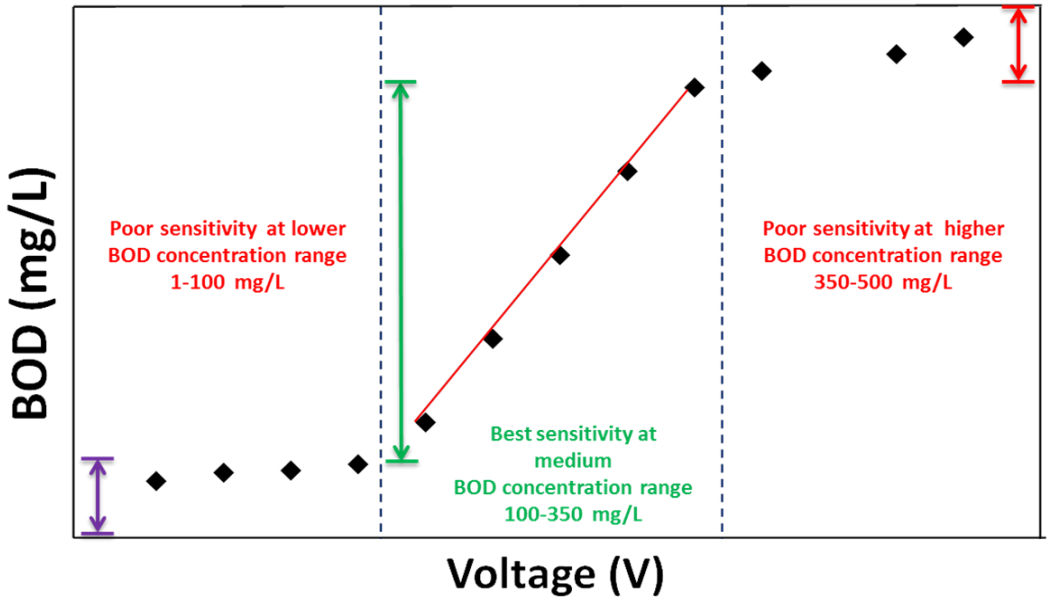

Figure 2.5: General pattern of BOD sensor sensitivity with respect to different concentration range.

2.7.4 Linearity

The linearity of BOD sensor can be an expression of the extent to which the actual measured curve of a sensor departs from the ideal curve (Gautschi 2002). According to the Monod's equation –

$$\mu = \mu_{max} \frac{S}{K_s + S} \qquad (2.12)$$

Where μ is the specid growth rage of mircroorganisms, μ_{max} is the specific growth rate of the microorganisms, S is the concentration of th limiting substrate for growth and Ks is the half-velocity constant.

As shown in the Fig 2.6, when substrate concentration is very high (i.e., non-limiting for growth), microorgansisms grow at their maximum rate, and under this conditions, S >> Ks and equation 2.12 becomes zero-order rate reaction (solid-lines in Fig 2.6). If the substrate concentration is limiting, microorganisms grow linearly with the substrate utilization, and equation 2.12 becomes first-order

reaction (dotted-lines in Fig 2.6). In the case of BOD sensor, linearity can be achieved by constructing what is known as the "Best fit straight line" through the calibration points in such a way that the maximum deviation of the curve from the line is minimised as indicated by dotted-lines in Fig. 2.6.

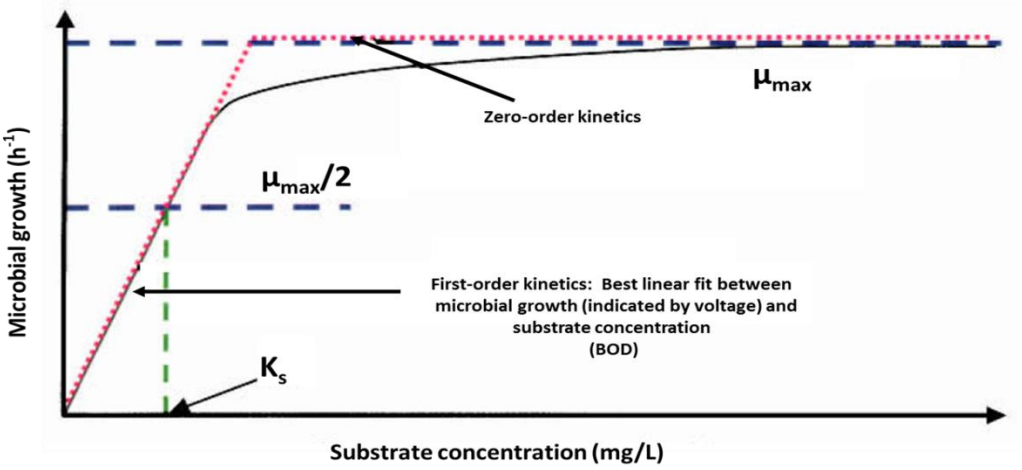

Figure 2.6: Microbial growth rate as a function of substrate concentration according to Monod Kinetics. Best linear relationship beween voltage and BOD can be estimated in the region of first-order kinetics (dotted lines).

2.8 MFC as a BOD sensor

Various limiting factors such as high internal resistance, low operational stability, higher power consumption, etc., still make MFCs very far from its commercialization as an alternative power source and for bioremediation. Nevertheless, fundamental research into how microorganisms oxidize organic compounds and generate electricity within MFCs has exhibited some other prospects of its practical applications such as the development of microbial energy based sensing devices for on-line control of biochemical processes and for environmental monitoring. As in environmental analysis, the most important application is BOD determination in polluted water or effluent, which is very crucial to have a fast, stable and economical technique for it. Rigorous process, off-line measurement and poor reproducibility (particularly at low concentrations)

of conventional 5-day BOD (BOD_5) impose tight constraints. Moreover, membrane fouling of the dissolved oxygen (DO) probe can become a serious problem with wastewater and therefore, frequent maintenance is needed to maintain high sensitivity (Liu and Mattiasson 2002). These severe issues stimulated the development of automated BOD sensor in recent years (Riedel 1998, Liu and Mattiasson 2002). Automated BOD biosensor can be defined as a self-sustainable and integrated device, which is capable to consume BOD in wastewater by means of biochemical reactions (generally oxidation-reduction reactions); and ultimately, BOD consumption is reflected in terms of response output, which can be measures using integrated transduction element (Thévenot et al. 2001). These types of biosensors can be categorized broadly based on their working principle (i.e., respirometric or optical detection), design (i.e., immobalized cell probe or biofilm) and substrate specificity, which will be discussed briefly in a separate section. The main advantages of these sensors may include rapid estimation of BOD, simplicity of system design and easy handling of on-line measurement at plant site. However, these sensors usually make use of single species microbial strains, which is not able to oxidize a broad range of substrates. Consequently, DO consumption may not be directly proportional to the total concentration of biodegradable organics present in solution (Reynolds and Ahmad 1997). Moreover, the intrinsic limitation of oxygen solubility in aqueous solutions, short-term stability of probes and lysis of immobilized microbial strains challenge the viability of such sensors (Riedel 1998, Tan and Wu 1999).

Besides the drawbacks of conventional BOD measurement technique, the above mentioned limitations of biosensors also supported the development of MFC as an alternative on-line BOD sensing device. MFC-based BOD sensor is quick,

portable and also contains mixed consortium of microorganisms in the form of biofilm at the anode side, which is capable to oxidize a wide range of substrates (Kim et al. 2003a, Kim et al. 2003b). In recent years, several studies have reported the development of MFC BOD sensor and its certain advantages over other type of microbial biosensors (Kim et al. 2003a, Di Lorenzo et al. 2009, Kumlanghan et al. 2007). However, certain factors that affect its performance have not been addressed explicitly. The main parameters which define the performance of MFC sensor are response time, sensitivity, detection limit, result reproducibility and long-term operational stability. The improvement in sensor design and operating conditions will enhance the performance of the MFC-based BOD sensor. Although fuel cell-based BOD sensor has been developed a decade before (Karube et al. 1977b), a lot of improvement is still required for its practical use and commercialization.

2.9 Advantages of MFC-BOD sensor

2.9.1 Better sensitivity

The sensitivity of any BOD sensor is majorly dependent on the type and size of the biofilm present. It has been observed that sensors with high cell density biofilm could be more sensitive (Liu and Mattiasson 2002). The sensitivity of any MFC-BOD sensor may be determined by the change in an electrical response (in terms of either current or voltage) per amount of biodegradable organic concentration present in the feed in a unit time interval. Sensitivity can be varied with the use of specific kind of substrate. In most of the studies, sensitivity is explained by the linear relationship between BOD concentration and the voltage generated, and based on the linear fit of curve, regression coefficient (r^2) is

determined (Kim et al. 2003a, Di Lorenzo et al. 2009, Moon et al. 2004). Generally, the r^2 values is observed in a range of 0.9 -0.99 when artificial wastewater and domestic wastewater were used as the substrate. This information acknowledges the advantages of MFC-BOD sensors over the other microbial BOD sensors, which are not capable of determining real time sensitivity. Although, MFC-BOD sensor has been observed with good sensitivity against artificial wastewater, it is still less sensitive with real wastewater. Some researchers reported the use of MFC-BOD sensor with real wastewater; however, sensitivity of MFC-BOD sensor was not discussed in detail (Di Lorenzo et al. 2009). Therefore, more research is needed to achieve better sensitivity of MFC-BOD sensor with real wastewater. Pre-treatment or pre-incubation of BOD sensor with the desired substrates could be helpful for increasing its sensitivity.

2.9.2 Substrate versatility

BOD sensors are aimed at being capable to rapidly analyse a sample of complex constituents with relatively low selectivity. Thus, the sensor should respond to all kinds of biodegradable organic solutes in the sample. In order to achieve this scenario, a biological recognition element with high detection capacity for a wide substrate spectrum is needed. The main advantage of MFC-BOD sensors is its versatility for several organic matters (Table 2.3). Since the anodic biofilm is generally developed using a mixture of activated sludge, anaerobic sludge, wastewater and artificial wastewater at the time of inoculation, it contains a rich microbial consortium capable of consuming a broad range of substrate (Holmes et al 2004, Kim et al. 2006). Different kind of sludge may allow versatile microbial species to be present in the biofilm and artificial wastewater may further allow their faster growth. On the other hand, single-microbial-species-based sensor

(Riedel et al 1988, Kim and Kwon, 1999) only have a specific substrate spectrum which disallow them to consume all biodegradable organic matter present in the sample, and subsequently interfere with their accuracy.

2.9.3 Real-time BOD measurement

Real-time or "on-line" BOD monitoring is imperative for the operator of a wastewater treatment plant to continuously monitor the evolution of BOD in effluent samples. It is also important for the process control of biological wastewater treatment systems. For this purpose, MFC-BOD sensor is a much suitable candidate in comparison to other microbial BOD sensors, with a response time of as short as 30 min (Kim et al. 2003a). This suggests that the MFC-BOD sensor would require 30 min for it to produce a new steady-state current after changing the strength of the wastewater, and hence it will be able to detect the BOD of next sample (of unknown BOD value) in next 30 min. In some other studies, BOD sensors have different response times of 60 min (Chang et al. 2004), 36±2 min (Moon et al. 2004) and 4.5 h (Di Lorenzo et al. 2009), and it fluctuated largely based on the measuring range of BOD concentration. Since MFC is a dynamic electrochemical system that is influenced by several physical parameters, it is hard to estimate the exact response time of the sensor. Yet, MFC BOD sensor has the advantages of on-line data documentation and remote data logging.

2.9.4 Long term stability

In order to match the criteria of its commercial use, BOD sensors are required to be of low maintenance cost and long-term stability. However, only few studies have addressed this criterion and reported the long-term stability of their developed BOD sensor. Table 2.3 summarizes most of the studies, which are related to MFC-BOD sensors. It also shows the main features of these studies,

including long-term stability of BOD sensors. However, some studies have not mentioned clearly about the stability of their developed sensor.

Table 2.4: Different design of MFCs with their main features.

MFC Design	Type of Wastewater	Response time	Sensitivity/ Deviation	Detection range	Long term stability	Reference
Mediator less Oligotrophic-type MFC, Pt coated graphite felt as anode and cathode, nafion450 as cation exchange membrane, external resistance of 500 Ω	AWW (glucose and glutamate) and surface water	60 min	10 %	2-10 mg/L (BOD_5)	-	(Moon et al. 2004, Kang et al. 2003)
Mediator less MFC, working 25 ml of anode and cathode volume, nafion, graphite felt and Pt wires, external resistance of 10 Ω	Wastewater from starch processing plant	30 min-10 h	3-12 %	<206 mg/L (BOD_5)	Over 5 years	(Kim et al. 2003a)
MFC based on glass tube bio-film reactor	AWW (glucose and glutamic acid)	6-9 min	-	≥20 mg/L	17 months	(Liu et al. 2013)
Single chamber air exposed MFC, anode volume of 50 ml and 12.6 ml. Nafion117, Pt coated carbon paper as cathode	AWW (glucose) and treated wastewater	40 min	0.53 %	≥ 350 mg/L	Over 7 months	(Di Lorenzo et al. 2009)
Mediator less MFC with working 20 ml of anode and cathode volume, nafion 450, graphite felt and Pt wires, external resistance of 10 Ω	AWW (glucose and glutamic acid), river water	60 min	10 %	≥ 100 mg/L	Over 1 year	(Chang et al. 2004)

Mediator less MFC with working 25 and 5 ml of anode and cathode volume, external 100 and 10 Ω resistance	AWW (glucose and glutamic acid)	5 ± 1 and 36 ± 2 min	-	50 to 100 mg/L	2 years	(Moon et al. 2004)
Submersible MFC, cathode is made of Pt coated carbon paper, nafion117, external resistance of 1000 Ω	DWW	30 min-10 h	-	17-183 mg/L (BOD_5)	-	(Peixoto et al. 2011)
MFC Design	**Type of Wastewater**	**Response time**	**Sensitivity/ Deviation**	**Detection range**	**Long term stability**	**Reference**
MEA based air cathode MFC, Pt coated carbon cloth as cathode, nafion 424, external resistance of 500 Ω	AWW (glucose and glutamic acid	-	4%	50-200 mg/L (BOD_5)	-	(Kim et al. 2009)
MFC with anode (graphite rods) volume of 100 ml and cathode (graphite rolls) volume of 1000 ml, nafion 117, external resistance 50-1200 Ω	AWW (glucose)	10-15 min	7.2 %	≥ 25 mg/L	11 days	(Kumlanghan et al. 2007)
Cation exchange membrane, graphite felt electrode, external resistance of 10 Ω	AWW and DWW	45 min	1.64 %	93-123 mg/L	Over 1 year	(Kim et al. 2003b)
Submergible MFC of 500 ml anode volume, anode and cathode are made of carbon paper, Pt based cathode catalyst, external resistance of 1000 Ω	Artificial ground water (acetate and glucose),	40 min	6-22 %	≥ 250 mg/L	5 months	(Zhang and Angelidaki 2011)

3. Material and Methods

This study was conducted in three main phases, which include development of MFC-BOD sensor, improvement of MFC-BOD sensor performance by the optimization of several parameters and effects of anodic film and other physical conditions in MFC-BOD sensor performance. Therefore, the material and methods used are described categorically, according to the nature of each phase. They are mainly divided into three main sections:

1. Construction and operation of MFC-BOD sensor;
2. Analytical analysis; and
3. Biological analysis.

Different section summarizes the material and methods used in different phases of this study. Construction and operation of MFC-BOD sensor is focused on the design and hardware of MFC reactors and optimization of operational parameters. Analytical analysis mainly includes methods used for the measurement of physical and chemical parameters, while biological analysis section is focussed on the analysis of the anodic biofilm.

3.1 Construction and operation of MFC-BOD Sensor

The MFC-BOD sensor was designed as a single-chambered reactor with an anode, a cathode and a proton exchange membrane sandwiched in between anode and cathode. The construction of MFC-BOD sensors includes four main steps:

3.1.1 Design and construction of MFC reactor frame

In this study, a single-chambered MFC (SCMFC), with an air exposed cathode, was constructed in order to make MFC more compact and simple with reduced cost of operation. An air-cathode MFC, where oxygen present in the air comes in contact of cathode and works as electron acceptor, provides potential advantages over the two-chambered system. Figure 3.1 shows three different designs of the MFC reactors, with differences in their volume and design. The first type of reactor type (Fig .3.1a) consists of a cylindrical chamber 1 cm wide by 6 cm diameter, resulting in an empty volume of 28.3 cm^3. The second type of reactor has similar design as the first type but with a smaller anodic volume of 12.6 cm^3 (Fig. 3.1b). The third type of reactor is rectangular in shape, with dimensions of 4 cm (length) x 2 cm (width) x 0.5 cm (height), and hence has a total anodic volume of 4 ml (Fig. 3.1c). The body of all the MFC reactors is made of acrylic glass sheets.

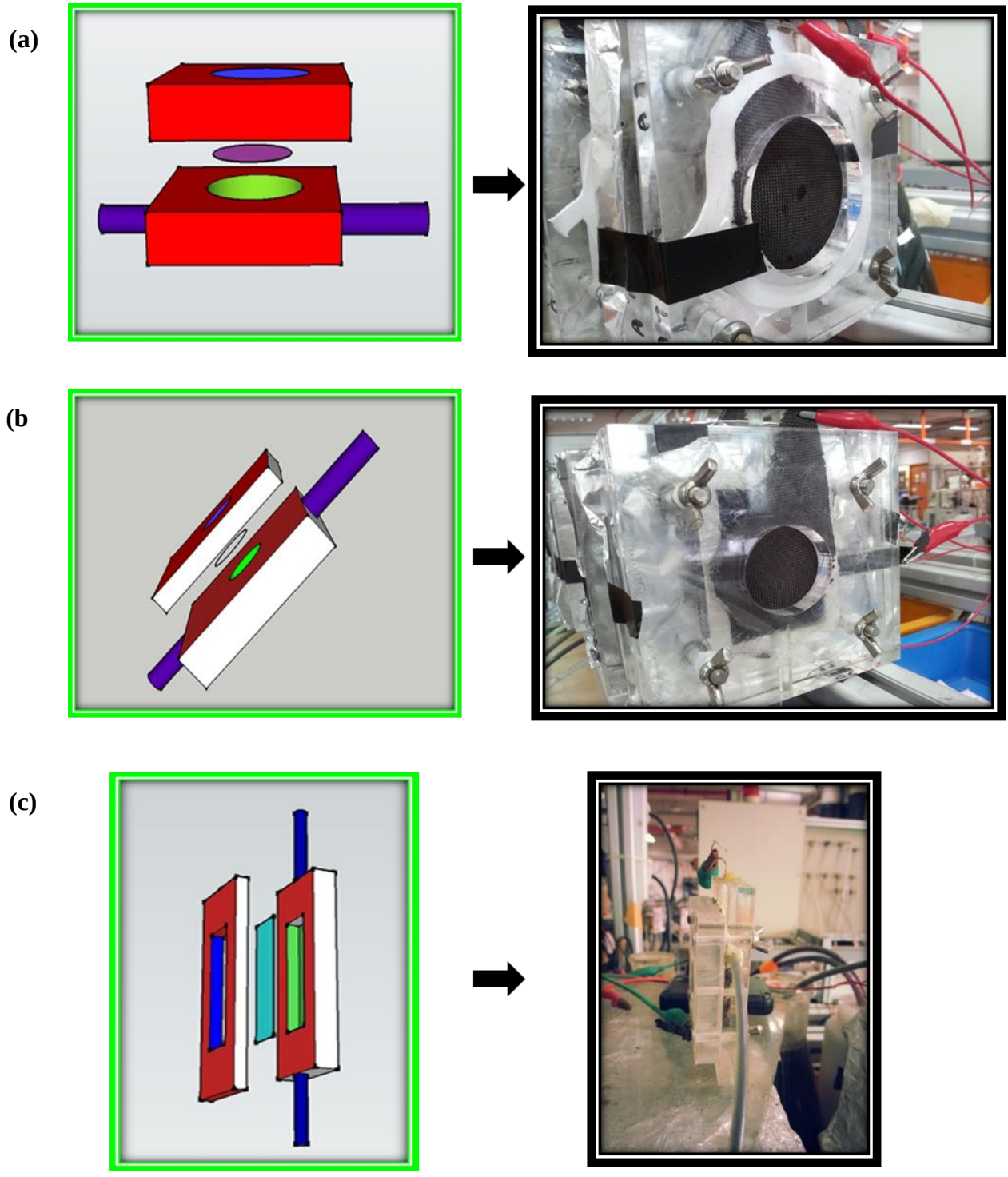

Figure 3.1: Schematic and photograph of different SCMFC used in study. (a) SCMFC in cylindrical shape with anodic volume of 26.3 ml. (b) SCMFC in cylindrical shape with anodic volume of 12.6 ml. (c) SCMFC in rectangular shape with anodic volume of 4 ml.

3.1.2 Fabrication of anode and cathode

Figure 3.2 shows the steps used in the preparation of membrane electrode assembly (MEA) and anode surface. The anode surface was prepared by gluing a piece of hydrophilic plain carbon cloth (non-wet proofed, type B, E-TEK, BASF Fuel Cell, Inc., USA) on top of an acrylic glass. A thin stainless steel wire was threaded into the carbon cloth to serve as a current collector.

Two different types of cathodes catalysts, MnO_2 and Pt, were used in this study. For MnO_2-based catalysts, three configurations (α, β, and γ-MnO_2) based on different preparation methods and crystalline structure, were characterized and investigated by cyclic voltammetry in neutral medium and were incorporated into air-cathode MFCs. Briefly, MnO_2 nanoparticals were mixed with carbon nanotubes as conductive material and polyvinylidene fluoride as binder.

Both the anode and cathode consisted of carbon cloth (wet proof, type B, E-Tek, USA), with the cathode sprayed on one side with MnO_2 ink at a catalyst loading of 3 mg cm^{-2} following the procedure of (Lu et al. 2011). Wet proof treatment at the air-side of cathode was also carried out in order to decrease the adhesion of the water and prevent flooding in the reactor. Polytetrafluoroethylene (PTFE) was used to form the hydrophobic layer due to its binding and hydrophobic nature. Carbon cloth coated with Pt catalyst was purchased (0.5 mg/cm^2, 30% wet proofed, E-TEK, BASF Fuel Cell, Inc., USA), which was coated with PTFE solution (Gashub, Singapore). Cathode cloth was hot pressed at 140^0C under 80 kg cm^{-2} for 90 sec with Nafion117 (DuPont Co., USA) with the catalyst layer at the inner side of the MEA (i.e., facing away from the anode chamber), while the

selemion membrane was just attached (without hot pressing and gluing) to the inner side of the cathode cloth.

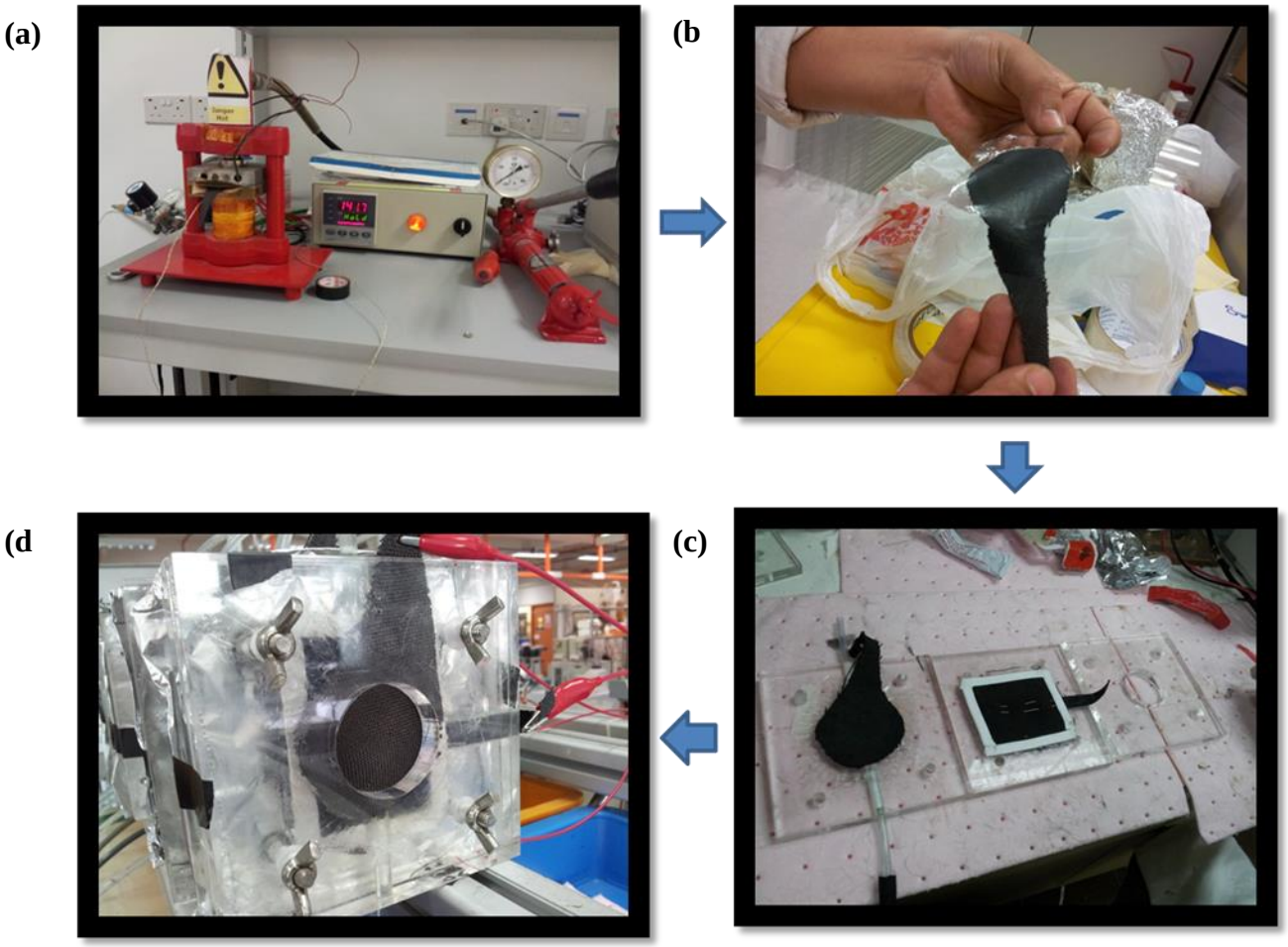

Figure 3.2: Different steps used in the preparation of MEA and assembling of MFC reactor. (a) Hot press equipment set up at 140 ^{0}C and 80 kg cm^{-2}. (b) MEA: hot pressed nafion membrane on cathode electrode after 90 second of hot pressing. (c) Demonstration of different parts of MFC. (d) Assembled MFC reactor.

3.1.3 Set up of MFC-BOD sensor system

Figure 3.3 shows the schematic diagram of the sensor setup, which is consisted of wastewater tank with mechanical stirrer, a feeding pump, (Masterflex 07523-70, Spectra-Teknik Pte Ltd., Singapore), MFC and a digital multimeter connected to a desktop computer. MFC requires microorganisms so that there would be biocatalysis of the substrate oxidation process that will cause a current to flow through the external circuit. However, there are no microbes on the anode when the MFCs are constructed. Hence, the reactors need to be first inoculated with an inoculum so that an electroactive biofilm would be formed on the anode. While several inoculums have been used in other studies, the inoculum used in this study is domestic wastewater (DWW) from the Ulu Pandan Water Reclamation Plant (UPWRP). The wastewater was fed to the reactors at 1.3mL/min for more than a month until a stable voltage was recorded before any experiment was carried out.

Between the experiments, DWW was fed to the MFCs to maintain the biofilm in the reactors. The MFCs were setup at room temperature (between 25 to 30^{o}C), which is suitable for bacteria growth. They were wrapped with aluminium foil to prevent light from entering in order to prevent algae growth in the MFCs. Otherwise, algae could produce oxygen in the anodic compartment and prevent anaerobic conditions.

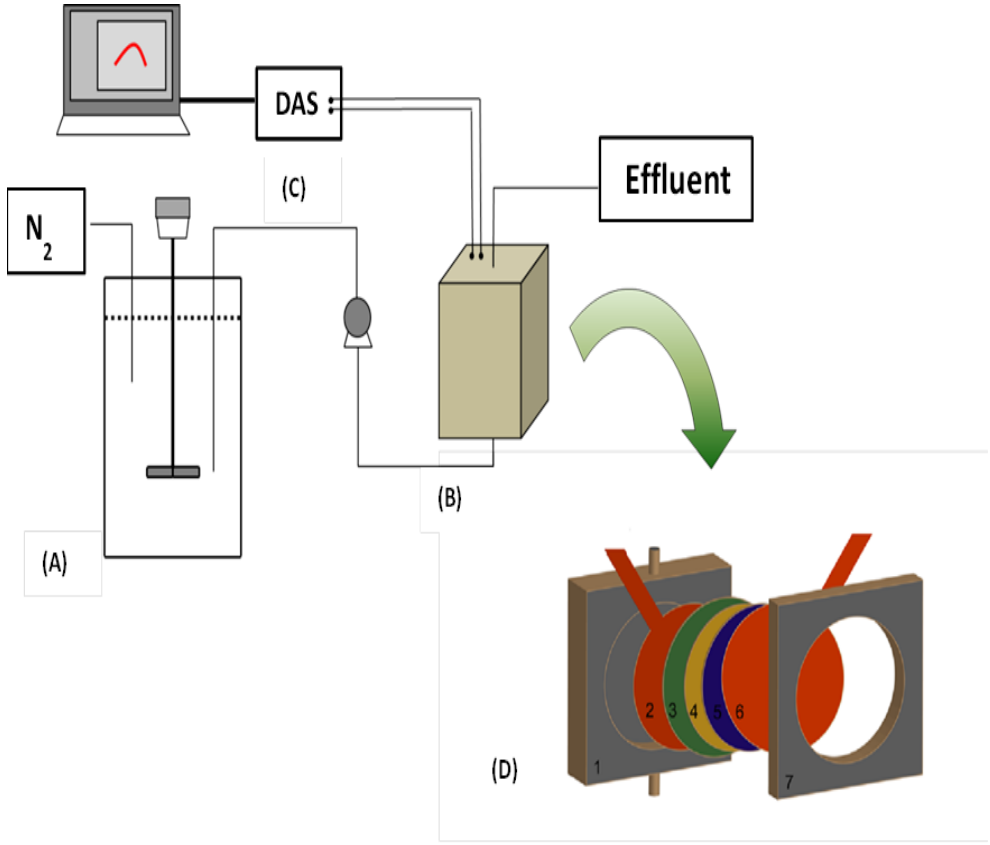

Figure 3.3: Schematic diagram of the microbial fuel cell sensor used in this study. (A) Influent tank. (B) Microbial Fuel cell. (C) Computer and data acquisition system. (D) Details of MFC configuration - 1: MFC body; 2: anode carbon cloth with current collector; 3: Nafion membrane; 4: catalyst layer; 5: carbon base layer; 6: cathode carbon cloth with current collector; and 7: cathode frame.

3.1.4 Feed preparation

3.1.4.1 Domestic wastewater

DWW was used as inoculum for the reactors. The anodic compartments were fed continuously with effluents collected from the primary clarifier of the Ulu Pandan Water Reclamation Plant in Singapore on a weekly basis and then stored in a cold room at temperature of 4^{o}C. Prior to feeding into the continuously stirred feed tank, the effluents was filtered with a fishing net of 0.45-mm pore size to remove bigger particles or solids which was left over from primary clarifier and allowed its temperature to raise naturally to room temperature (between 25 to 30^{o}C). The

filtered wastewater was thus drawn out from feed tank to the MFCs using a pump. The wastewater fed to the MFCs had a pH ranging between 7.0 to 8.0 and an average COD of 310±75 mg/L. In order to use different BOD concentration for the experiments, several dilutions of the DWW was prepared using deionized water. The main characteristics of the DWW are summarized in Table 3.1.

Table 3.1: Main characteristics of the influent DWW.

Wastewater component	Concentration
COD	310.0 ± 75.0 mg/L
TSS	218.5 ± 105.0 mg/L
TDS	110.2 ± 62.3 mg/L
VSS	182.5 ± 76.0 mg/L
pH	7.30 ± 0.4
Conductivity	0.855 ± 0.085 (ms/cm)

3.1.4.2 Artificial wastewater

Synthetic wastewater was made up of nutrient solution, vitamins, minerals, and sodium acetate. The chemical composition of the solutions used is shown in Table 3.2. In order to avoid the early oxidation of sodium acetate in the presence of nutrient solution, both the solutions were kept in separate tanks before they were mixed well and immediately fed to the MFCs. Figure 3.4 shows the actual set-up of the experiment. Sodium acetate was dissolved in deionized water in a feed tank, while nutrient solution was poured into another feed tank. 12.5 ml of each vitamin and mineral solutions per litre of nutrient solution were added into the nutrient

solution feed tank. The solutions were then drawn from the two feed tanks and fed into the influent mixing tank, which was in turn pumped to the MFCs.

Table 3.2: Constituents of nutrient solution of the artificial wastewater used in the experiments.

Nutrient Solution (Oh et al., 2004)		**Trace Minerals (Balch et al., 1979; Lovley & Phillips, 1988)**		**Trace Vitamins (Balch et al., 1979)**	
Compound	**Concentration (mg/L)**	**Compound**	**Concentration (mg/L)**	**Compound**	**Concentration (mg/L)**
$NaHCO_3$	3130	$ALK(SO_4)_2$	10	Biotin	2
NH_4Cl	310	$CaCl_2.2H_2O$	100	Folic Acid	2
$NaH_2PO_4.H_2O$	750	$CoCl_2$	100	Pyridoxine hydrochloride	10
NaH_2PO_4	4220	$CuSO_4.5H_2O$	10	Thiamine hydrochloride	5
Na_2HPO_4	2750	$FeSO_4.7H_2O$	100	Riboflavin	5
KCl	130	H_3BO_4	10	Nicotine acid	5
		$MgSO_4.7H_2O$	3000	DL-Calcium pantothenate	5
		Na_2MoO_4	500	Vitamin B_{12}	0.1
		$Na_2MoO_4.2H_2O$	5	*p*-aminobenzoic acid	5
		NaCl	1000	Lipoic acid	5
		$NiCl_2.6H_2O$	24		
		Nitrilotriacetic Acid	1500		
		$ZnSO_4$	100		

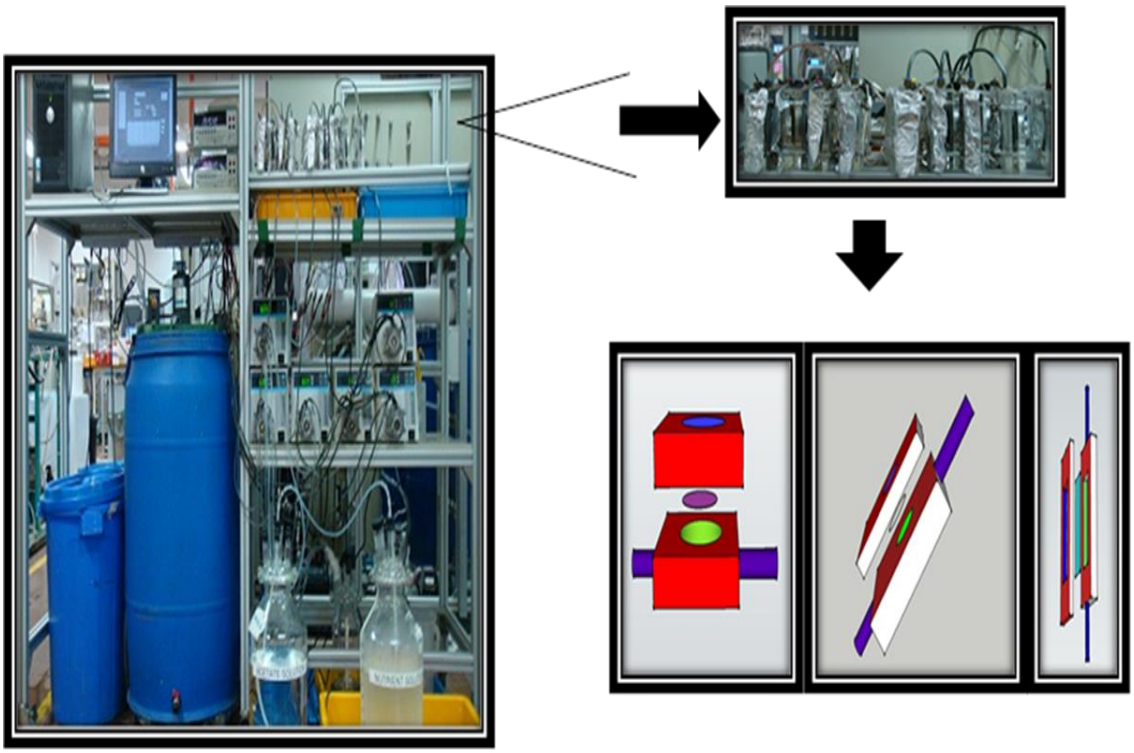

Figure 3.4: Laboratory set up for BOD sensor system with both overview and closer view.

3.1.5 Data collection and electrical performance analysis

3.1.5.1 Voltage measurement and collection

The potential drop across an external resistance was measured using a digital multimeter (M3500A, Array Electronic, Taiwan), which was further recorded into a personal computer through a data acquisition system (PC1604, TTi, RS, Singapore), and exported to Microsoft Excel for analysis.

3.1.5.2 Polarization curves

In order to evaluate the power output of a MFC system, polarization curves were obtained to determine the maximum amount of power that could be generated from the MFC system. At pseudo-steady-state condition, the external resistance

was varied (in certain steps) from high to low resistance. Figure 3.5 shows three different zones categorized in the polarization curve.

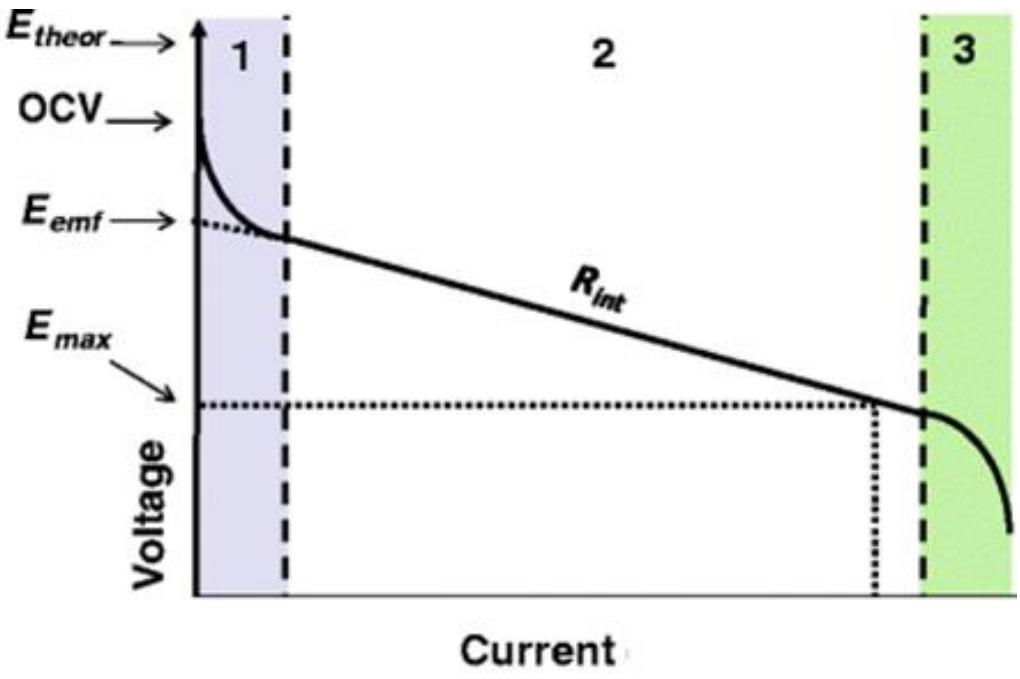

Figure 3.5: Typical polarization curve for an MFC showing the three overpotential zones that affect the cell voltage at increasing current density; 1: activation polarization, 2: ohmic losses, and 3: concentration polarization (Lefebvre et al. 2011).

The characteristics of the three zones are as follows:

1. Starting from the open circuit voltage (OCV) with zero current, the initial steep decrease of voltage is caused by the dominance of activation losses;
2. The voltage decreases at a slower rate and linearly with current due to the dominance of ohmic losses; and
3. Voltage decreases quickly at high current due to the limitation of the mass transport rate of the substrate to the electrode or the transport rate of proton across the membrane.

Using the polarization curve, the internal resistance of the system could be obtained from the slope of the linear curve and can be expressed as:

$$R_{int} = -\frac{\Delta E}{\Delta I} \quad (3.1)$$

The maximum power output could be obtained when R_{ext} was equivalent to R_{int}, and calculated as:

$$P_{max} = -\frac{OCV^{2}}{4R_{int}} \quad (3.2)$$

Polarization curves of the MFCs were obtained by varying the applied external resistance and recording the pseudo-steady-state voltage every minute. The MFC had to be disconnected for several hours before the commencement of the polarization curve experiment, so that it could reach up to the open circuit voltage (OCV). In this study, a broad range of external resistance, from 100 to 10,000 Ω, was applied by decreasing resistance gradually at every 1-min interval.

3.1.5.3 Power Curves

A power curve plots the power (or power density) against current (or current density) using the data obtained from the polarization curve (Fig. 3.6).

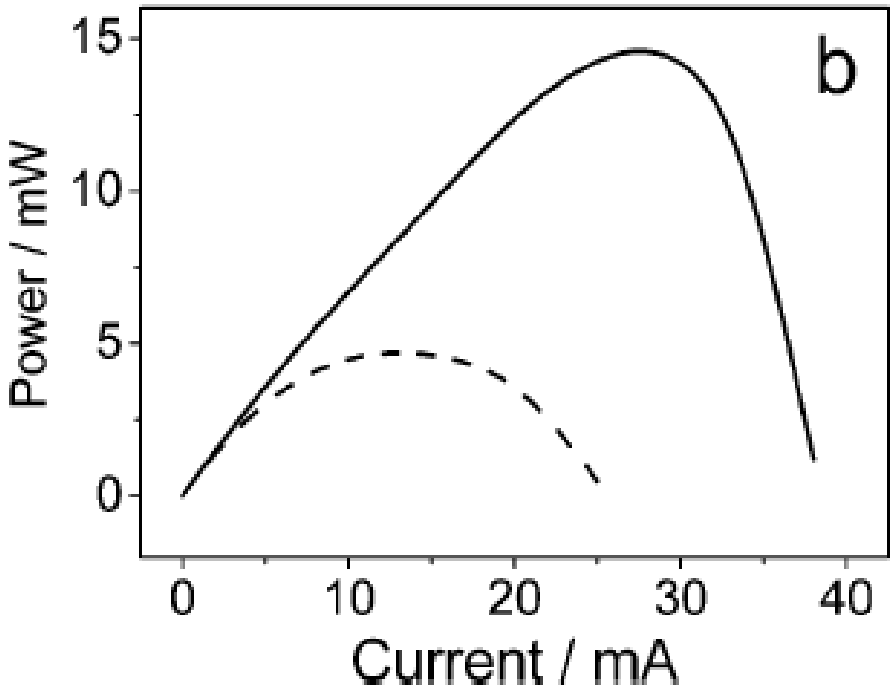

Figure 3.6: Power curves of an actual MFC (solid line); and a mathematically manipulated dataset with additional internal resistance added (dotted line) (Logan et al., 2006).

The curve starts from the origin (no power output in OCV, when no current flows) to a maximum power point. Power output starts decreasing after reaching the maximum power due to increasing ohmic losses and electrode overpotential, and drops till the point of no power production (short circuit).

3.1.5.4 Coulombic efficiency

Although power (current) is generated in MFCs, the amount of power extracted is only a proportion of total amount of stored energy within the metabolized substrate. To determine the coulombic efficiency of the system, the ratio of the number of electrons moving through the external circuit to the theoretical number

of electrons produced from the substrate metabolism is determined. Coulombic efficiency of MFCs in batch mode can be calculated as:

$$\epsilon_C = \frac{M \int_0^{t_b} I \, dt}{Fbv_{An}\Delta COD} \tag{3.3}$$

where *M* is the molecular weight of oxygen (32g/mol), *F* is the Faraday's constant, *b* is the number of electrons needed per mole of oxygen, v_{An} is the liquid volume of the anode chamber and ΔCOD is the change in COD over time.

For continuous flow systems, the coulombic efficiency can be determined based on the current in the steady state as follows

$$\epsilon_C = \frac{MI}{FbQ\Delta COD} \tag{3.4}$$

Where *Q* is the volumetric influent flow rate and ΔCOD is the difference between influent and effluent COD.

3.2 Analytical analysis

3.2.1 Ion concentration

Samples were first filtered through a 0.45-μm pore-sized membrane (GN-6 grid 47-mm, Gelman Science, Pall Corporation, Ann Arbor, Mich.) before measurement. Cations of Na^+, NH_4^+, K^+, Mg^{2+}, Ca^{2+} and anions of F^-, Cl^-, NO^{2-}, NO^{3-}, Br^-, PO_4^{3-}, and SO_4^{2-} was measured using an Ion Chromatogram (DIONEX-500 fitted with GP50 Gradient pump and CD20 conductivity detector) with IonPac CS12A cation and IonPac AS9-HC anion column.

3.2.2 Total suspended solids (TSS) and volatile suspended solids (VSS)

The TSS and VSS were determined according to the Standard Methods (APHA, 2005). An empty porcelain dish is initially weighed (W1). The glass microfiber filters (GF/F, Whatman) were rinsed with 25 mL of distilled water and baked in a furnace (Thermolyne 48000, Omega Medical Scientific) at 550^{o}C for 20 min prior to analysis. The samples were then filtered through the filter to collect the TSS and then dried at 105^{o}C for 1 h. After cooling the porcelain dish in a desiccator, it is reweighed again (W2). The TSS content is calculated as follows:

$$TDS\ (ppm) = \frac{W2-W1}{Volume\ of\ sample} \tag{3.5}$$

In order to determine the VSS, filter with the collected TSS was further heated at 550^{o}C for 20 min and weighed (W_3) after being cooled in the desiccator. The VSS is calculated as follows:

$$VSS\ (ppm) = \frac{W2-W3}{Volume\ of\ sample} \tag{3.6}$$

3.2.3 Conductivity analysis

A conductivity probe (Thermo scientific Orion 4 star, pH – conductivity probe, USA) was used to measure the conductivity of the DWW and acetate. The conductivity probe was calibrated for molar concentration using NaCl.

3.2.4 Acetate concentration

Acetate was analyzed using a gas chromatograph (Shimadzu, AOC-20i) equipped with a FIT detector and a 25 m × 0.32 mm × 0.5μm HP-FFAP column. Samples

were also filtered through a 0.2-μm pore-sized membrane and acidified using formic acid before analysis.

3.2.5 pH

The pH values of the feed and effluent were measured using a pH meter (F-54BW, Horiba Instruments Incorporation, USA) to determine condition for bacteria growth and behaviour of the MFCs.

3.2.6 Chemical oxygen demand

The chemical oxygen demand (COD) of the feed and effluent was measured in accordance to the Standard Methods (APHA, 2005). The samples were filtered through a glass microfiber filter (0.45 μm pore-sized, Whatman, UK) prior to analysis. The percentage of COD removal was calculated as:

$$\frac{COD_{in} - COD_{out}}{COD_{in}} \times 100\% \tag{3.7}$$

where COD_{in} is the influent COD (mg/L) and COD_{out} is the effluent COD (mg/L).

3.2.7 Biochemical oxygen demand

Biochemical oxygen demand (BOD) is an empirical test to provide a measure of the level of degradable organic material in a water sample. The most common dilution method was used to measure BOD_5 in this study. Water sample were filled inside the BOD bottles (300 ml of volume) followed by the initial measurement of dissolved oxygen initially. Subsequently, the bottles were sealed and incubated for a specified time period of 5 days at a constant temperature of 20 ℃ in the dark. The BOD_5 was then computed from the difference between the initial and final readings of dissolved oxygen.

3.2.8 Statistical analysis

The analysis of variance (ANOVA) was used as a statistical analysis tool to examine and interpret the linear model equations obtained during calibration. ANOVA is a simple regression analysis which uses the Fisher's *F*-test and its associated probability to assess the robustness of linear models and overall model significance. "Prob > F" (probability that null hypothesis is correct) less than 0.05 and a large F-value indicate that the model terms are significant.

3.3 Biological analysis

3.3.1 Scanning electron microscopy (SEM)

Anodic biofilm and the PEM surfaces were observed under scanning electron microscope (SEM). The anode cabon cloth and membrane sections were first soaked in a 2.5% Glutaraldehyde solution for 30 min at room temperature (25^{o}C) for fixation. They were then rinsed with ethanol, which was used in an ascending concentration order of 25, 50, 75, 90, and 100%, in order to dehydrate the samples. Prior to observation, the samples were critical-point dried and coated with gold in a sputtering device. An SEM (XL-30-FEG, Philips, Germany) was used to take images of the anodic biofilm and fouled PEM surface.

3.3.2 Fluorescent- in situ hybridisation (FISH)

3.3.2.1 Fixation

FISH analysis was performed in order to check the presence of exo-electrogens in the biofilm. *Geobacter sulfurreducens* was assumed as a representing community of exo-electrogens in anodic biofilm. Biofilm was extracted using PBS buffer carefully, and centrifuged at 12000 rpm to remove the supernatant. The cells were then fixed overnight at 4^{o}C in 750 µl of fresh 4% paraformaldehyde, then washed

three times with 500 µl of 1x PBS. The biomass pellets were then re-suspended in the mixture of 1x PBS and 96 % ethanol (1:1) and stored at deep freezer (-22^{o}C).

3.3.2.2 Hybridization

In-situ hybridization was performed with the FISH probe of *Geobacter sulfurreducens* (termed as "GEO-2"), having a total length of 19mers sequence, which was labelled at 5' end with FITC and CY3 dyes (synthesized by Supernom Pte Ltd). Before the hybridization, 2 ul of the sample (100x dilutions) was applied to polo-L-lysin (0.01 %) coated slides and dried in the air. A volume of 10 µl of hybridization solution (30% deionised formamide + 0.9 M NaCl + 20mM Tris-HCl (pH 7.2)), 0.01 % sodium doecyl sulphate and 50 ng of each fluorescence labelled probe were added to each sample, and the mixture was incubated at 46 ^{0}C for 3 h. The samples were rinsed well with the washing buffer (20mM Tris-HCl (pH 7.2), 0.01 % sodium doecyl sulphate, 20 mM NaCl) and incubated in the washing buffer at 48 ^{0}C for 20 min. The samples were then stained with DAPI solution (6.25ug/ml) for 3 min before rinsing with the sterile water and air dry. Finally, the samples were covered with a fade retardant (VECTASHIELD vector Laboratories, Inc) prior to apply a glass cover slip on it.

3.3.2.3 Epi-fluroscence microscope investigation

The capture-ready sample slide was then viewed under an epi-fluroscence microscope (Olympus BX51) connected to a PC, and the digital image capture and analysis were performed using DP manager, version 3.3.1.222 (Olympus Corp.). The images bonding with DAPI, EUB338 (FITC) and ARC915 (CY-3) were captured under the wideband of UV, blue and green excitation, respective. DAPI images represent the whole microbe communities within the objective field, while the images with two specific probes show the individual cell distribution in

the communities separately. The abundance and intensity of signals indicate the corresponding community structure.

3.3.3 Flow cytometric analysis

To determine the viability of the culture, cells were stained using the LIVE/DEAD BacLight (Molecular Probes, Eugene/Portland, OR) using the procedure described previously (Sachidanandham et al. 2005). *E. coli* cells and scrapped out biofilm were grown in 30 ml of Luria-Bertani broth medium (DifcoTM, Becton Dickinson, MD, USA) broth using 50-ml culture tubes, and kept inside a shaker incubator at 150 rpm at 37^{o}C. The cells of exponential phase (4 h of incubation) and early stationary phage (15 h of incubation) were taken out and 1ml of each sample was transferred into 1.5-ml micro-centrifuge tubes. The culture was then stained with 0.5 µl of SYTO9 and 5 µl of propidium iodide (PI). After vortexing the stained cell suspension, it was incubated at 30℃ in the dark for 25-30 min. The suspension was then washed twice in PBS buffer and centrifuged for 10 min at 4000g. The pellet was re-suspended in PBS buffer for flow cytometry analysis. For making control, cells were killed either by 30 min of incubation using 20% (vv-^{1}) allyl alcohol (Sigma-Aldrich Chemical Co., St. Louis, MO, USA) solution or by autoclaving cells at 121^{o}C for 20 min, followed by staining. For the former case, allyl alcohol was later removed by washing the cells twice with PBS and centrifuged for 10 min at 4000g. Since the autoclaving method was found to be more effective and convenient, it was followed for killing the cells in later experiments.

4. Development of MFC-BOD Sensor

4.1 Introduction

In the recent years, microbial fuel cell (MFC) has been examined as an alternative BOD sensing device (Kim et al 2003, kang et al 2003). MFC-based BOD sensors are quick, portable and also contain a mixed population of microorganisms capable to oxidize a wide range of substrates (Kim et al. 2003a; Kim et al. 2003b). Yet the design and operation conditions as reported in the literature are suboptimal, consisting of two-chambered MFC systems (Kumlanghan et al. 2007; Moon et al. 2004) functioning in batch mode (Chang et al. 2004; Chang et al. 2005; Pandit et al. 2012). For the operator of a wastewater treatment plant, to continuously monitor the evolution of BOD in effluent samples, a continuous "on-line' system is needed. Furthermore, the use of single-chambered MFCs should be preferred as these are easier and cheaper to operate than their two-chambered counterparts, mostly because the cathode can directly be exposed to ambient air as a free and sustainable source of oxygen.

In MFCs, the electron acceptor is one of the critical components, which affects the performance of MFCs dramatically. Many electron acceptors with high redox potential such as ferricyanide (Oh and Logan 2006) and permanganate (You et al. 2006) have been tested to maximize the electricity generation in MFCs, but the usage of these high-energy catholyte materials is not sustainable or cost effective. Nitrate and nitrite are also good candidates for their potential application in wastewater treatment process which have been tested in laboratory-scale MFCs, yielding good treatment efficiency but relatively lower electricity performance (Lefebvre et al. 2008, Virdis et al. 2010). Comparing with other electron acceptors,

oxygen has been reported as one of the most suitable candidates, which is sustainable, cost effective and scalable for practical applications (Logan 2008). However, due to the slow reaction kinetics of oxygen reduction reaction (ORR), different electrocatalysts were externally used to increase the rate of cathodic reactions. Therefore, another source of improvement for MFC sensors consists in the choice of an affordable and sustainable cathode catalyst.

So far, most sensors reported in the literature have made use of expensive platinum (Pt) (Di Lorenzo et al. 2009; Kang et al. 2003; Kim et al. 2009) as cathode catalyst. However, considering its high cost and low durability due to corrosion and degradation of catalytic activity over time (Shao et al. 2009), alternative metal catalysts such as indium/tin (Chhina et al. 2006), cobalt (Lefebvre et al. 2009), titanium (Ekström et al. 2007), tungsten (Maiyalagan and Viswanathan 2008) or manganese (Lu et al. 2011) should be sought.

This phase of the research was aimed to explore an affordable and sustainable cathode catalyst for better cathodic reactions, and subsequently better performance of MFC. Keeping this in mind, the efficacy of manganese dioxide (MnO_2) as a catalyst for the oxygen reduction reaction was tested. Manganese oxide is a representative metal oxide that has been studied as a promising alternative electrocatalyst for ORR, and has been tested in air-cathode fuel cells recently (Li et al. 2010, Zhang et al. 2009a, Roche et al. 2010, Cheng et al. 2010**,** Roche and Scott 2009). ORR has been widely investigated by electrochemical methods for different applications, and multiple mechanisms have been proposed (Roche and Scott 2009, Zhang et al. 2007, Lima et al. 2006, Roche et al. 2008). It has been shown that oxygen is reduced to hydroxide (OH^-) through a dual pathway, consisting of competition between 1) the four-electrons mechanism, and 2) a

partial reduction with two electrons yielding hydrogen peroxide ions (HO_2^-) followed by either a 2-electrons reduction or a disproportionation reaction of HO_2^- in solution (Mao et al. 2003). However, in these studies, the electrolytes reported were mostly acidic or alkaline, which was reasonable for the applications in fuel cells and metal-air batteries but not suitable for MFCs. To our knowledge, neutral electrolyte for air-cathode MFCs was rarely reported till now (Zhang et al. 2009a, Roche and Scott 2009). In this study, catalytic capabilities of three different configurations of MnO_2 (α, β, and γ-MnO_2) based on different preparation methods in neutral medium and crystalline structure were characterized and investigated with their use as catalyst in air-cathode MFCs.

4.2 Performance of MnO_2-catalyst based MFC

The performance of MFCs was determined with DWW, which was reported to produce nearly 30% power of that can be produced by artificial wastewater (sodium acetate solution) with similar reactor designs (Liu et al. 2004, Liu et al. 2005). The performance order of MFCs with different catalysts was found to be Pt > β > γ > α-MnO_2 as illustrated in Table 4.1 and Fig. 4.1. The MFC performance showed that β-MnO_2-catalyst-based-cathode MFC generated comparable amount of power with that using Pt catalyst considering the lower cost of catalyst. Comparing with the Pt-based MFCs, β-MnO_2-based MFCs with a loading of 3 mg/cm^2 produced the maximum power of 0.277 mW. In addition, the value reached up to 64.1% of the maximum power density for the Pt-based MFCs, which was almost the value of 64.2% reported recently (Zhang et al. 2009a, Zhang et al. 2009b). The internal resistance of β-MnO_2-based MFCs measured was even lower than that of Pt-based MFCs and the COD removal efficiency of β-MnO_2-based MFCs was slightly higher than that of Pt-based MFCs. Comparing with the

other previous reported study of similar kind, the maximum power output for our β-MnO_2-based MFC was found higher than the β-MnO_2-based cubic MFC (0.277 vs. 0.198 mW) (Zhang et al. 2009a). However, since total anode area (1.15x 10^{-3} m^2) reported by Zhang et al. 2009 was lower than the total anode area (2.83 x 10^{-3} m^2) reported in our study, the maximum power density in our study was found lower (97.8 vs. 172 mW/m^2).

Table 4.1: Summary of air-cathode MFC performances with different cathode catalysts.

Catalysts	**Electromotive Force (V)**	**Open Circuit Voltage**	**Internal Resistance (Ω)**	**Maximum Power (mW)**	**Maximum Power Density**	**COD Removal Efficiency**
α-MnO_2	0.36	0.425	540	0.063	22.1	**84.1**
β-MnO_2	0.427	0.473	165	0.277	97.8	**84.8**
γ-MnO_2	0.400	0.470	172	0.234	82.6	**83.8**
Pt	**0.632**	**0.664**	**234**	**0.432**	**152.7**	**81.6**

This was the first case where domestic wastewater was applied to examine the performance of MnO_2-based catalysts in MFCs to our knowledge.

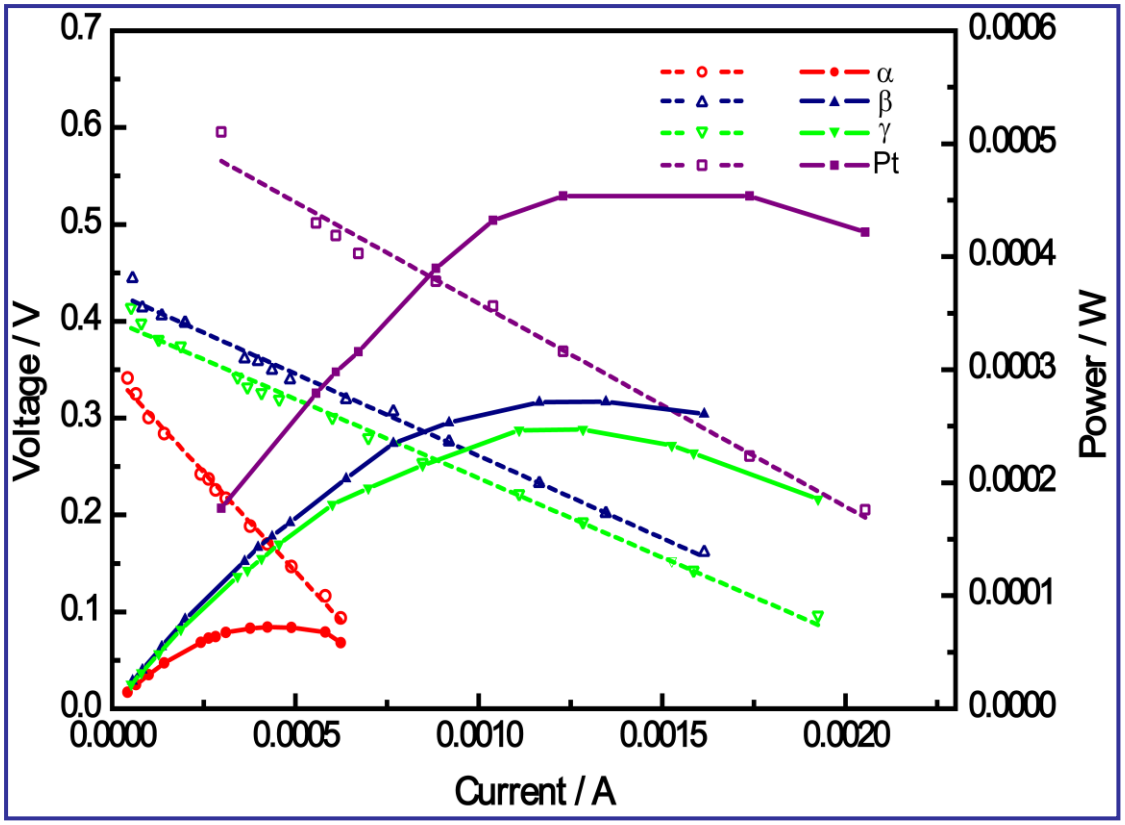

Figure 4.1: Polarization and power curves for air-cathode MFCs respectively on Day 11 when MFCs have reached their performance stabilization. Cell voltage (E) data were collected by data acquisition system across different external resistance (R_{ex}), and current and the power was calculated using R_{ex} and E. Voltage and power were plotted as the functions of the current to make polarization and power curves respectively. The dash lines with empty symbols were polarization curves and the solid lines with close symbols were for power curves. α: α-MnO_2 based catalyst; β: β-MnO_2 based catalyst; γ: γ-MnO_2 based catalyst; Pt: Pt based catalyst.

4.3 Exploring MnO_2-based MFCs as BOD sensor

Results showed that β-MnO_2- and γ-MnO_2-based MFCs were able to produce high power with domestic wastewater mainly because of low internal resistance. Considering the economic aspect besides their reasonable performance, this kind of design and configuration of MFC could be promising for its use as BOD sensor in future. Motivated with the performance of β-MnO_2 and γ-MnO_2-based MFCs, they were further explored as BOD sensor.

4.3.1 HRT optimization and response time determination

A good sensor should provide a strong signal (in this case, voltage output) and a quick response time. For this purpose, the operating conditions (in terms of HRT) were optimized. In order to avoid the variability of DWW and achieve better repeatability, sodium acetate solution was used at a fixed BOD_5 concentration of 386 ± 10 mg/L. Figure 4.2 shows the variations in the maximum steady-state voltage generated by the MFC-BOD sensors at different HRT, obtained by varying the flow rate from 0.6 to 1.1 ml/min. The range of HRT tested varied between 26 and 47 min with β-MnO_2, and between 31 and 47 min with γ-MnO_2. For both types of catalyst, the voltage generally increased with decreasing HRT, indicating that the signal became stronger and therefore, that the sensor was more sensitive. A maximum steady-state voltage of 23.1 mV was obtained with β-MnO_2 at a HRT of 28 min (equivalent to a flow rate of 1.1 ml/min) and further decrease in HRT did not increase the maximum steady-state voltage beyond that value. With γ-MnO_2, a maximum steady-state voltage of 20.5 mV was achieved at an HRT of 33 min (equivalent to a feed flow rate of 0.85 ml/min). A HRT of around 30 min could therefore be considered as being optimal, and was selected for the rest of the experiments.

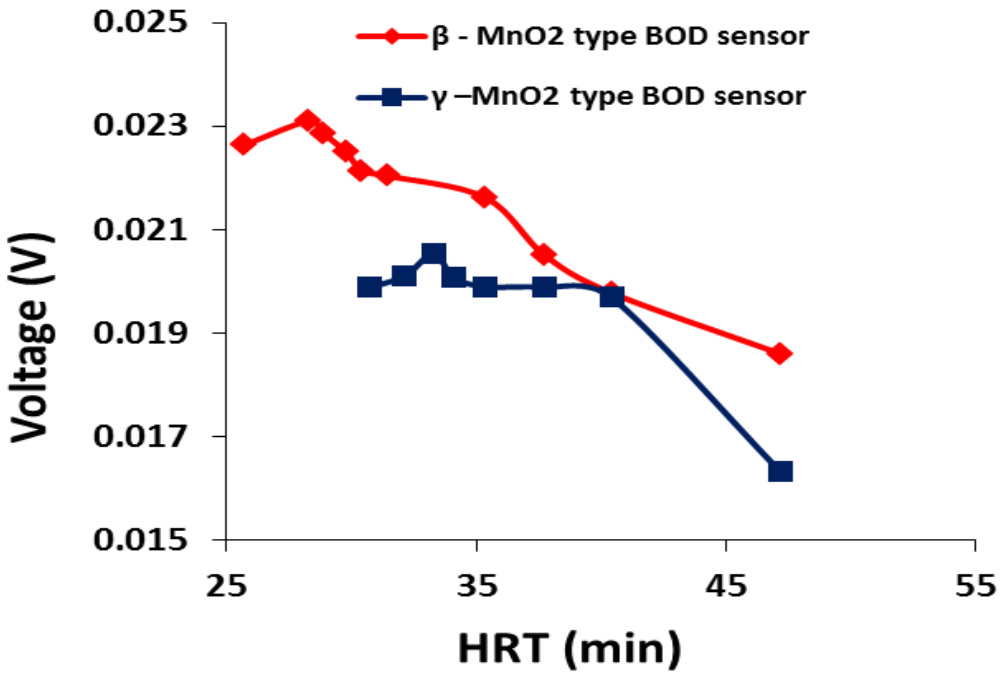

Figure 4.2: Optimization of HRT for the β-and γ–MnO_2 type MFC BOD biosensors.

The observation of increasing maximum steady-state voltage with decreasing HRT (i.e., increasing feed flow rate) illustrated the effect of mass transfer rates, which increased at lower HRT and were accompanied by increasing electrochemical activity of the biofilm. Lower HRT also allowed the limiting substrate condition inside the anode chamber, and the substrate utilization happened in accordance with the first-order reaction kinetics, abiding the Monod equation.This result was in accordance with the findings of Di Lorenzo et al. (2009), who reported that the dynamic response of MFC sensors became faster at lower HRT. It also showed that microorganisms in the MFC sensor were capable of handling high organic loading rates and translated them into a higher voltage. Furthermore, a shorter HRT allowed the bulk liquid in the MFCs to be replaced more rapidly, which could help in reducing the response time.

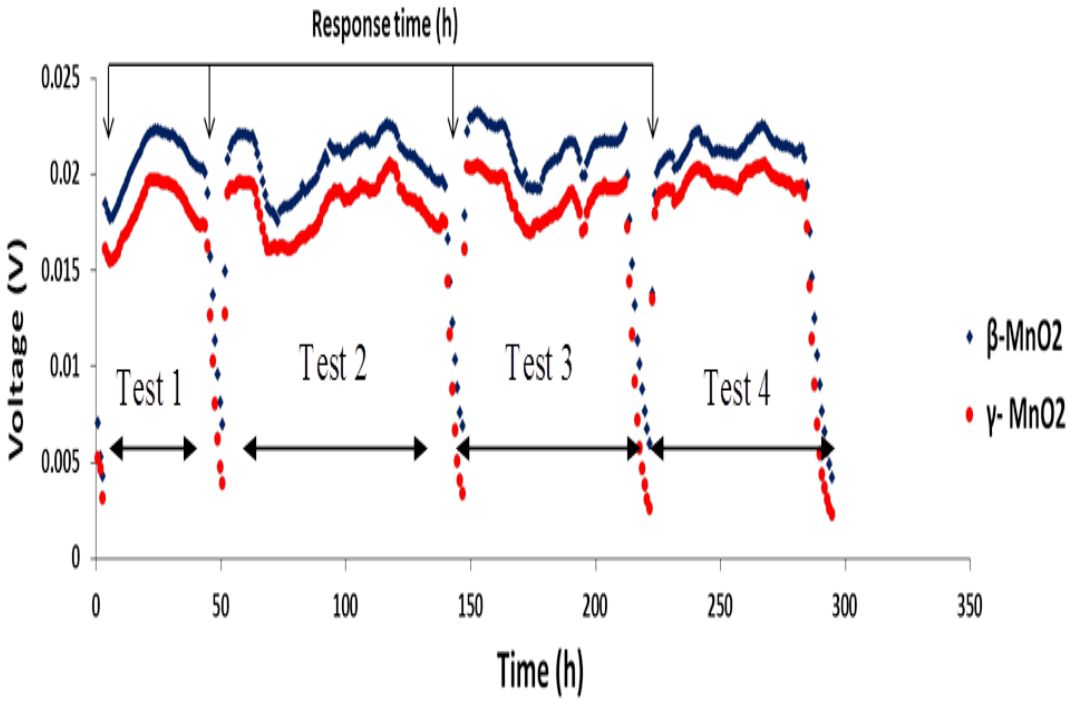

Figure 4.3: Demonstration of voltage pattern over time and estimation of response time for the β-and γ–MnO_2 type MFC BOD biosensors. Every data point represents the time interval of 1 h.

The shortest response time of the MFC was determined with sodium acetate by alternating the phases of feeding and starvation periods and monitoring the time taken for the voltage output to reach a stable value (Fig. 4.3). The response times of the MFC-BOD sensors over 4 consecutive tests were obtained with sodium acetate at the optimized HRT of 30 min, and were found similar for both types of sensors, in the range of 2-3 h.

4.4 MFC-BOD sensor calibration

4.4.1 Impact of the catalyst

The response of MFC-BOD sensor was measured in terms of voltage generation. A calibration of steady-state voltage versus BOD_5 (44– 483 mg/L) was conducted with an external load of 10 Ω, which was able to give the fastest response at the time change in voltage due to the change in BOD concentration. Figures 4.4a and b show the dynamic response of the β-MnO_2-MFC-BOD sensor against different inlet BOD_5 concentrations.

The MFC-BOD sensors were fed with AWW containing different concentrations of BOD_5, until the maximum steady voltage was generated. Afterwards, they were starved till the voltage dropped to the value of 0.0015 ± 0.005 V, followed by feeding with a new feed solution of a different BOD concentration. In order to get a reliable maximum voltage at different BOD concentration, all the experiments were done in duplicate. The reproducibility of the response was found good.

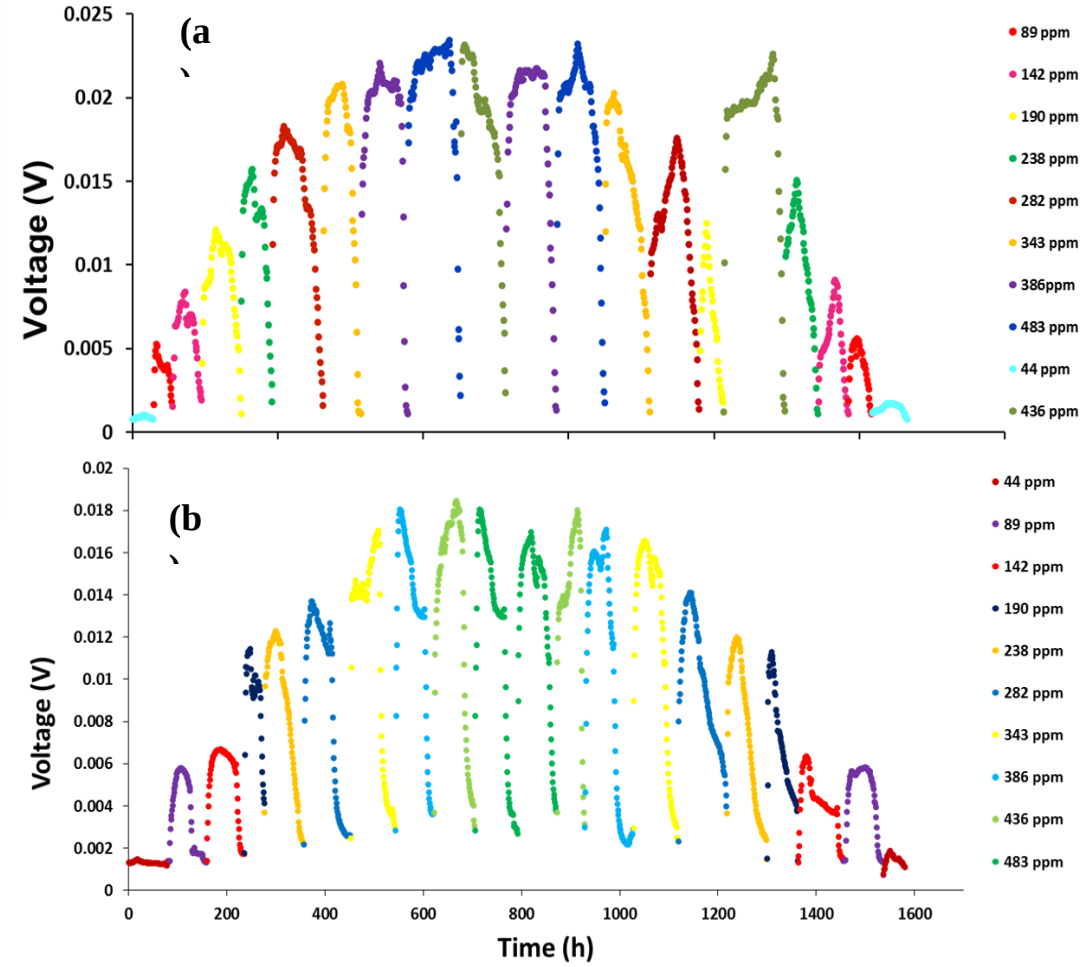

Figure 4.4: Dynamic response of β -MnO_2 type BOD sensor in terms of voltage for a broad range of BOD concentration of 44-483 ppm. (a) Dynamic response after 3 months of sensor operation. (b) Dynamic response after 1 year of sensor operation.

Similar experiment was done with γ-MnO_2-MFC-BOD sensor. BOD_5 concentration was varied from 44- 483 mg/L, with an increment of 50 mg/L for each time (Figs. 4.5a and b). The MFC-BOD sensors were again allowed to be fed with feed solution of a specific BOD_5, until the maximum steady voltage was generated. Afterwards, they were starved till the voltage dropped to the value of 0.0015 ±0.005 V, followed by feeding of a new feed solution with different BOD concentration.

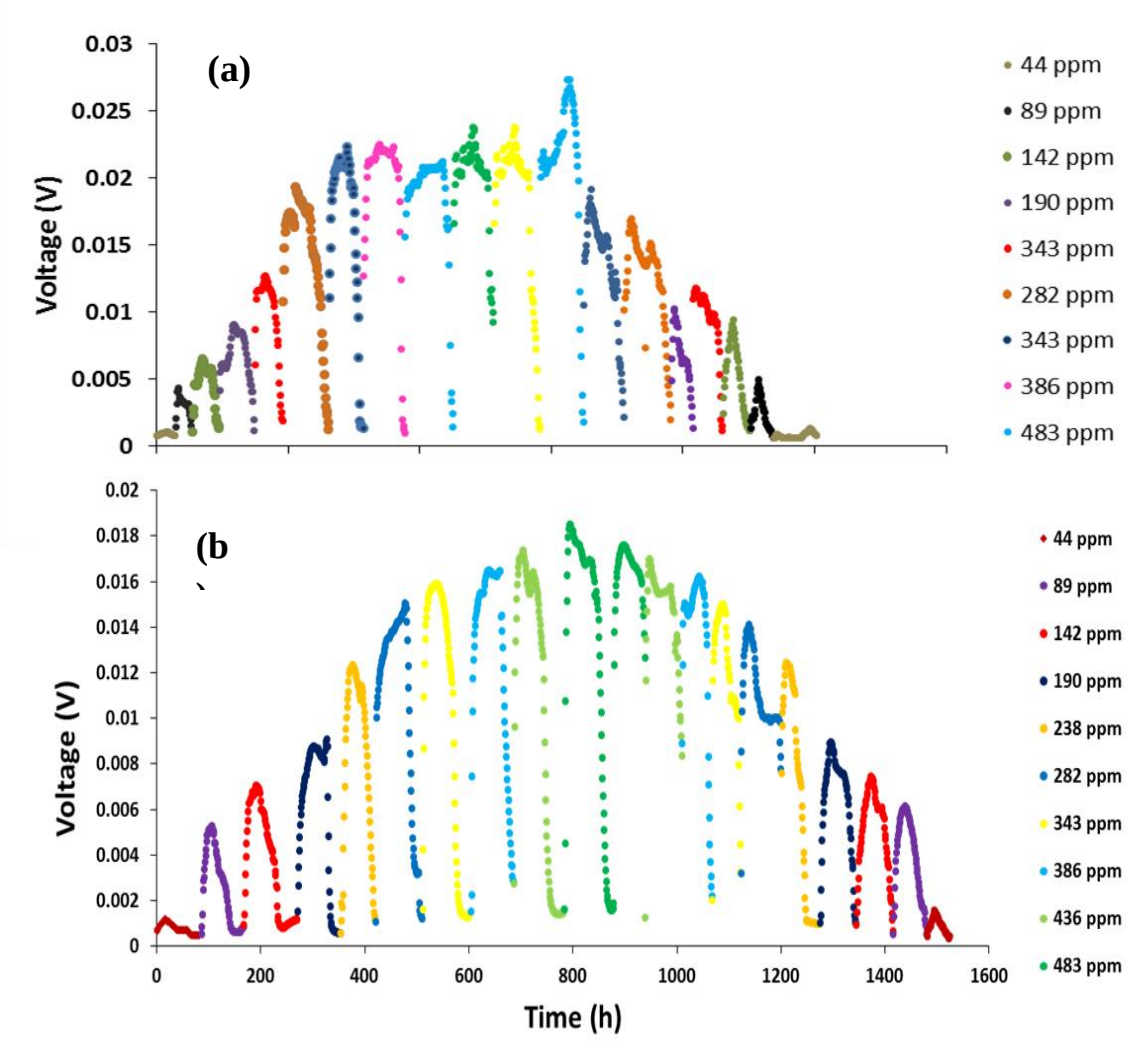

Figure 4.5: Dynamic response of γ-MnO_2 type BOD sensor in terms of voltage for a broad range of BOD concentration of 44-483 ppm. (a) Dynamic response after 3 months of sensor operation. (b) Dynamic response after 1 year of sensor operation.

Figures 4.6a and b show the calibration results with sodium acetate at different BOD_5 concentrations, ranging from 44-483 mg/L, after 3 months of operation. A linear-relationship was obtained between the BOD_5 and the maximum steady-state voltage as long as the BOD_5 concentration remained in the range of 44-343 mg/L. The r^2 value was high, at 0.99 and 0.97 for the β- and γ-MnO_2, respectively. The reproducibility of the sensor response was found better with β-MnO_2 (standard deviation of 0.05%) than with γ-MnO_2 (standard deviation of 0.22%). The

statistical significance of the model equations and the adequacy of models were verified by ANOVA. As shown in Table 4.2, the *F*-values were 511 and 236 for the β- and γ-MnO_2-based-MFC-BOD biosensor, respectively, implying that the model was significant. Additionally, the value of "Prob > *F*" remained below 0.05, indicating that the model terms were significant at a 95% level of confidence. In both types of MFC-BOD sensor, a good relationship was obtained between the voltage output and the BOD_5, indicating reliable performance and calibration. However, in terms of reproducibility, the β-MnO_2-MFC-BOD sensor performed better than the γ-MnO_2-MFC-BOD sensor.

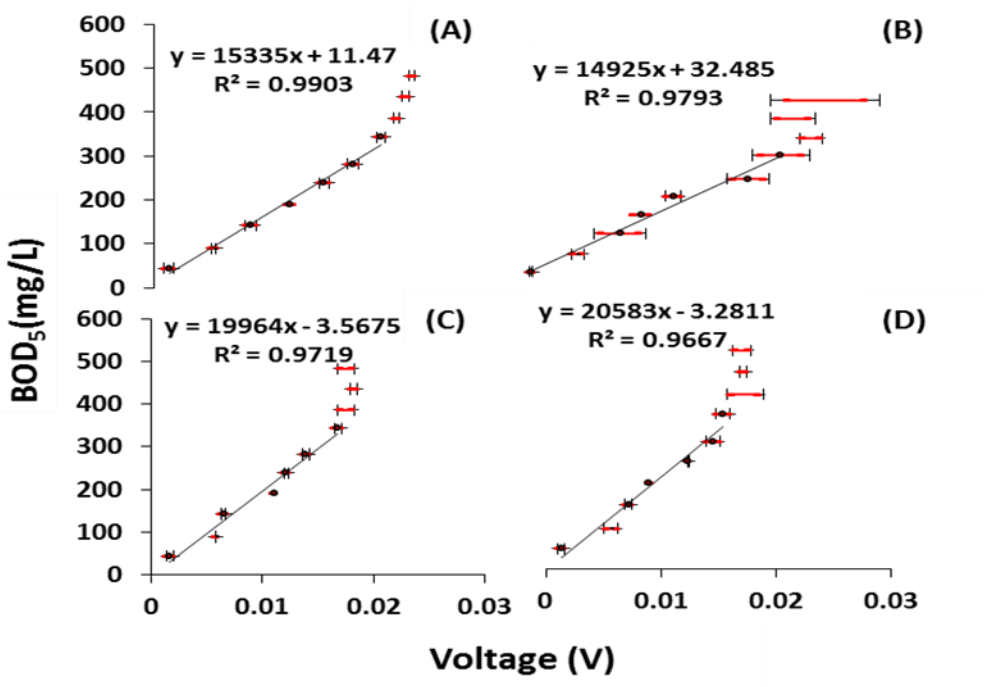

Figure 4.6: Dynamic response of the MFC BOD biosensors against organic concentration in sodium acetate solution at different time interval. (A) and (B) show a linear-relationship between maximum steady-state voltage generated and BOD_5 of the β- and γ-MnO_2 type MFC BOD biosensors, respectively, after 3 months. (C) and (D) demonstrate the same type of linear- relationship after 1 year.

In the previous study, it has been shown that β-MnO_2 yielded the best performance, as assessed by cyclic voltammetry and confirmed by actual MFC experiments (Lu et al. 2011). Nevertheless, the performance of γ-MnO_2 was good

enough that we decided to assess its efficacy in a BOD sensor. The present study confirmed the superiority of β-MnO_2-MFC-BOD sensors over γ-MnO_2-MFC-BOD sensors in terms of sensitivity and stability over time. This can be explained by the different crystallographic structures of β- and γ-MnO_2 catalysts. Indeed, β-MnO_2 presents a homogeneous nano-rod structure, while γ-MnO_2 forms fine needles, dispersed in clusters around carbon nanotubes (Lu et al. 2011). The improved structure of the former is likely to allow for better adsorption of O_2 on its surface and overall higher catalytic activity. In our sensor, this translated into a stronger and more stable signal. This is in accordance with other studies that have correlated the higher catalytic activity of β-MnO_2 to its higher average oxidation state, as compared to γ-MnO_2 (Zhang et al. 2009b). The linear relationship between voltage (indicating bacterial growth) and BOD_5 (indicating substrate concentration) of both MFC-BOD sensors followed the Monod' kinetics, showing a good linearity when BOD_5 is a limiting factor and deviating from lineratiy when BOD_5 is high and not a limiting factor.

4.4.2 Performance with real wastewater

One of the main goals of this study is to provide the operators of wastewater treatment plants with an efficient and sustainable BOD sensor. For this purpose, it is essential to assess the MFC-BOD sensor performance not only with synthetic feed but also with real DWW. The calibration with DWW was done both with β- and γ-MnO_2 after 6 months of operation (Fig. 4.7). In those conditions, a linear-relationship between the voltage output and the BOD_5 concentration was again obtained, confirming the results obtained with synthetic substrate. Figures 4.7a and b show a linear-relationship between the BOD_5 concentration (ranging from 36−178 mg/L) and the maximum steady-state voltage with r^2 values of 0.98 and

0.96, and *F*-value of 360 and 209 for β- and γ-MnO_2, respectively. Additionally, the very low value of model parameter, "prob >*F*", indicated that the model was statistically significant.

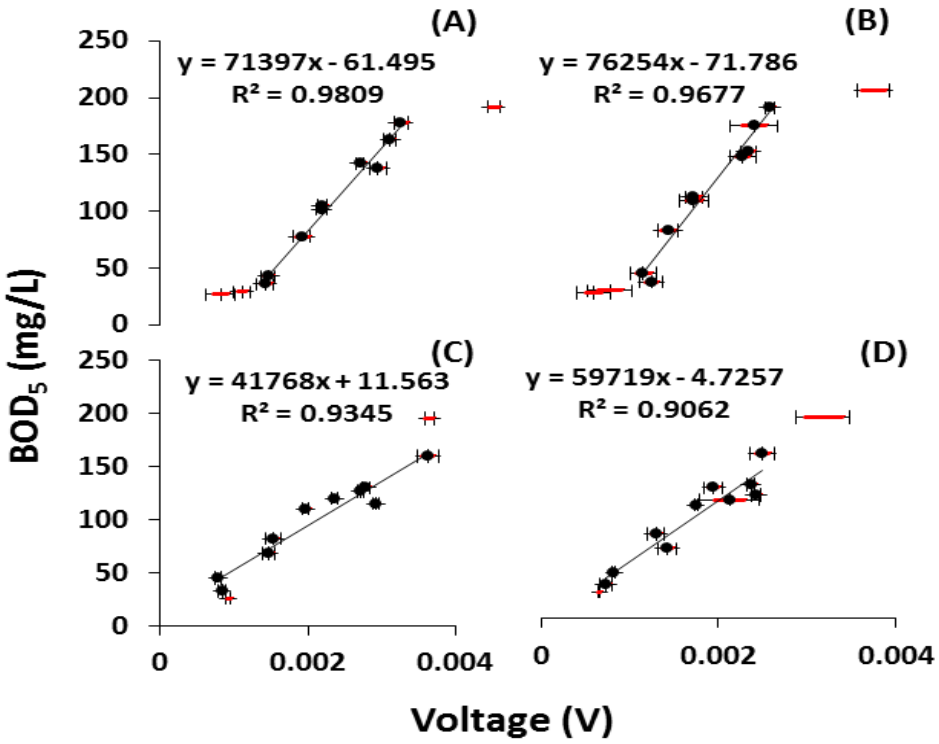

Figure 4.7: Dynamic response of MFC BOD biosensors against organic concentration in DWW. (A) and (B) show linear- relationship between independent variable (maximum voltage) and dependent variable (BOD_5) of the β-and γ-MnO_2 type MFC BOD sensors respectively, after 6 months. (C) and (D) demonstrate the same type of relationship after 1.5 years.

It is a well-known fact that simple substrates like acetate are more readily assimilable at the anode of an MFC than complex effluents, leading to higher coulombic recoveries (Lefebvre et al. 2009). This can explain the lower mass transfer rates with DWW, which led to slightly reduced sensitivity; nevertheless, a good linear-relationship was established with DWW too, at a BOD_5 ranging between 33 and 172 mg/L, making our sensor applicable for practical use.

4.4.3 Long term stability

The performance of the sensors was determined again under the same conditions after 1 year with sodium acetate and 1.5 year with DWW. Figures 4.7c and d show again a good linear relationship, obtained with sodium acetate within a BOD range of 44-343 mg/L, with r^2 value of 0.97 (*F*-value of 173) and 0.96 (*F*-value of 145), for β- and γ-MnO_2, respectively. Repeatability of the sensors was still good with a standard deviation of 0.075% and 0.16 %, for β- and γ-MnO_2, respectively. These results were again supported and confirmed by the performance check using DWW with BOD_5 ranging from 33-160 mg/L. The regression coefficient, r^2, remained high at 0.93 and 0.90 (F-value of 114 and 77), respectively, with β- and γ-MnO_2 (Figure 4.7c and d).

These results show that over a long time period of 1 to 1.5 years, the voltage generated by both the β- and γ-MnO_2-MFC-BOD sensors eventually decreased, probably due to changes in biofilm composition, biofouling on the proton exchange membrane (Xu et al. 2012) and decreased catalyst activity (Rismani-Yazdi et al. 2008). Kim et al. (2003) reported that their MFC-BOD sensor remained stable for 5 years, but provided little evidence to support their claim. In particular, re-calibration was not addressed. In this study, we noticed that re-calibration is one of the critical factors that affected the performance of sensor, and it was definitely required after 1 year; however, the exact frequency of re-calibration should be evaluated, in order to maintain a good proportionality between BOD_5 and the recorded voltage at all times.

4.5 Compliance of predicted BOD values (BODp) with BOD_5

The compliance of the BOD_5 values as predicted by the MFC-BOD sensors (BODp) with BOD_5 was determined using 5 random samples of DWW after 1.5

years, using the calibration curves obtained at that time. Figure 4.8 plots the BODp values measured with β- and γ-MnO_2 against BOD_5 for all the five DWW samples. The BOD_5 of the 5 samples ranged from 56 to 155 mg/L, with a standard deviation comprised between 14-27%. For both types of catalyst, a good correlation was obtained between BOD_5 and BODp; yet, the standard deviation obtained with β-MnO_2 (3-12%) was lower than that of γ-MnO_2 (8-21%). Nevertheless, these standard deviations of BOD sensors remained lower than that of BOD_5, therefore showing the improved reliability of the sensors over conventional BOD_5 method, especially when β-MnO_2 was used as the catalyst.

Results also showed that for higher BOD value (>150 mg/L), the MFC-BOD sensors had a tendency to slightly overestimate the BOD. Yet, the compliance was extremely good at the lower BOD range (between 50 and 100 mg/L), which corresponds to the typical BOD of treated effluents from a wastewater treatment plant. This, along with good accuracy, result reproducibility, fast response time and ability to measure BOD continuously emphasizes the suitability of the MFC-BOD sensor developed in this study for application in wastewater treatment plants.

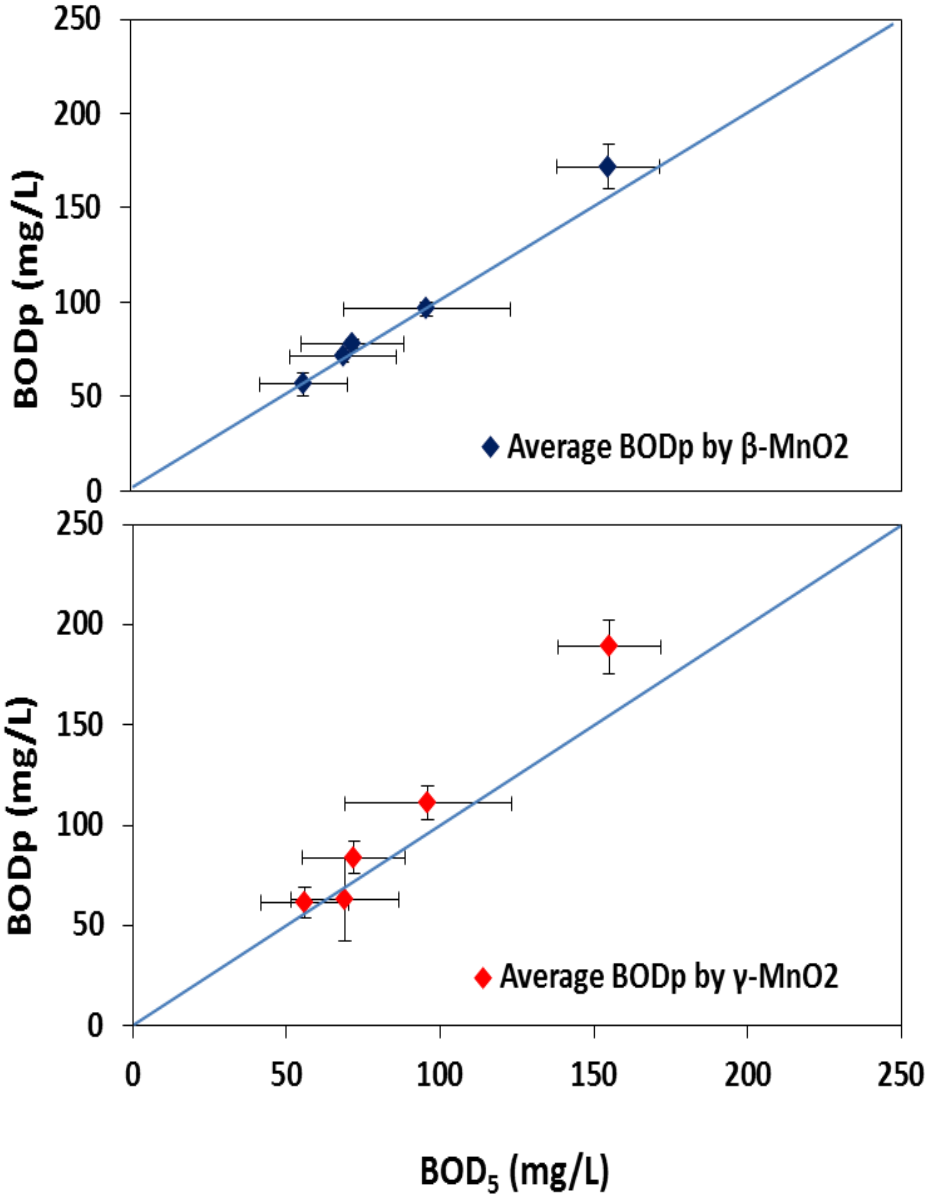

Figure 4.8: Variation between BODp by the β-and γ–MnO_2 type BOD sensors and BOD_5 measured with conventional 5-day BOD method.

4.6 Summary

This comprehensive study demonstrated the development of an on-line MFC-BOD sensor system based on an inexpensive and innovative catalyst, and tested its performance for a long time interval to minimize the production and

maintenance cost. Table 4.2 summarizes the overall performance of MFC-BOD sensors developed in this study.

Table 4.2: Overall performance shown by β-and γ –MnO2 type MFC BOD sensor for linear regression between the voltage and BOD concentrations.

Type of Sensor	Time period	Type of wastewater	Range of Organic concentration measured (ppm)	*R* Square	*F* - Value	Prob > *F*
β- MnO_2	3 months	AWW	44-343	0.990	511	3.14E-06
β- MnO_2	6 months	DWW	36-178	0.980	360	2.28E-07
β- MnO_2	1 year	AWW	44-343	0.971	173	4.55E-05
β-MnO_2	1.5 years	DWW	33-160	0.934	114	5.18E-06
ϒ- MnO_2	3 months	AWW	44-343	0.979	236	2.12E-05
ϒ- MnO_2	6 months	DWW	36-178	0.967	209	1.79E-06
ϒ- MnO_2	1 year	AWW	44-343	0.966	145	6.93E-05
ϒ- MnO_2	1.5 years	DWW	33-160	0.906	77	2.20E-05

Main conclusions of this study are summarized as below:

- This study is first to use MnO_2 catalyst (in place of expensive Pt catalyst) for MFCs applied as an on-line BOD sensor. Good linear-relationship between the voltage generated by the MFC-BOD sensor and BOD_5 (ranging from 44-483 mg/L, using sodium acetate solution), reasonable performance with DWW (BOD_5 ranging from 36-178 mg/L and 33-160 mg/L), fast response time of 2-3 h, stable performance after more than 1.5 years of operation, and good result reproducibility demonstrated the potential of these MFCs as BOD biosensor.
- The influence of HRT on the performance of the MFC-BOD sensors was first optimized. Several HRT were examined by changing the flow rate, and HRT

of 28 min and 33 min were found as the optimal HRT for the β- and γ-MnO_2-MFC-BOD sensors, respectively. Both type of MFC-BOD sensors showed fair sensitivity probably due to the low HRT.

- The applicability of MFC-BOD sensors was verified with real DWW and both the β- and γ-MnO_2-type-MFC-BOD biosensors exhibited good performance with a regression coefficient of r^2 of 0.93 and 0.90, respectively after 1.5 years.
- The β-MnO_2-type-MFC-BOD sensors exhibited an impressive performance by establishing a close compliance between BODp and BOD_5 with slight variations of only ± 3 to 12%.
- Inexpensive manufacturing and maintenance cost, and reliable operational stability of MnO_2-type-BOD-MFC sensors indicate their potential to substitute the conventional BOD_5 methods, which takes longer analytical time of 5 days and suffers from huge variability. However, sensor's performance still needs to be improved in terms of response time and sensitivity.

5. Sequential Optimization of MFC-BOD Sensor

5.1 Introduction

The performance of MFC-BOD sensors can be influenced by various parameters, such as response time, detection limit, linearity of the calibration curve, etc. As described earlier, the response time of any sensor can be defined as the time taken by a sensor to approach its true output when subjected to an input. In the case of MFC-BOD sensor, the response time was described as the time required to reach 95% of the steady-state voltage for a fixed organic concentration (Moon et al, 2004). However, this definition is applicable for any specific organic concentration. In the steady-state mode, response time can rather be defined as the time taken to reach a new steady- state. It may vary with the change in concentration of feed. Therefore, in practice, the response time of any continuous system should be the time taken by sensor to reach 95% value of the maximum output from its baseline output.

For the practical use of BOD sensor, a broad organic concentration range with reliable and accurate measurement is desirable. The MFC-BOD sensor claims to measure a wide substrate range and higher detection limit, because of using mixed microbial consortium in anodic biofilm. However, either very low or very high concentration of organics hampers the accuracy of sensor. In order to monitor the effluent discharge from any industrial plant, BOD sensor should also be sensitive to lower BOD_5 concentrations.

Optimization of a BOD sensor is a complex task, since often the improvement of one parameter leads to impairing of another one. Keeping this in mind, a

sequential optimization approach was applied for achieving better performance of the MFC-BOD sensor. Sequential optimization approach dealt with the use of several combinations based on the HRT and design of the MFC-BOD sensor (Table 5.1). With the concept of varying one parameter at any one time, while keeping other parameters unchanged, the MFC-BOD sensor was calibrated for achieving lower response time and higher sensitivity (especially for the lower range of BOD_5 concentration).

Table 5.1: Sequential optimization approach for better performance of BOD sensor.

Study	Varied parameter/ MFC constituent	Fixed parameters / MFC constituent
HRT based	HRT	Volume, PEM, cathode catalyst, anode material
Volume based	Anodic volume	HRT, PEM, cathode catalyst, anode material
Membrane based	PEM	HRT, volume, cathode catalyst, anode material
Cathode based	Cathode catalyst	HRT, volume, PEM, anode material
Anode based	Anode material	HRT, volume, PEM, cathode catalyst

In Chapter 4, the performance of both β- and γ-MnO_2-MFC-BOD sensor were examined, and based on these results, β-MnO_2 was chosen as the catalyst for further optimization studies.

5.2 HRT optimization

A decrease in the HRT (or increase in flow rate) may cause an increase in the biofilm's electrochemical activity due to higher mass transfer rates (Di Lorenzo et al, 2009). Subsequently, increased mass transfer rate may accelerate the response of bacteria exposed to a given feed concentration. Although the HRT was optimized in chapter 4, it needed to be re-optimized due to the reasons listed below:

1) One of the main concerns for estimating HRT in chapter 4 was to achieve a strong output signal (in terms of voltage) in the sensor, along with high mass transfer rate. However, the role of HRT in determining BOD_5 removal rate was not considered at that time. It was learned later that the BOD removal rate could also be a decisive parameter for determining the performance of the MFC-BOD sensor. Lower BOD_5 removal rate indicates the measurement of the "true" influent BOD_5 concentration, which is the desired BOD_5 measurement. However, theoretically, higher HRT causes higher removal of BOD_5, which does not provide the measurement of the "true" influent BOD_5 concentration (Logan, 2008). Therefore, HRT was re-optimized to decrease the BOD_5 removal rate.

2) In chapter 4, the time taken for the MFC-BOD sensors to reach the maximum steady-state voltage (with HRT of 28.3 min) was still high and inconsistent. Therefore, the assumption was made that lowering the HRT might help lower the response time by increasing the electrochemical activity of microorganisms.

For achieving low BOD_5 removal rate, several HRT were tried and the BOD_5 removal rate was measured. Figure 5.1 shows that the BOD_5 removal rate decreased with increasing HRT. It was observed that a HRT of 28.3 min removed

85% of BOD_5 in the influent feed, while HRT of 1 and 2 min decreased the BOD_5 removal efficiency up to 6%. Considering the higher voltage signal obtained with 2-min HRT as compared to 1 min, future experiments were carried out at a HRT of 2 min.

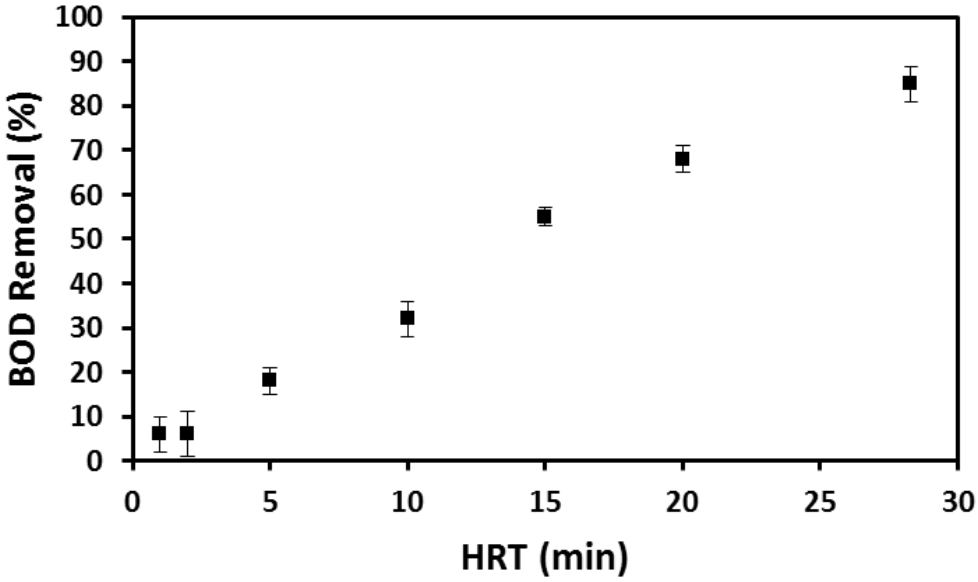

Figure 5.1: BOD_5 removal efficiency at different HRT.

Figure 5.2 shows the voltage profile produced by the MFC-BOD sensor operated at a HRT of 2 min. Different BOD_5 concentrations were applied and the time required to achieve the maximum steady-state voltage was measured. Feed was changed at after certain time interval (around 7 h) to induce a different BOD concentration. It was observed that the response time, at the time of up-shift of substrate concentration, lowered drastically; however, it lowered gradually during the down-shift of substrate concentration. The same trend was also observed by Di Lorenzo et al. (2009) and Moon et al. (2004).

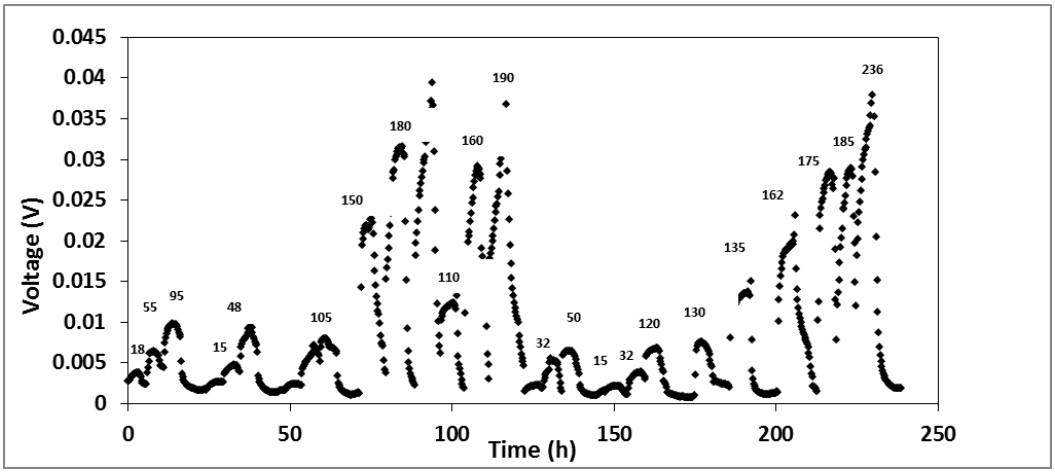

Figure 5.2: Voltage pattern at different BOD_5 concentration at HRT of 2 min.

Figure 5.3 shows the comparison of the time required to produce the maximum steady-state voltage at the HRT of 2 min and HRT of 28.3 min. It was observed that the time lowered from 5-26 h (at the HRT 28.3 min) to 2-4 h (at the HRT 2 min) for different BOD_5 concentration. Faster mass transfer rate and higher electrochemical activity of microorganisms at a short HRT helped to lower the response time of sensor. These results were supported by Di Lorenzo et al. (2009) and Moon et al. (2004), who observed the decrease in COD removal rates by increasing the flow rate or reducing the HRT.

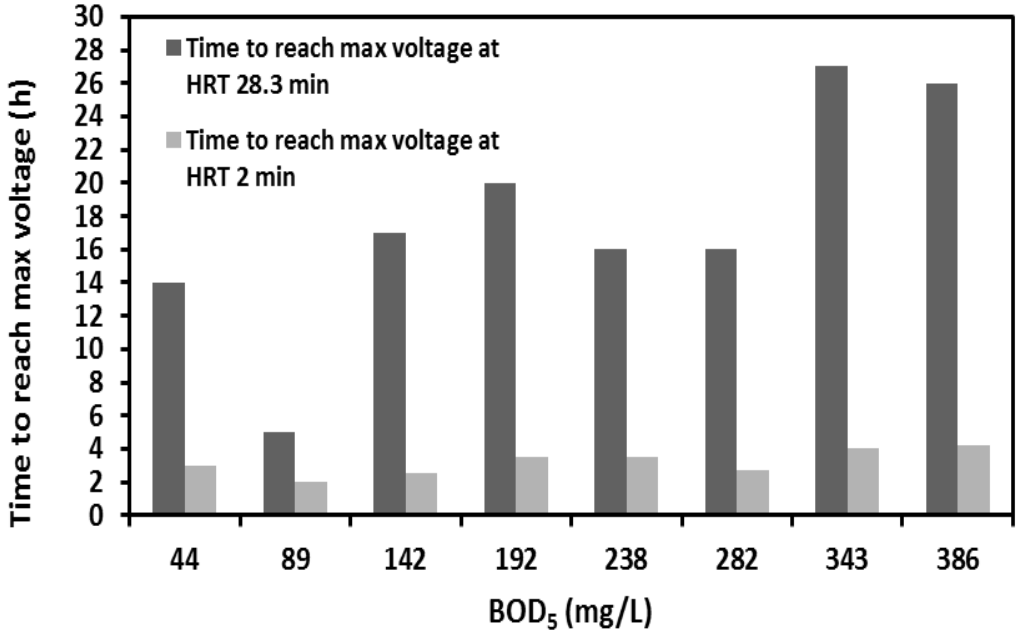

Figure5.3: Time to reach maximum steady state voltage at different HRT.

5.2.1 Sensor performance with AWW at HRT of 2 min

The response time of the MFC-BOD sensor was decreased, however, was still inconsistent against different substrate concentration (in a range of 2-4 h) at a HRT of 2 min. Therefore, with the aim of checking the MFC-BOD sensor's performance at any fixed time interval, instead of waiting for the time to reach the maximum steady-state voltage, the voltage was recorded at the exact time period of 30, 60, 90 and 120 min. The voltage recorded at that time period were calibrated against different BOD_5 concentration of AWW, ranging from 8-236 mg/L. Figure 5.4 shows a linear calibration relationship between the generated voltage at different time interval (30, 60, 90 and 120) and BOD concentration. BOD_5 concentration above 236 mg/L was found to be non-linear with the produced voltage. This pattern abided the Monod Kinetics, showing a non-linear microbial growth (indicated by voltage) when substrate (BOD_5) is high and a non-limiting factor. For BOD_5 concentration $\leq$ 236 mg/L, the linear calibration

relationship clearly indicated good performance of MFC-BOD sensor even at the time interval of 30 min (R^2=0.95), showing quicker response of the MFC-BOD sensor against influent BOD concentration.

A positive change in BOD_5 concentration was associated with a positive change in voltage. Steeper slope indicated that a greater rate of change in BOD_5 concentration could be reflected by a small change in the voltage. This rate of change in voltage with respect to the change in BOD_5 determined the sensitivity of the MFC-BOD sensor. The change in the slope was only around 6% over a specific time period (30 to 120 min). This change noticeably indicated that the sensitivity of MFC-BOD sensor did not change much over time.

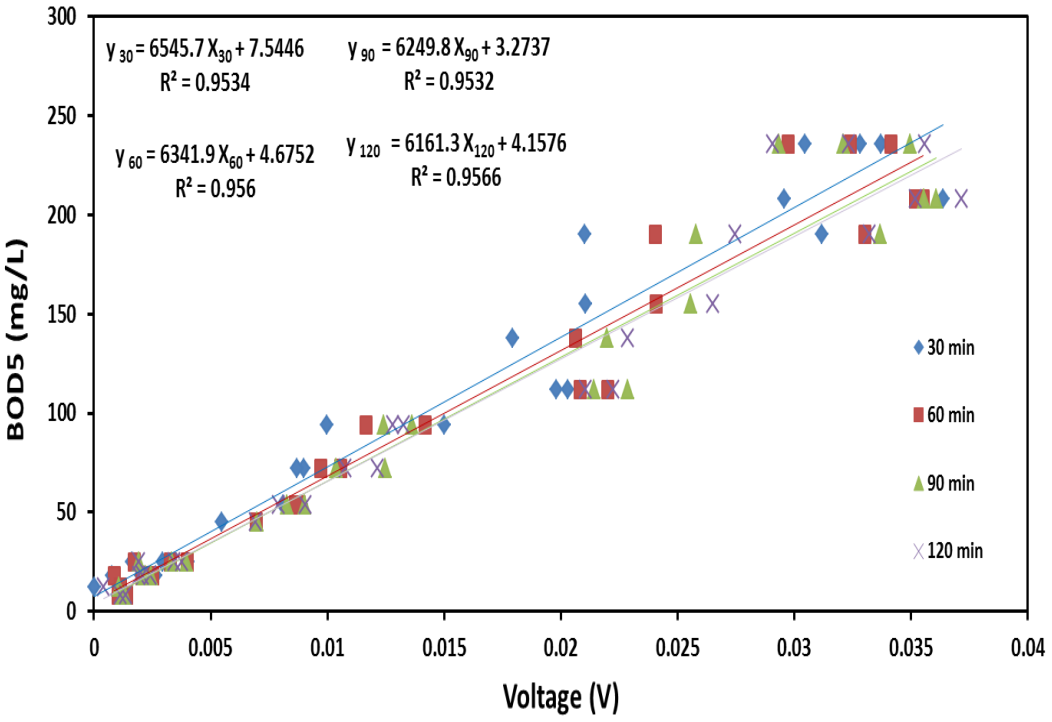

Figure 5.4: Linear calibration between BOD_5 (using AWW) and voltage recorded at different time interval for MFC-BOD sensors with a HRT of 2 min.

5.2.2 MFC-BOD sensor performance with DWW at HRT of 2 min

In the later phase of this study, the performance of the MFC-BOD sensor at a HRT of 2 min was measured with DWW. A linear calibration relationship was established between BOD_5 concentration ranging from 13-121 mg/L and the voltage generated at time interval of 30, 60, 90 and 120 min (Fig. 5.5).

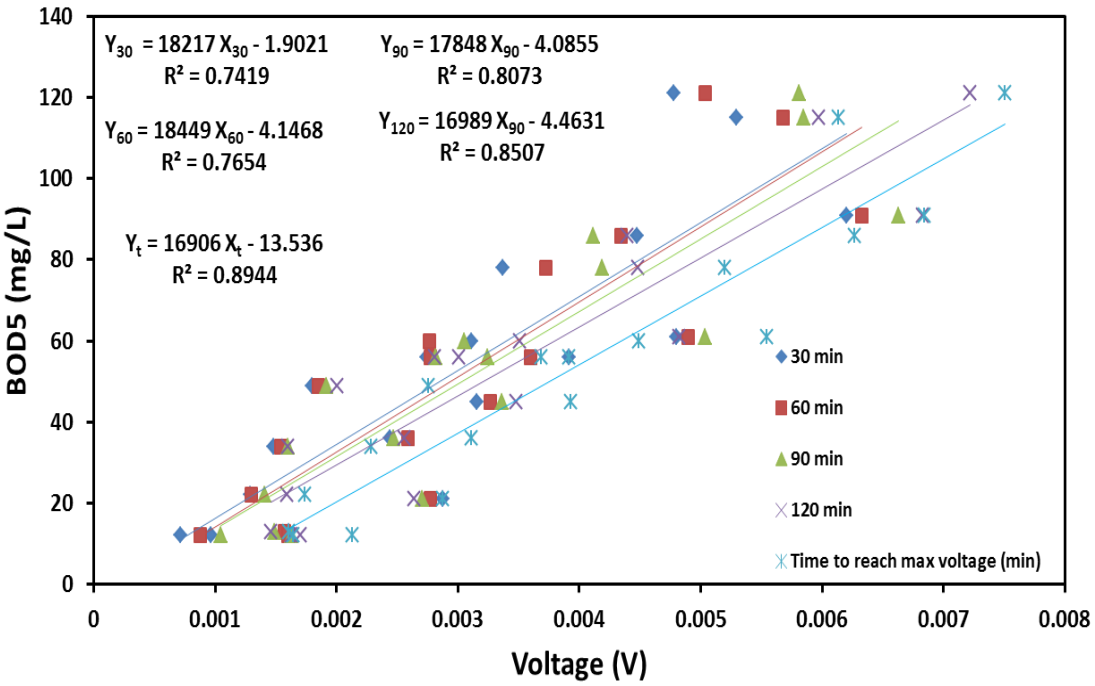

Figure 5.5: Linear calibration between BOD_5 (using DWW) and voltage recorded at different time interval for MFC-BOD sensors with a HRT of 2 min.

In Figure 5.5, the terms "Y_t" and "X_t" were used to demonstrate a linear relationship that which was established for the maximum steady-state voltage. Poorer performance of MFC-BOD sensor with DWW was indicated by lower regression coefficient; however, the sensitivity of sensor did not change much over the time period. Complex composition of the DWW, unlike easily biodegradable substrate in the AWW, was the probable reason behind the poorer performance of the MFC-BOD sensor. This trend was also confirmed by Di

Lorenzo et al. (2009), who observed lower regression coefficient of R^2=0.93 with DWW in comparison to R^2=0.97 with with AWW.

Summary of HRT-based-optimization is shown in Table 5.2. It clearly indicated that 2-min HRT was able to enhance the performance of BOD sensor with improved response time and sensitivity. Therefore, further studies were carried out using this HRT.

Table 5.2: Summary of HRT-based optimization.

Parameter	**Features**	
	HRT 28.3 min	***HRT 2min***
Volume	28.3 ml	28.3 ml
PEM	Nafion	Nafion
Cathode catalyst	β- MnO_2	β- MnO_2
BOD removal	85 %	6 %
Response time	Varied from 5-27 h	Varied from 0.5-2 h
Detection limit	BOD concentration range was 44-343 mg/L	BOD concentration range was 8-236 mg/L
Linearity	Regression coefficient was high (R^2=0.98). However, response time was high and fewer samples were used.	Regression coefficient was comparable (R^2=0.95) considering lower response time, higher detection range, and more number of samples.
Sensitivity	-	± 6 %

5.3 Optimization of MFC-BOD sensor volume

Scaling down the volume of a MFC-BOD sensor reduces non-ideal flow and induces plug flow inside the reactor, which helps voltage or current to respond linearly to the change in BOD concentration (Moon et al., 2004). Therefore, MFC-BOD sensors with three different volumes - 28.3 (described earlier in chapter 4), 12.6 and 4 ml were examined. The design and construction of all the three MFC-BOD sensors have been discussed in chapter 3 (Fig. 3.1). The produced voltage profile of the MFC-BOD sensor having an anodic volume of 12.6 ml showed that the MFC-BOD sensor had good response time for both upper shift and lower shift. It was assumed that smaller volume of reactor might have helped increase the electrochemical activity of biofilm due to higher mass transfer rate (Fig. 5.6). This was in line with the observations made by Moon et al. (2004) and Di Lorenzo et al. (2009), who experienced lower response time with smaller anode volume.

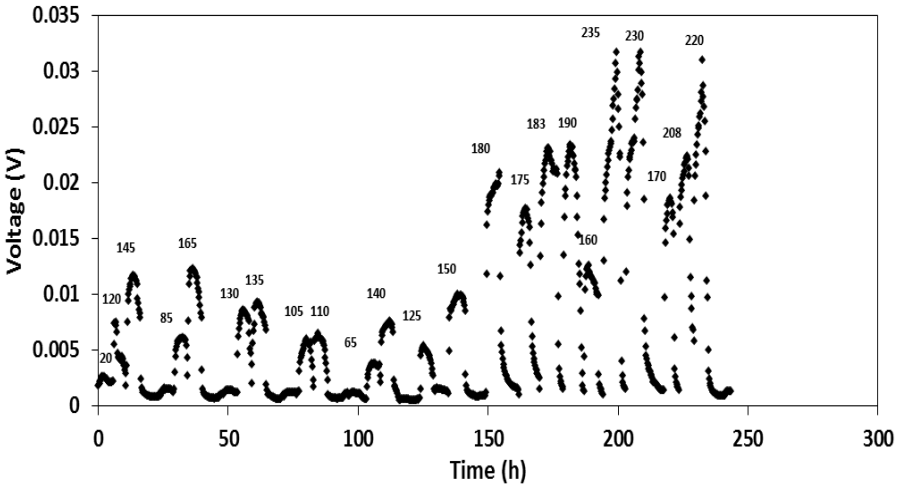

Figure 5.6: Voltage profile at different BOD_5 concentration for MFC-BOD sensor with volume of 12.6 ml.

5.3.1 MFC-BOD sensor performance with a volume of 12.6 ml

Figure 5.7 shows the performance of MFC-BOD sensor with AWW ranging from 8-236 mg/L. It was observed that scaling down the sensor volume (56% less than the original volume of 28.3 ml) performed equally well at every time interval (R^2=0.93-0.95). It helped attain a good linear relationship at the time interval when maximum steady-state voltage was reached. It was worthy to note that a smaller volume also increased the sensitivity of the sensor. There was only a slight change of 2.3% in the sensitivity of the sensor between the time interval of 30 to 120 min for the MFC-BOD sensor with a volume of 12.6 ml. Shorter response time was measured when the fuel concentration (i.e., BOD_5) was increased, which was believed to be due to the reduced void volume resulting from microbial growth and to the non-ideal flow in the anode compartment.

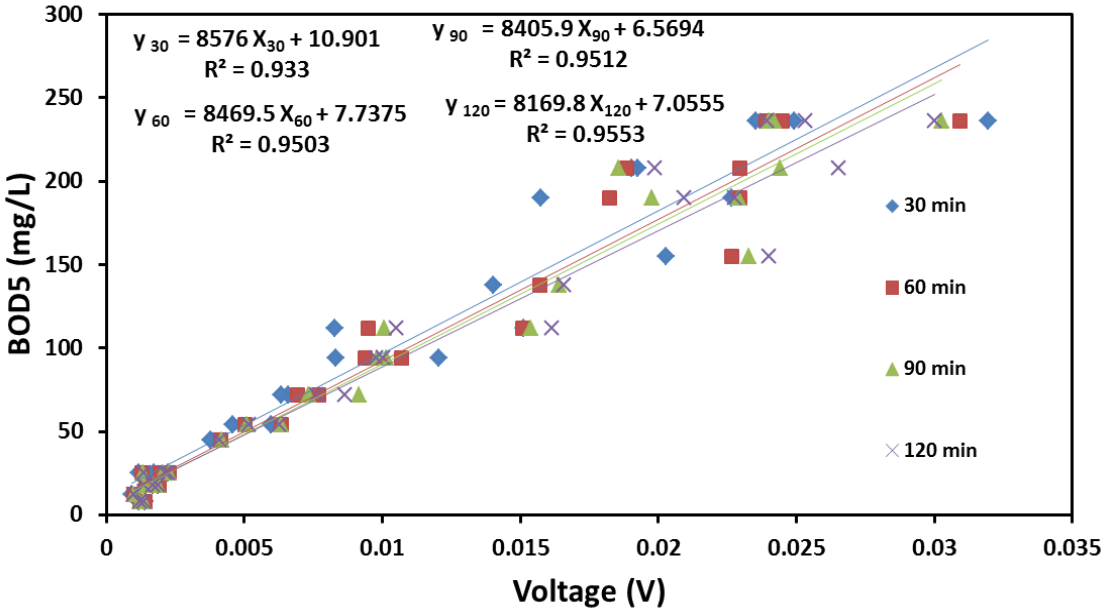

Figure 5.7: Linear calibration between BOD_5 (using AWW) and voltage recorded at different time interval for MFC-BOD sensor with a volume of 12.6 ml.

With DWW, the MFC-BOD sensor again followed similar trend, starting with a lower regression coefficient at 30 min (R^2 = 0.70) but steadily increased to higher

regression coefficient of R^2 = 0.82 at 120 min (Fig 5.8). However, the best linear relationship between BOD and voltage was established only at the time period when the maximum steady-state voltage was obtained (R^2 = 0.92). Inspiringly, excellent sensitivity with only a slight change of 5.5% (with DWW) was observed over a time interval of 30-120 min. These results were supported by Di Lorenzo et al. (2009) who showed better performance with small sized BOD sensors over bigger one.

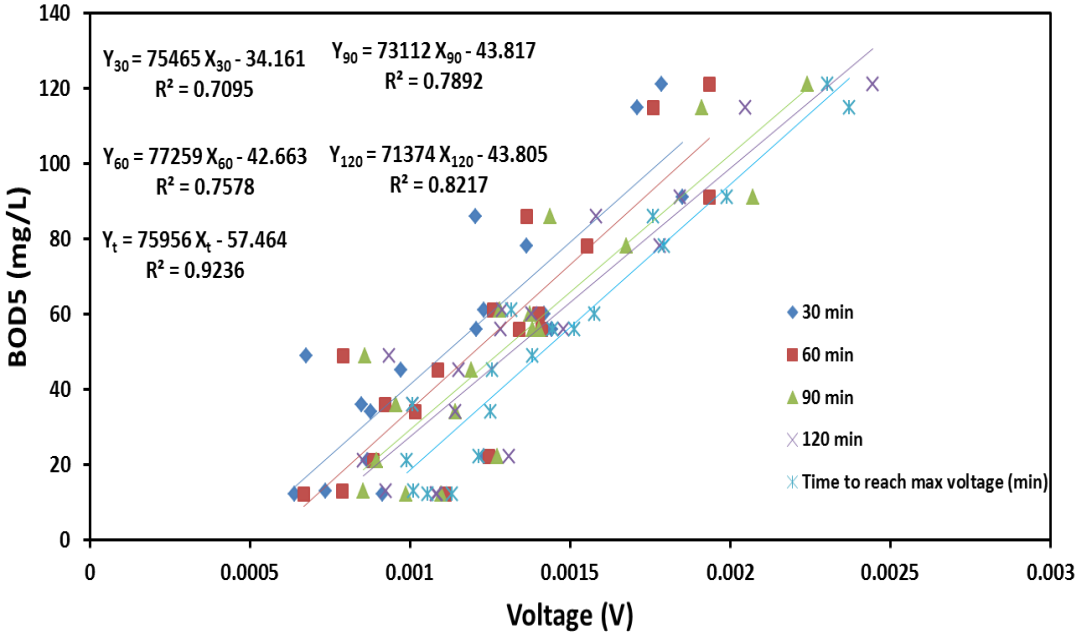

Figure 5.8: Linear calibration between BOD $_5$(using DWW) and voltage recorded at different time interval for MFC-BOD sensor volume of 12.6 ml.

5.3.2 MFC-BOD sensor performance with a volume of 4 ml

Besides investigating the effects of different volume in the performance of MFC-BOD sensor, another interest in decreasing the volume of MFC-BOD sensor is to make it compact and portable. Keeping that in mind, a smaller volume of MFC-BOD sensor (volume of 4 ml) was designed and constructed. The performance of

the MFC-BOD sensor was tested both with AWW and DWW. Fig 5.9 shows the voltage pattern of MFC-BOD sensor of volume 4 ml.

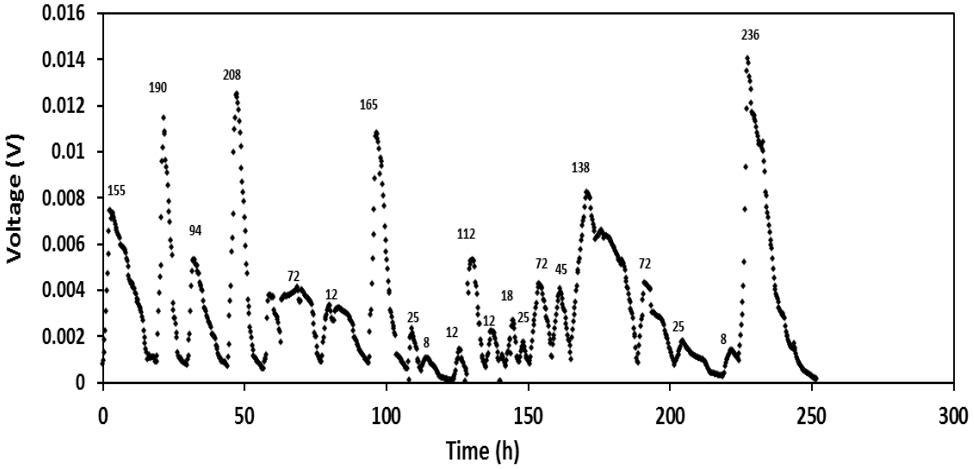

Figure 5.9: Voltage profile at different BOD_5 concentration for MFC-BOD sensor with volume of 4 ml.

The performance of the MFC-BOD sensor was first measured with AWW with BOD_5 ranging from 8-236 mg/L. However, the performance of MFC-BOD sensor decreased drastically with a poor linear relationship and sensitivity. Figure 5.10 shows that the maximum linearity between voltage and BOD concentration was measured at the time interval of 120 min. However, sensitivity was decreased to 34% from its original value. Moreover, the signal strength of MFC-BOD sensor (i.e., voltage output) was very low (in the range of 0.0015-0.0135 V).

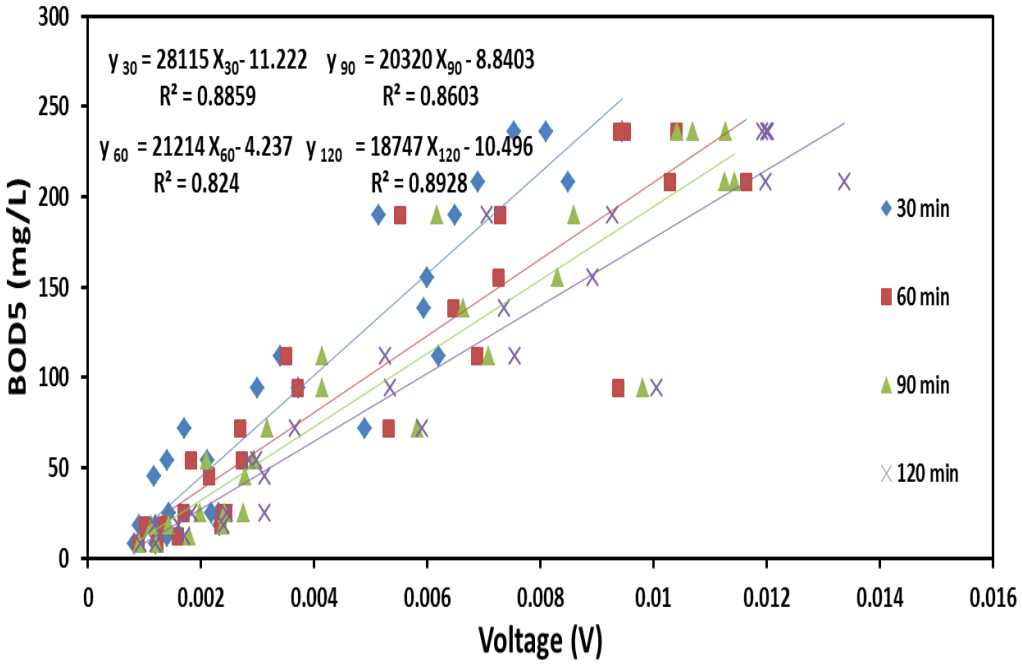

Figure 5.10: Linear calibration between BOD_5 (using AWW) and voltage recorded at different time interval for MFC-BOD sensor with a volume of 4 ml.

Again, very poor linear relationship between BOD_5 and produced voltage was measured when the MFC-BOD sensor was calibrated with DWW (Fig 5.11). The results showed that the MFC-BOD sensor was not able to provide a good linear relationship between BOD_5 and produced voltage (R^2 = 0.67) and good sensitivity (deviation of 33.4%). The probable reason of the poor performance was the very small anode surface area, which did not allow biofilm to grow homogeneously but promoted the growth of patchy biofilm (Biffinger et al, 2007). Additionally, with only limited biofilm growth, microorganisms were not able to reciprocate the exact response of BOD_5 concentration, and hence showed poor linear relationship between the produced voltage and BOD_5.

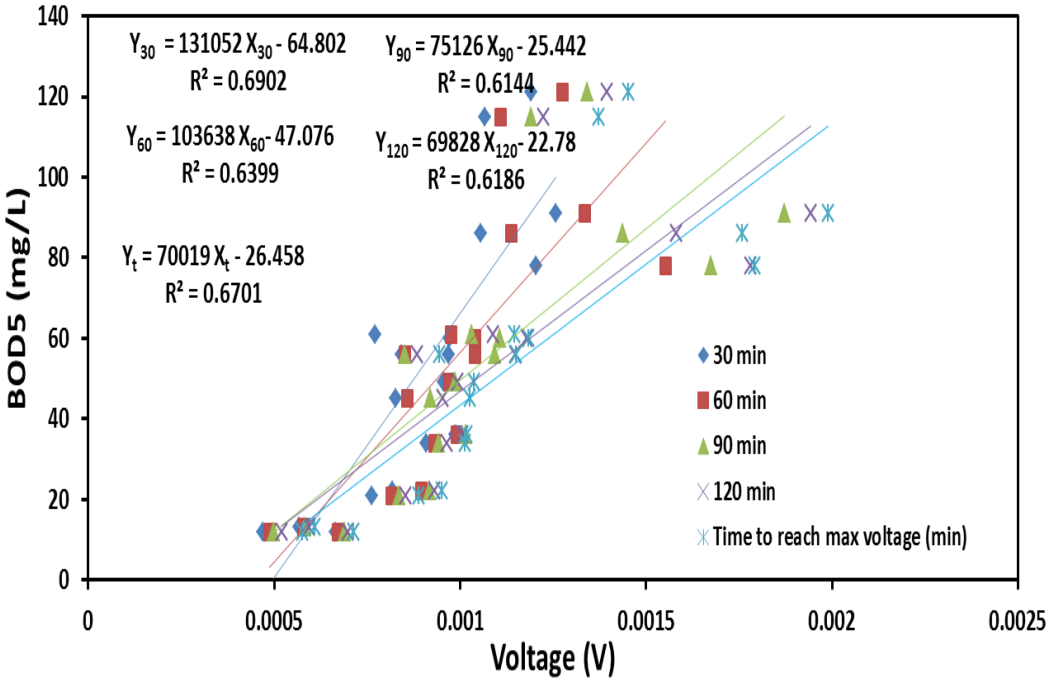

Figure 5.9: Linear calibration between BOD_5 (using DWW) and produced voltage recorded at different time interval for MFC-BOD sensor with a volume of 4 ml.

Table 5.3 summarizes the major findings of volume-optimization of the MFC-BOD sensor. Two conclusions were derived from his study. First, a smaller anodic volume (12.6 ml versus 28.3 ml) probably caused non-ideal flow to become plug flow and helped to increase the electrochemical activity of biofilm due to higher mass transfer rate. Second, further decrease in the anodic volume (4 ml vs 12.6 ml) probably allowed the growth of patchy biofilm, which was not able to respond to the BOD_5 concentration linearly.

Table 5.3: Summary of volume-based optimization of MFC-BOD sensor.

Parameter	**Features**		
	Volume 28.3 ml	***Volume 12.6 ml***	***Volume 4 ml***
HRT	2 min	2 min	2 min
Flow rate	14.1 ml/min	6.3 ml/min	2 ml/min
Detection limit	BOD concentration range was 8-236 mg/L	BOD concentration range was 8-236 mg/L	BOD concentration range was 8-236 mg/L
Linearity	Regression coefficient was high and in the range of R^2 = 0.95–0.95 for the response time of 30-120 min	Regression coefficient was slightly lower and in the range of R^2 = 0.93–0.95 for the response time of 30-120 min	Regression coefficient was the lowest and in the range of R^2 = 0.88–0.89 for the response time of 30-120 min
Sensitivity	± 6 %	± 4.8 %	± 33.4 %

5.4 Choice of PEM

The ability of separating the anode and cathode compartments, and enabling the transfer of protons from the anode to cathode side in order to allow electrical current production through an external circuit, makes proton exchange membrane (PEM) as one of the most important components in MFCs. Nafion 117 membrane had been used as the choice of PEM for MFC till now. Nafion membrane is generally regarded as a PEM having highly selective permeability of protons and high conductivity to various cations (Oh & Logan et al, 2006). However, some of its drawbacks, such as oxygen leakage from cathode to anode, substrate loss, cation transport and accumulation rather than protons and biofouling in its

application in MFCs (Kim et al, 2007), have led us to compare its performance with other type of PEM, which is the Selemion membrane. Selemion membrane has been reported as less expensive and durable substitute of Nafion membrane, while having comparable cation conductivity (Shen et al, 2013). Lefebvre et al. (2011b) reported higher value of oxygen diffusion coefficient of 0.90×10^{-6} cm^2/s for the Nafion membrane, while lower value was observed for the Selemion membrane (0.08×10^{-6} cm^2/s), suggesting that the Nafion membrane allowed the most O_2 to be diffused into the MFC that was harmful to the system. Moreover, the chance of binding of sulfonic acid groups in the Nafion membrane with ammonia (if present in the solution) may pollute the membrane (Rabaey and Verstraete, 2005; Chae et al., 2007). The positive features of the Selemion membrane motivated us to compare its performance with that of the Nafion membrane in MFC-BOD sensor application.

5.4.1 MFC-BOD sensor performance using Selemion membrane as PEM

The performance of the MFC-BOD sensor using Selemion membrane as the PEM was studied using both AWW and DWW, and it was compared with the performance of the MFC-BOD sensor which used Nafion membrane as the PEM. The performance of the MFC-BOD sensor with Nafion membrane was already discussed in the previous section of this chapter.

5.4.1.2 MFC-BOD sensor performance using AWW

Several BOD_5 concentrations ranging from 8-236 mg/L were used for investigating the performance of the sensor. Figure 5.12 shows the calibration relationship between the BOD_5 concentration and the produced voltage at different time period. The linear relationship between BOD_5 and voltage was not

found robust in terms of regression coefficient. Only at 90 and 120 min, the MFC-BOD sensor was able to establish regression coefficients of $R^2 > 0.90$. Less selectivity of Selemion membrane for protons might be the reason behind lower performance of BOD sensor.

The slope of every linear equation indicated that the rate of change in BOD_5 concentration could be reflected by a small change in the voltage, and determined the sensitivity of the MFC-BOD sensor, which decreased up to 21% with increasing time interval. The poor performance of the Selemion membrane can be supported by its lower proton selectivity and conductivity for ions than the Nafion membrane. Le (2013) reported overall conductivity of Selemion membrane of 0.86 ms/cm when equilibrated in electrolyte solution of H_2SO_4, which was approximately 100 times lower than the proton conductivity of the Nafion 117 membrane (90 ms/cm) (Sone et al., 1996). Additionally, the use of Nafion allowed the MFC to be designed as MEA (using hot-press method), which helped in reducing the distance between the anode and cathode (Liu et al., 2005a). However, MEA design was not possible with Selemion membrane because of its lower tensile strength of 0.2 Mpa (Lefebvre et al., 2011) than that of the Nafion 117 membrane (32 Mpa) (manufacturer data).

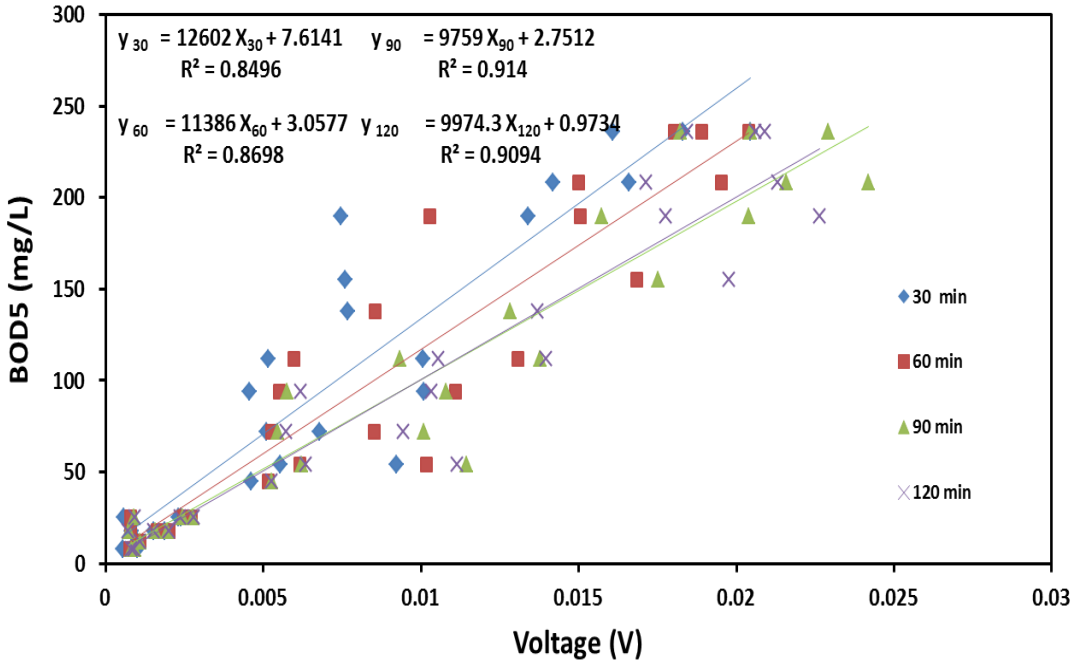

Figure 5.10: Linear calibration between BOD_5 (using AWW) and produced voltage recorded at different time interval, and comparison of the change in sensitivity of MFC-BOD sensor over time using Selemion membrane as PEM.

5.4.1.3 MFC-BOD sensor performance using DWW

Figure 5.13 demonstrates a linear calibration relationship established between produced voltage at different time interval and BOD concentration of DWW. The MFC-BOD sensor did not perform well in the presence of DWW. The regression coefficient, even at the a time interval of 120 min was observed as $R^2 = 0.77$, while it improved ($R^2 = 0.85$) at the time period when the BOD_5 concentration was calibrated with the maximum steady-state voltage. Results were consistent with the finding that lower selectivity for protons led to higher resistance of the membrane (Selemion membrane) and resulted in lower performance (Rabaey et al., 2005).

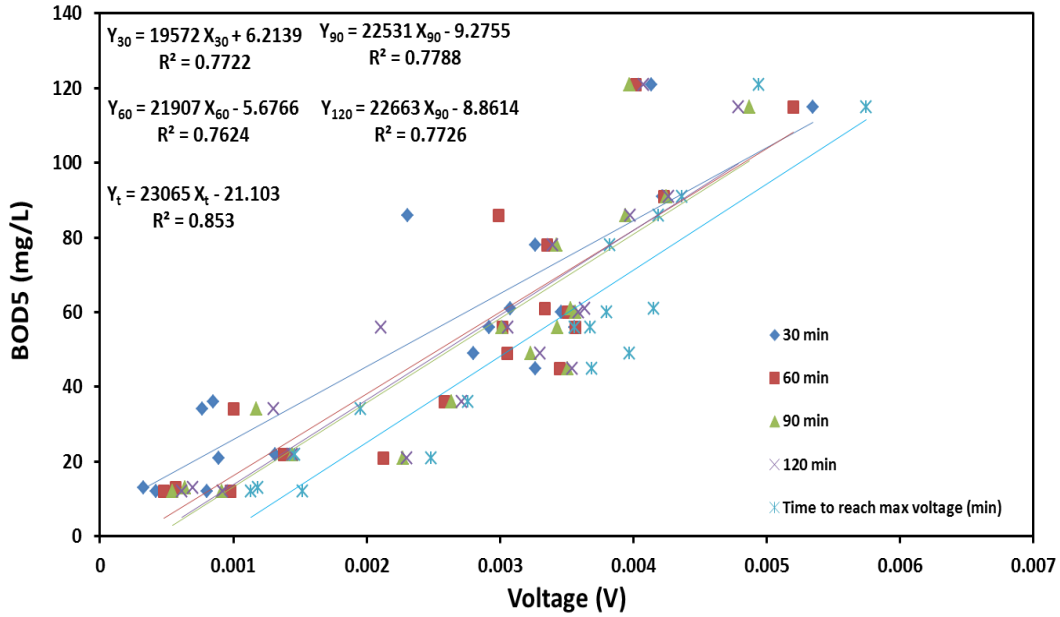

Figure 5.11: Linear calibration between BOD_5 (using DWW) and produced voltage recorded at different time interval, using Selemion membrane as PEM.

The summary of membrane-based-optimization of the MFC-BOD sensor is shown in Table 5.4.

Table 5.4: Summary of the study on the choice of PEM.

Parameter	**Features**	
	Nafion membrane	***Selemion membrane***
Volume	12.6 ml	12.6 ml
HRT	2 min	2 min
Cathode catalyst	β-MnO_2	Pt
Detection limit	BOD concentration range was 8-236 mg/L	BOD concentration range was 8-236 mg/L
Sensitivity	±4.8 %	±21%
Linearity	Regression coefficient was high and in the range of R^2 = 0.93 – 0.95 for the response time of 30-120 min	Regression coefficient was lower and in the range of R^2 = 0.84-0.90 for the response time of 30-120 min

5.5 Choice of cathode catalyst

Recently, metal-based materials have been investigated as alternative catalysts for oxygen reduction in MFCs (Lu et al, 2011; Lu et al, 2013; Zhao et al, 2006). Especially, MnO_2 has been shown as a successful cathode material for primary or secondary battery, and is believed to be a promising cathode catalyst for alkaline fuel cells and metal-air batteries applications (Wei et al., 2000) since oxygen reduction activities can be achieved on manganese dioxide in alkaline media (Lima et al., 2006; Zhang et al., 2007). In chapter 4, three different MnO_2 catalysts (α, β, and γ-MnO_2) were examined for catalysing ORR at the cathode in

MFCs. Among them, β-MnO_2 catalyst was identified as the best suitable catalyst for MFC-BOD sensor application.

On the other hand, Pt is still the most commonly used cathode catalyst for ORR in MFC-based applications; however, high cost prohibits its use for commercial MFC applications. Yet, it has been widely used as the most common precious metal catalyst in cathode materials of MFC because of having favourably low overpotential for oxygen reduction (Logan et al, 2005). Keeping all these factors in mind, in this part of study, we compared the performance of β-MnO_2-MFC-BOD sensor with Pt-MFC-BOD sensor. All other parameters and sensor components such as HRT (2 min), volume of the reactor (12.6 ml), and PEM (Nafion) were kept similar. It should be noted that the loading concentration of MnO_2 catalyst on the cathode was 3 mg/cm^2, while the loading concentration of Pt catalyst on the cathode was 0.5 mg/cm^2. However, the Pt catalyst was estimated around 50 times costlier than MnO_2 catalyst. The performance of β-MnO_2-MFC-BOD sensor has been discussed already in earlier section (section 5.3).

5.5.1 Pt-MFC-BOD sensor performance with AWW

Figure 5.14 shows the calibration relationship between BOD_5 concentration and produced voltage at different specific time period. Several BOD_5 concentrations ranging from 12-288 mg/L were used to investigate the performance of the MFC-BOD sensor. With $R^2 > 0.94$, even at the response time of 30 min, the results clearly indicated a robust linear relationship between BOD_5 and voltage. This relationship further improved with time interval of 60, 90 and 120 min, with a R^2 value of 0.96. The higher catalytic activity of Pt might have increased the rate of ORR, and resulted with the higher performance of Pt-MFC-BOD sensor. This result was supported by the observations of Lu et al. (2011) and Zhang et al.

(2009), who reported higher performance of Pt-MFC than MnO_2-MFC due to better catalytic activity of the Pt.

Figure 5.14 also shows the rate of change in BOD_5 with the change in produced voltage (measured by the slope of linear relationship), indicating excellent sensitivity of Pt-MFC-BOD sensor with a slight change of 3.5% over the time interval from 30 to 120 min. The slopes of all the linear curves were rather similar, with an improvement in regression coefficient, R^2 from 0.94 to 0.96.

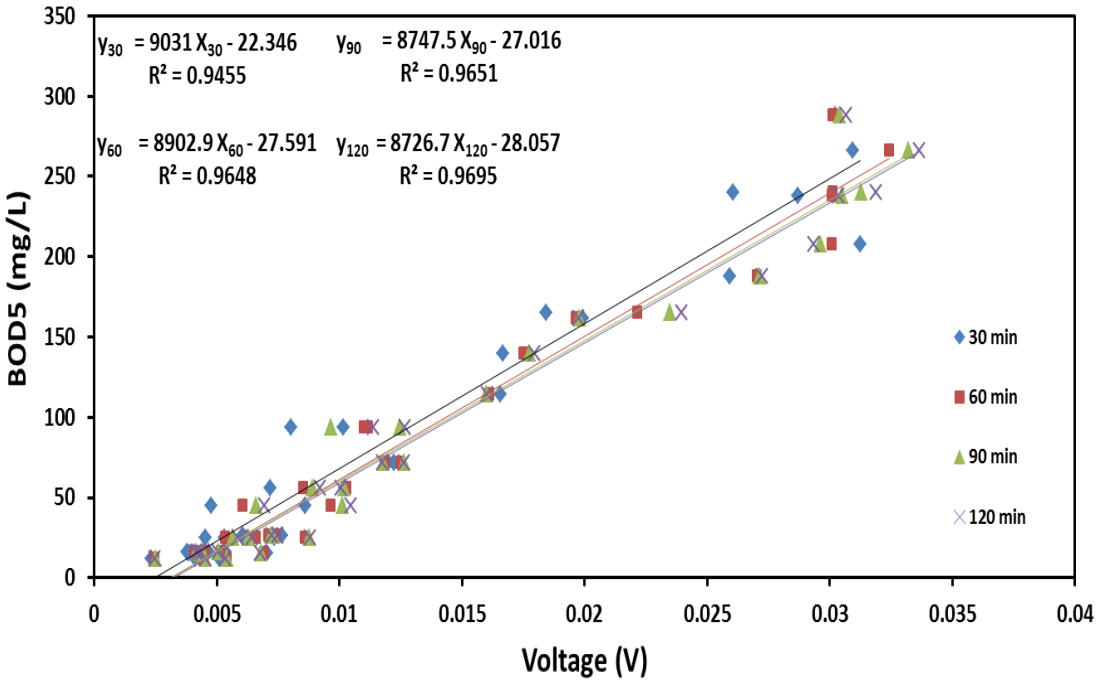

Figure 5.12: Linear calibration between BOD_5 (using AWW) and produced voltage recorded at different time, and comparison of the change in sensitivity of MFC-BOD sensor, using Pt as the catalyst at the cathode.

5.5.2 Pt-MFC-BOD sensor performance with DWW

Pt-MFC-BOD sensor performed better than the MnO_2-MFC-BOD sensor when examined with DWW. The regression coefficient of Pt-MFC-BOD sensor at 30 min interval was measured with $R^2 = 0.89$, which was better than the $R^2 = 0.70$ of

MnO_2-MFC-BOD sensor. In addition, at every specified time interval, the Pt-MFC-BOD sensor performed better than the MnO_2-MFC-BOD sensor. However, the performance with DWW dropped comparatively to that with AWW. This was probably due to complex composition of wastewater, which might have caused slower bacterial metabolism. For example, for the same BOD_5 concentration of 1 g/L of AWW (acetate based) current density of 0.8 mA/cm^2 was produced (Logan et al., 2007), while DWW (corn stover biomass) produced a current density of 0.15 mA/cm^2 (Zuo et al., 2006). Figure 5.15 illustrates that the sensitivity of Pt-MFC-BOD sensor decreased up to 18% over the time (from 30-120 min). Results showed that the regression coefficient improved (R^2 = 0.95) for the linear relationship of BOD_5 with maximum steady-state voltage, however the sensitivity again decreased to 24%.

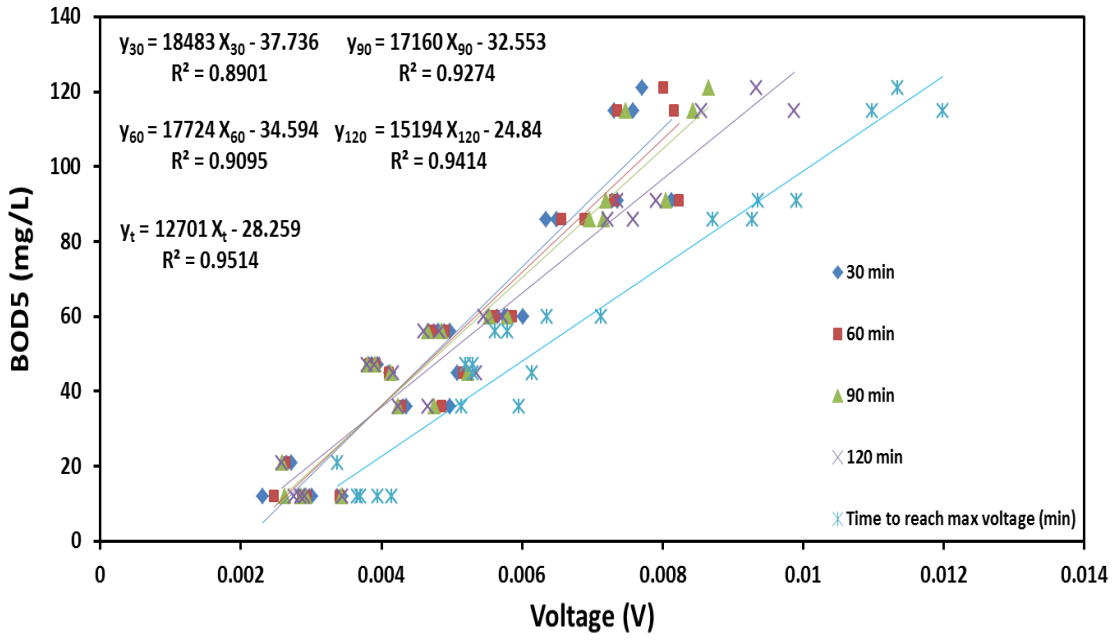

Figure 5.13: Linear calibration between BOD_5 (using DWW) and produced voltage recorded at different time interval, using Pt as the catalyst at the cathode.

The summary of cathode-catalyst-based-optimization of the MFC-BOD sensor is shown in Table 5.5. This part of the study showed that Pt was found to be a better catalyst (irrespective of its higher cost) than MnO_2 catalyst, for MFC-BOD sensor application. Pt performed better in terms of shorter response time (high regression coefficient at early response time of 30 min) and excellent sensitivity (3.4%). Better capability of Pt to reduce the activation energy needed for oxygen reduction at the cathode made it a better catalyst choice over MnO_2 for MFC-BOD sensor.

Table 5.5: Summary of the study on the choice of cathode catalyst.

Parameter	**Features**	
	MnO_2-MFC-BOD sensor	***Pt-MFC-BOD sensor***
Volume	12.6 ml	12.6 ml
PEM	Nafion	Nafion
HRT	2 min	2 min
Sensitivity	± 4.8 %	± 3.4%
Linearity	Lower regression coefficient of R^2 = 0.93 – 0.95 for the response time of 30-120 min	Higher Regression coefficient of R^2 = 0.94-0.97 for the response time of 30-120 min

5.6 Choice of anode material

In MFC, the anode material should be highly conductive, enable the attached growth of electrophilic microorganisms, allow electronic transfer to the anode

body from microorganisms and facilitate lower internal resistance, anodic potential and stability.

Considering all these aspects, carbon cloth (Fuel Cell Earth LLC) was used as an anode material in earlier part of this study. The carbon cloth used was a carbon fiber fabric, which was made from spun yarn. The spun yarns had many surface fibrils that protruded in various directions at various lengths from the surface. However, in order to achieve higher response and sensitivity of the MFC-BOD sensor, the choice of better anode material is crucial. In this regard, highly conductive Graphite plate (Graphtek LLC) was explored as an alternative anode material. High conductivity (48 BTU) and smaller grain size (1 mm) were the rationale behind the choice of graphite as anode material. Graphite plate was made up of very fine graphite grains, which were isostatically pressed and isomolded, and having high strength and density.

5.6.1 MFC-BOD sensor performance using graphite as anode material

The performance of MFC-BOD sensor, using graphite as an anode material, was studied with both AWW and DWW. It was compared with the performance of MFC-BOD sensor that used carbon cloth as an anode material (results shown in earlier section).

5.6.1.1 MFC-BOD sensor performance using AWW

Figure 5.16 shows the calibration relationship between BOD_5 concentration and produced voltage at different time period. Several BOD_5 concentrations ranged from 12-288 mg/L were used for assessing the performance of the MFC-BOD sensor. With $R^2 > 0.96$, even at 30 min of time interval, the results clearly indicated a robust linear relationship between BOD_5 and the produced voltage

from the regression coefficient. This relationship further improved with time interval of 60, 90 and 120 min, with a R^2 value of 0.97. The higher conductivity of graphite might have increased the rate of electron transfer from the anode to cathode side, resulting with the higher performance of Pt-MFC-BOD sensor.

The use of graphite as an anode material significantly improved the performance of the MFC-BOD sensor, achieving high voltage generation, faster response time and better sensitivity. Figure 5.16 shows the change in sensitivity (rate of change in BOD with the change in voltage), which was measured through the slope of the linear relationship. MFC-BOD sensor exhibited an excellent sensitivity with almost no change (around 0.2%) over the time interval from 30 to 120 min. The slope of all the linear curves were rather similar with regression coefficient, R^2 ranging from 0.96 to 0.97. These results confirmed the observation of Heijne et al. (2008), who reported better performance of non-porous material (flat graphite) than porous material (graphite cloth) due to better mass transfer.

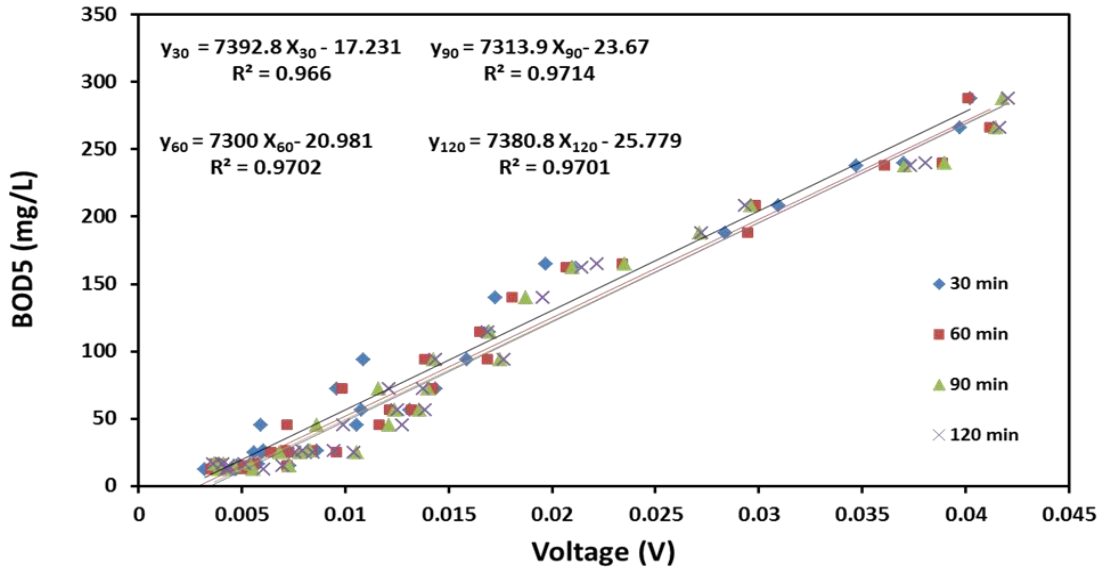

Figure 5.14: Linear calibration between BOD_5 (using AWW) and produced voltage recorded at different time interval, using graphite plate as anode material.

5.6.1.2 MFC-BOD sensor performance using DWW

The performance of the MFC-BOD sensor improved significantly with the use of graphite as anode material. Graphite, as a conductive material, not only enhanced voltage generation, but also decreased the response time and increase sensitivity. Figure 5.17 shows the performance of the MFC-BOD sensor with DWW. The MFC-BOD sensor using graphite performed better than that using carbon cloth. The regression coefficient of graphite-based-Pt-MFC-BOD sensor at 30 min was measured as $R^2 = 0.92$, which was much better than the $R^2 = 0.89$ of carbon-cloth-based-Pt-MFC-BOD sensor. Additionally, at every specified time interval, the Pt-MFC-BOD sensor performed better than the MnO_2-MFC-BOD sensor. However, the performance of the MFC-BOD sensor dropped with DWW, when comapred to that with AWW; yet the sensitivity decreased to only 7% over time (from 30 to 120 min) when compared to a decrease of 18% for the carbon-cloth-based-Pt-MFC-BOD sensor. The regression coefficient improved ($R^2 = 0.98$) at the time period when BOD_5 concentration was calibrated with the maximum steady-state voltage, with 13% decrease in the sensitivity.

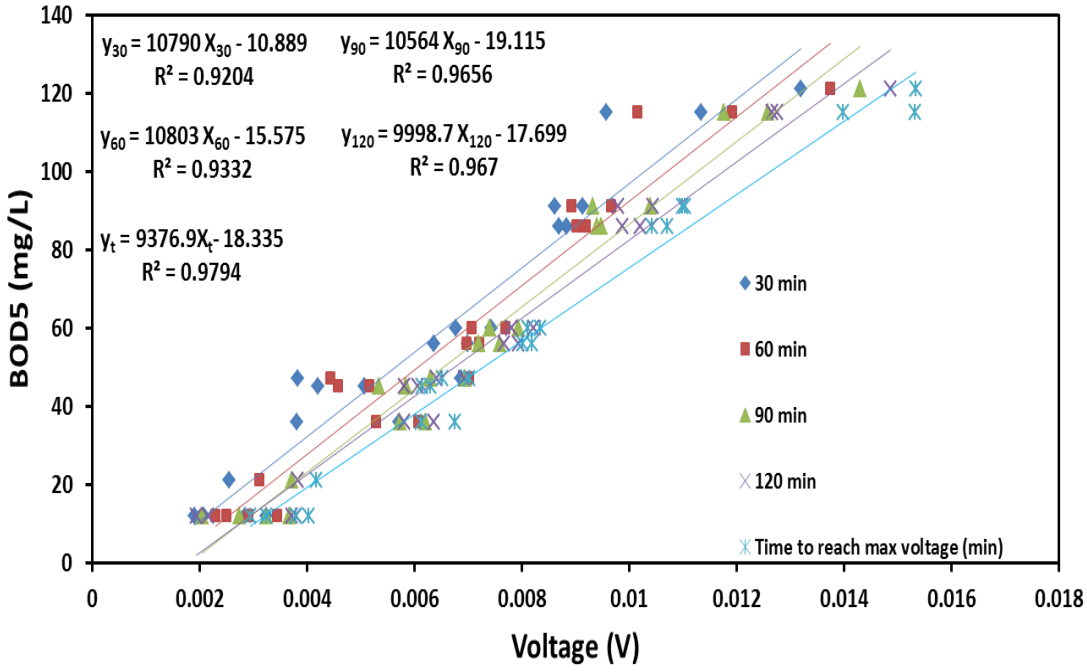

Figure 5.15: Linear calibration between BOD_5 (using DWW) and produced voltage recorded at different time interval, using graphite plate as anode material.

The summary of anode-material-based-optimization of the MFC-BOD sensor is shown in Table 5.6.This study showed that graphite performed as a better anode material than the MnO_2-carbon cloth in MFC-BOD sensor application. Graphite-based-Pt-MFC-BOD sensor performed better in terms of shorter response time (i.e., high regression coefficient even at 30 min time interval) and excellent sensitivity (i.e., change of 0.2% over time). Better conductivity and lower inner resistance of graphite (1-1.5 Ω) than carbon cloth (1.2-2 Ω) helped in better transfer of electrons from the anode to cathode side, and made it a better choice over carbon cloth for MFC-BOD sensor.

Table 5.6: Summary of study on the choice of anode material.

Parameter	**Features**	
	Carbon cloth	***Graphite plate***
HRT	2 min	2 min
Volume	12.6 ml	12.6 ml
PEM	Nafion	Nafion
Cathode catalyst	Pt	Pt
Sensitivity	± 3.5 %	± 0.2%
Linearity	Lower regression coefficient of R^2 = 0.94–0.97 for the response time of 30-120 min	Higher Regression coefficient of R^2 = 0.96-0.97 for the response time of 30-120 min

5.7 Summary of sequential optimization study for MFC-BOD sensor

The approach of sequential optimization was performed by varying one parameter at a time. This approach avoided the chances of interference, which might have occurred due to the changes in multiple parameters at any one point of time. Table 5.7 summarizes the main observations of this comprehensive study.

Table 5.7: Overall summary of the sequential optimization of MFC-BOD sensor.

Type of study	Remarks
HRT based	HRT of 2 min was estimated to be more effective for "true" BOD_5 measurement with shorter response time
Volume based	Sensor volume of 12.6 ml was found better than 28.3 ml and 4 ml in terms of better sensitivity
PEM based	Nafion membrane performed better than Selemion membrane, in terms of better sensitivity and linearity
Cathode catalyst based	Pt was a better catalyst than MnO_2 , in terms of faster response, better sensitivity and better calibration relationship
Anode material	Use of graphite plate as an anode material was better than carbon cloth in terms of higher strength of signal output, better sensitivity and better linearity

5.8 Compliance of predicted BOD values (BODp) with BOD_5

After the sequential optimization study, an optimized parameter and components of MFC-BOD sensor were established and developed. The optimized MFC-BOD sensor was comprised of a volume of 12.6 ml, HRT of 2 min, Nafion membrane as the PEM, Pt as the cathode catalyst and graphite as the anode material. The compliance of the BOD_5 values as predicted by the optimized BOD sensor (BODp) with BOD_5 was determined using some random samples of DWW, using the calibration curve (at a response time of 2 h) obtained by the optimized MFC-BOD sensor. Figure 5.18 plots the BODp values measured with optimized MFC-BOD sensor against BOD_5 for all DWW samples. The BOD_5 of DWW samples ranged from 15-120 mg/L, with a standard deviation comprised between 7-26%.

However, inspiringly, for optimized MFC-BOD sensor, a standard deviations obtained were small (ranging from ±3-13%). It was worthy to note that smaller standard deviations of BOD_5 obtained from the MFC-BOD sensors demonstrated improved reliability of the MFC-BOD sensors over conventional BOD_5 method.

In addition, a good correlation was obtained between BOD_5 and BODp. Results showed that, for high BOD_5 value (>120 mg/L) and for low BOD_5 value (< 15 mg/L), the MFC-BOD sensors had a tendency to slightly overestimate the BOD_5. Yet, the compliance was extremely good with a slight variation of ±2-6% at the intermediate BOD_5 range (between 40-110 mg/L), which corresponds to the typical BOD_5 of treated effluents from wastewater treatment plant. This, along with good accuracy, result reproducibility, fast response time and the ability to measure BOD continuously demonstrated the potential of the MFC-BOD sensor in on-line monitoring of wastewater.

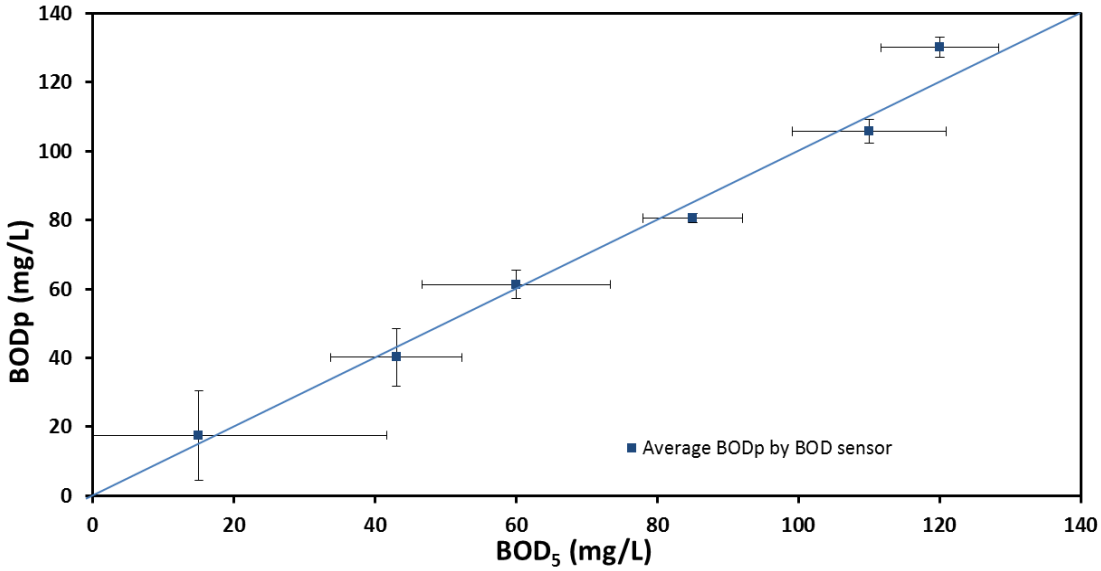

Figure 5.16: Variation between BODp obtained by optimized MFC-BOD sensor and BOD_5 measured with conventional 5-day BOD method.

6. Biofilm Analysis and Effect of Environmental Conditions

6.1 Introduction

In order to maintain the high performance of the MFC-BOD sensor, it is very important to study the changes in the anodic biofilm. Biofilm of MFC is generally categorized as a mix consortium of anaerobic and facultative anaerobic bacteria. Generally, these microbial communities are attached to the MFC electrodes, harvesting electricity from a variety of sediments and activated sludge. Microbial populations in MFC biofilm have been studied by several groups, attempting to elucidate their electrochemical roles (Bond et al., 2002; Holmes et al., 2004b; Lee et al., 2003; Tender et al., 2002). However, these analyses were mainly aimed to isolate and study specific species of anodophiles such as *Geobacter sulfurreducens* (Bond & Lovley, 2003), *Geobacter metallireducens*, *Geopsychrobacter electrodiphilus* (Holmes et al., 2004c), *Desulfuromonas acetoxidans* (Bond et al., 2002) and *Desulfobulbus propionicus* (Holmes et al., 2004a). The performance of MFC-BOD sensor varied in long term, and the changing composition of biofilm over the time period might have played a crucial role behind the changed performance. Considering this factor, we tried to estimate the changes in anode biofilm by analysing the composition of live and dead cells in biofilm at certain time period. Change in the ratio of live and dead cells in anode biofilm was eastimated by calculating the population of live and dead cells at certain time period such as 1 month, 3 months, 6 months and 1 year . Since the structure of biofilm also plays a significant role in the performance of MFC-BOD sensor, the thickness and density of biofilm were analysed.

For a wide application of MFC-BOD sensor, it is very important to evaluate the performance of sensor at different environmental conditions such as operating temperature, anodic pH and conductivity. The voltage and current generation by the MFC-BOD sensor depends on these environmental conditions. Thus, a correction factor should be applied to measurements done under different environmental conditions from the ones used in the calibration.

6.2 Flow cytometric measurements for the quantification of live and dead cells in biofilm

In the case of anodic film, the death of a bacterial cell could be defined as an inability of cell to grow in the form of biofilm using growth medium such as DWW, acetate, glucose, etc. When subjected to any food starvation situation, certain bacteria lose their culturability and convert themselves to a transitional state of dormancy, known as active but non-culturable (or viable but non-culturable) state, where they continue to retain their activity and cell membrane integrity (Peneau et al., 2007; Sachidanandham et al., 2005; Smith & Oliver, 2006). This kind of cell state is difficult to be detected with the conventional plating method. Nevertheless, there are several viability indicators available that could be assessed at the single-cell level without culturing the cells. These indicators are mainly based on the criteria that reflect different levels of cellular integrity or functionality. They are mostly based on the fluorescent molecules, which could be detected by the epifluorescence microscopy, solid state cytometry or flow cytometry.

Biofilm structure of MFC-BOD sensor changes over time. Therefore, in order to assess the performance of the MFC-BOD sensor over a long period of time, it is

important to know the proportion of active microorganisms (live cells) present in the anodic biofilm. In this study, flow cytometry, a powerful tool in microbiology in last 20 years particularly in biotechnological processing, food preservation and chemical disinfection processes (Berney et al., 2006; Joux & Lebaron, 2000; Porter et al., 1997), was applied to measure the proportion of live and dead cells in the anodic biofilm, because of its quick single-cell analysis. Cells were stained using the LIVE/DEAD BacLight (Molecular Probes, Eugene/Portland) using the procedure described elsewhere (Sachidanandham et al., 2005). The kit consisted of two stains, propidium iodide (PI) and SYTO9. Green fluorescing SYTO9 was able to enter through the cell wall of all cells, and was used for assessing total cell counts, whereas red fluorescing PI could enter only through the cells with damaged cytoplasmic membranes. The emission properties of these stain mixture were bound to DNA change due to the displacement of one stain by other and quenching by fluorescence resonance energy transfer (Stocks, 2004; Boulos et al., 1999). The differentiation between active and dead cells was enabled by the detection of intact and damaged cytoplasmic membranes, respectively (Sachidanandham et al., 2005). Cytometric data was analysed using the software FlowJo. Figure 6.1 shows the population of pure live (extracted from the exponential phase of LB broth culture) and pure dead (autoclaved) culture, which were used as a control for the real time samples of biofilm. Since some bacterial cells had tendency to autofluorescence, one unstained sample was first used for compensating the error. Results showed 99.4% of live cells in pure live culture and 99.5% of dead cells in pure dead culture.

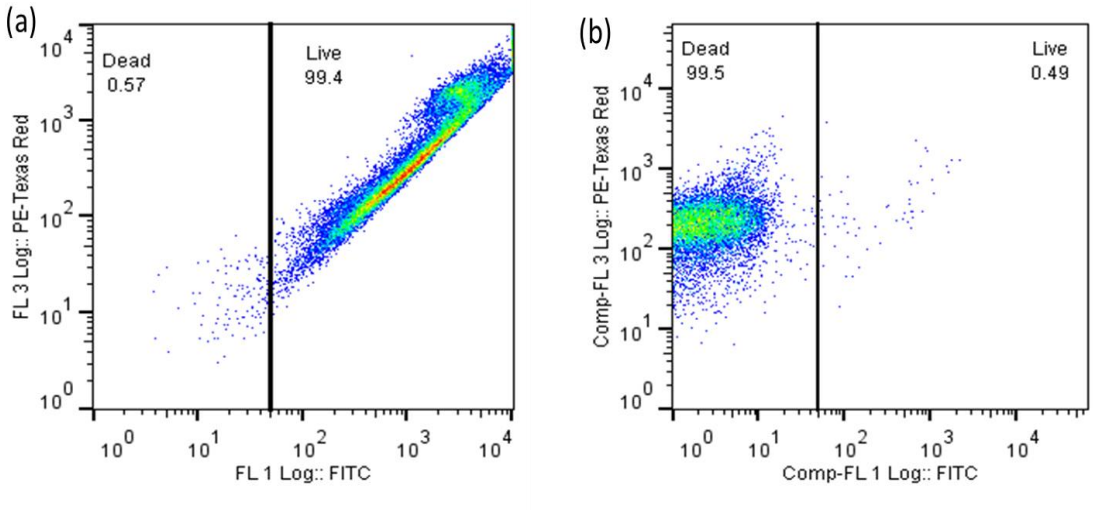

Figure 6.1: Population of live and dead cells in the control samples measured by flow cytometric analysis. (a) Pure live culture extracted from the exponential phase of LB broth; and (b) Pure dead culture used after autoclaving it for 20 min. FL 3Log:: PE-Texas Red is the logarithmic scale of red fluorescence and FL 1Log:: FITC is the logarithmic scale of green fluorescence.

In order to assess the proportion of live and dead cells in the biofilm of different ages, biofilm was extracted (just before the experiment) from four different MFC-BOD sensors of different time period and stained with dyes after slowly vortexing the suspension. Figure 6.2 shows the proportion of live and dead cells at different time period (1 month, 3 months, 6 months and 1 year).

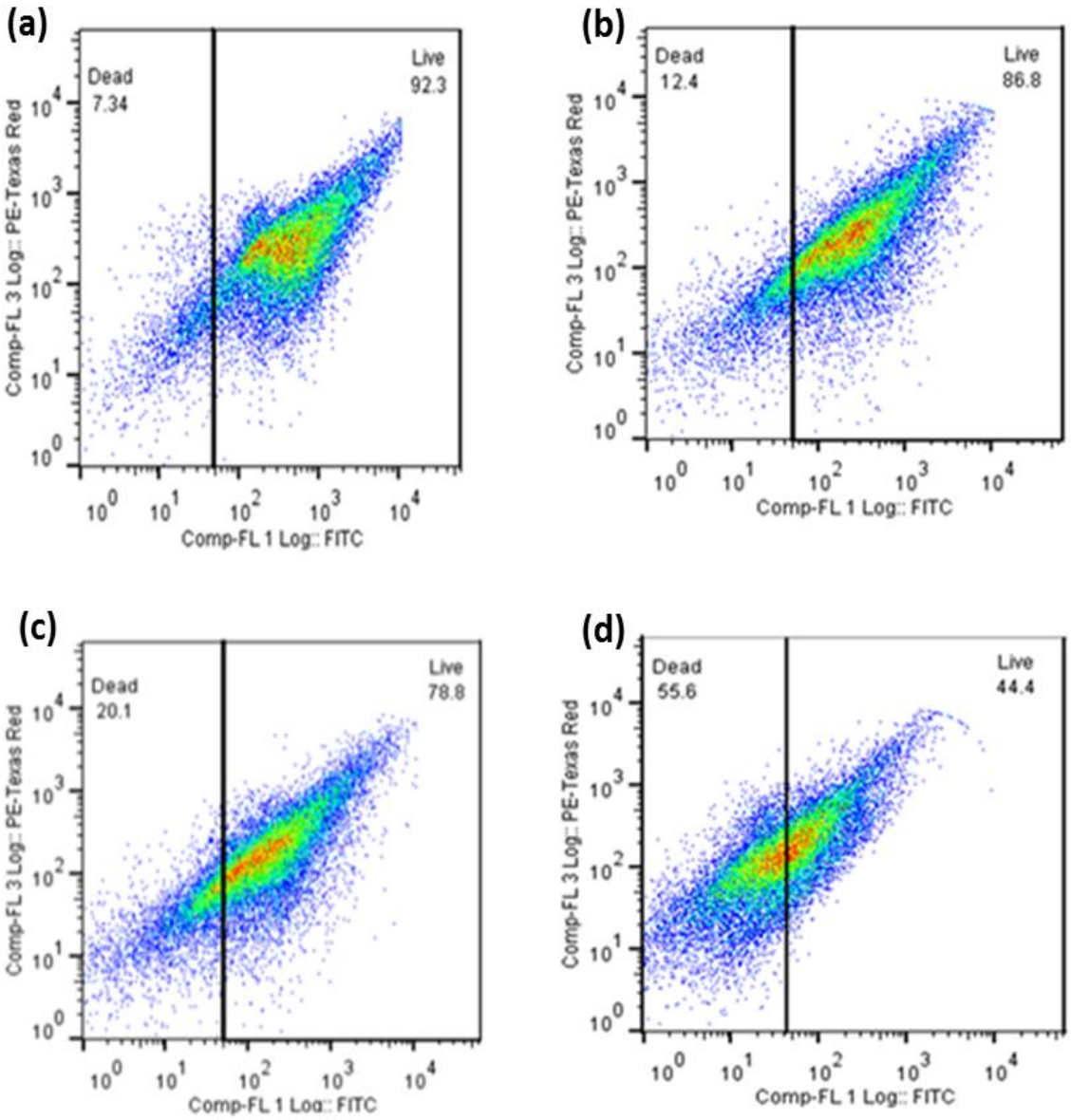

Figure 6.2: Population of live and dead cells in the biofilm of different time period. Age of biofilm was: (a) 1 month; (b) 3 months; (c) 6 months; and (d) 1 year. Comp-FL 3Log:: PE-Texas Red is the logarithmic scale of red fluorescence and Comp-FL 1Log:: FITC is the logarithmic scale of green fluorescence.

The total number of cells counted for every sample was in the range of 25,000-30,000 cells/ml of sample, ensuring the high diversity of bacterial cells. Bifurcation in the cluster of dots of all the samples (except pure live and pure

dead) suggested the presence of mixed variety of cells in biofilm. Figure 6.2 indicates that the biofilm was quite active and highly grown at the age of 1 month, comprising about 92.3% of live cells and 7.3% of dead cells. Gradually, the proportion of live and dead cells in biofilm started to change over time. The amount of live cells started decreasing to 87% (3 months), 78% (6 month), and finally 44% (1 year). It could be explained as - biofilm developed slowly at first, because only a few organisms could attach, grow, and multiply. As populations increased exponentially (in 15-20 days), the depth of biofilm increased rapidly, producing high and stable voltage during that period of time. Biofilm polymers, which are generally sticky, allowed the attachment of new cells to the colonized surface as well as the accumulation of dead (non-living) debris and sludge from the bulk liquid (Mai-Prochnow et al., 2004). Gradually, such debris or sludge (consist of various inorganic chemical precipitates, organic flocs and dead cell masses) started accumulating on the surface area of living cells, and subsequently, the proportion of live cells started decreasing. An increase in the number of dead cells (7 to 55%) in the period of 1 month to 1 year was reflected with the drop in the performance of MFC-BOD sensor (chapter 4). These results could be helpful in estimating the appropriate time for reviving the anodic biofilm in order to enable a long time operation of the MFC-BOD sensor.

6.3 SEM analysis for characterizing anodic biofilm and PEM fouling

Biofilm was analysed by SEM in order to characterize biofilm density and morphology. Figure 6.3 displays SEM micrographs taken for different volume of MFC-BOD sensor at different flow rates. It is evident from the micrographs that

the biofilm developed on the the carbon cloth fibers and had a mixed bacterial consortium, predominated by rod shaped, elongated and spherical bacteria.

For measuring the density of biofilm, VSS (present in 1 cm^2 of biofilm area) was measured according to the Standard Methods (APHA, 2005), and biofilm density (*D*, g VSS/L) was determined using the formula - $D = m/L \times 10^4$, where *m* (mg/cm^2) is the VSS content of the biofilm collected from the $1cm^2$ carbon cloth and *L* is the thickness of the biofilm (μm) (Xing et al., 2010). The biofilm density indicates the amount of biomass (g) per volume of biofilm (L). Differences in biofilm density may occur due the thickness of biofilm, presence of different types of microorganisms and hydrodynamic conditions (Kwok et al. 1998). Table 6.1 lists the thickness and density of the biofilm of MFC-BOD sensors of different volumes and flow rates.

Table 6.1: VSS, thickness and density of the anodic biofilm of MFC-BOD sensors of different volumes and flow rates.

Sensor volume (ml)	**Flow rate (ml/min)**	**VSS (mg/cm^2)**	**Biofilm thickness (μm)**	**Density (g VSS/L)**
28.3	14.1	3.43 ±43	187 ±2.5	183.42
12.6	6.3	3.28 ±36	248 ±1.2	132.25
4	2	3.13 ±23	253 ±3.8	123.71

Not much difference in VSS was observed between the MFC-BOD sensors of 28.3 ml and 12.6 ml in volume; however, the VSS of the MFC-BOD sensor with volume of 4 ml was lower. The thickness of biofilm differed with the change in volume and flow rate. The biofilm thickness of the 28.3-ml MFC-BOD sensor was about 187 μm, while it increased to about 248 μm and 253 μm for the 12.6-ml and

4-ml MFC-BOD sensor, respectively. Thinner biofilm increased the biofilm density, showing dense population of microorganisms. This was supported by the SEM analysis (Fig. 6.3). The SEM micrographs show denser biofilm in the 28.6-ml MFC-BOD sensor (less thickness) (Fig. 6.3a) than the biofilm in the 12.6-ml MFC-BOD sensor (Fig. 6.3b), which was more porous and thick. The biofilm of the 4-ml MFC-BOD sensor was observed scattered, patchy and fragile (Fig. 6.3c).

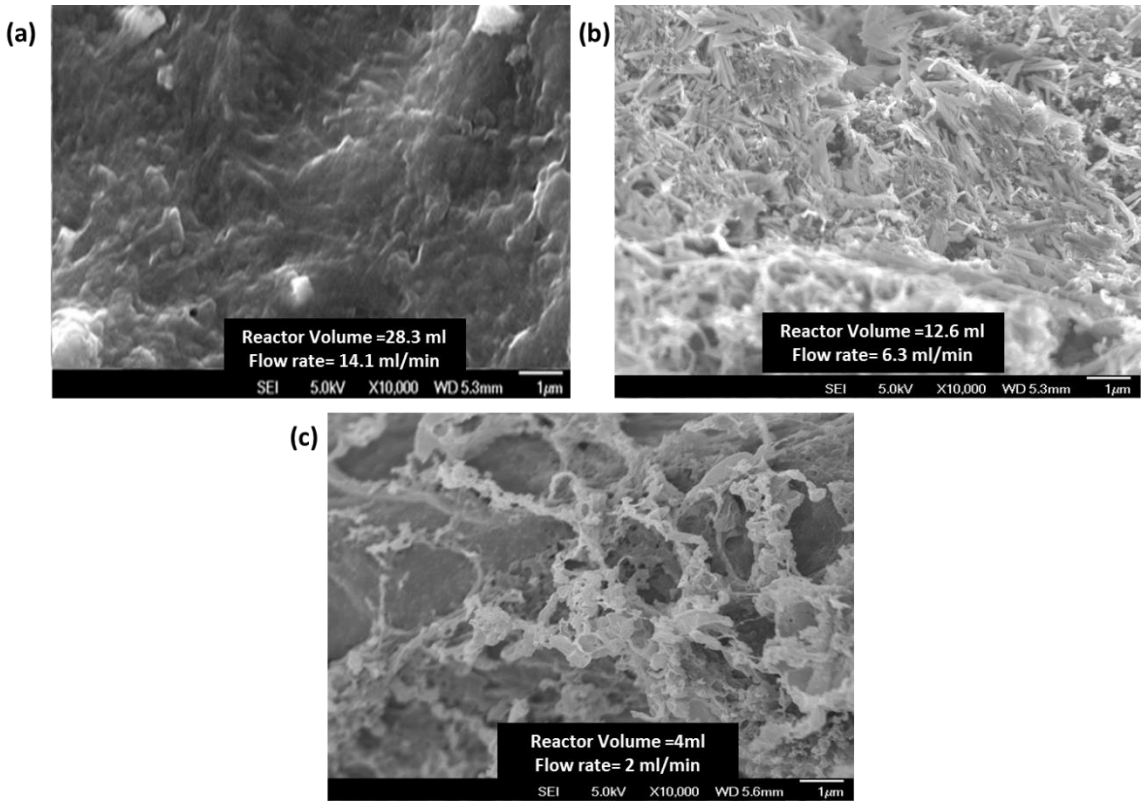

Figure 6.3: Scanning electron micrographs (x10, 000) of the anodic biofilms of MFC-BOD sensors of different volume and flow rate.

Hu et al. (2007) observed that low biofilm density along with increased porosity observed under low shear rates were expected to increase the diffusivity of substrate. In the case of MFC-BOD sensor, less diffusivity of substrate might decrease the mass transfer rate, and subsequently, lower the sensitivity of the sensor. The observation of Hu et al. (2007) was confirmed in this study, where denser biofilm of the 28.3-ml MFC-BOD sensor was less sensitive than that of the

12.6-ml MFC-BOD sensor. However, in the case of the 4-ml MFC-BOD sensor, scattered, fragile and patchy structure of biofilm might have reduced its sensitivity.

Besides analysing the anodic biofilm, SEM was used to observe the biological and chemical fouling of the PEM (Nafion membrane) after long-term operation of the MFC-BOD sensor (about1.5 years). Figure 6.4 shows the micrographs of the PEM, indicating biological (Fig. 6.4a) and chemical (Fig. 6.4b) fouling on the Nafion membrane.

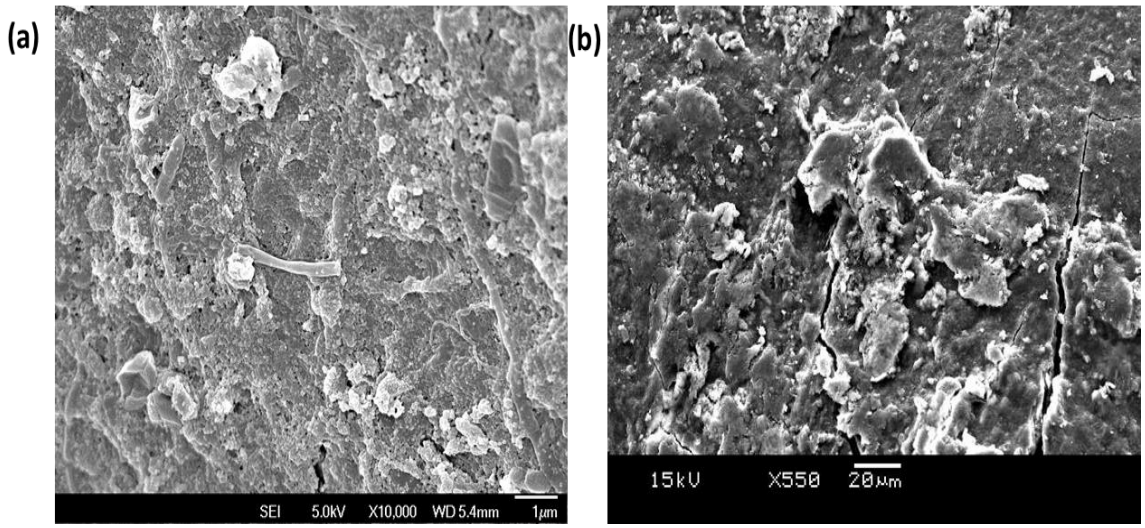

Figure 6.4: Scanning electron micrographs (x10, 000 and x550) of the PEM showing: (a) biological; and (b) chemical fouling on it.

The fouling on the membrane reduced the transfer of protons from the anode to cathode side and caused a decrease in the performance of the MFC-BOD sensor, which was shown by the results in chapter 4. This study suggested the need of changing the PEM after a long-term operation of the MFC-BOD sensor.

6.4 Elemental Analysis of anodic biofilm

Biomass present in the anodic biofilm was analysed to determine its elemental composition such as carbon (C), hydrogen (H), nitrogen (N) and sulphur (S).

Table 6.2 shows the CHNS composition of the anodic biofilm of MFC-BOD sensors with different volumes. All MFC-BOD sensors showed maximum carbon composition, which was probably due to the presence of acetate, the main BOD source for microorganisms. Other than the carbon, composition of other compounds was quite similar in every type of MFC-BOD sensor. The difference in the deposited carbon might be due to the ability of different biofilm to consume the carbon substrate.

Table 6.2: CHNS composition of MFC-BOD sensors with different anode volumes.

Sensor volume (ml)	C wt % (ppm)	H wt % (ppm)	N wt % (ppm)	S wt % (ppm)
28.3	39.10	5.07	5.11	1.91
12.6	41.58	5.00	5.39	1.73
4	51.69	4.85	4.57	1.88

6.5 Determination of metal ions in biofilm sludge

The MFC-BOD sensor may face adverse effects of toxicity present in wastewater in the form of heavy metals such as Cu^{2+}, Cd^{2+}, Ni^{2+}, Pb^{2+}, etc. The presence of a these toxic substances can potentially inhibit the metabolic activity of electrochemically-active bacteria and reduce the electron transfer eventually. For practical use of the MFC-BOD sensor, the effects of toxicity, if present, should be included as one of the influencing parameters. The effective concentration range of heavy metals in wastewater may vary from a small dose of 0.4 to as high as 12.5 ppm; however, clear mechanism of their inhibition effect on planktonic cells and electrochemically-active biofilm is still a matter of debate (Altaş, 2009; Kim

et al., 2007b; Patil et al., 2010). In order to check if heavy metals are deposited in the biofilm, the amount of metal ions present in the anodic biofilm were determined using ion chromatography. Table 6.3 shows the concentration of different heavy metals present in the biofilm.

Table 6.3: Composition of metal ions present in the biofilm of sensors of different anode volumes.

Sensor volume (ml)	Cu (ppm)	Zn (ppm)	Na (ppm)	Pb (ppm)	Ni (ppm)	Cd (ppm)
28.3	1.85	4.42	9.91	ND	< 0.10	ND
12.6	3.13	5.46	8.47	ND	< 0.10	ND
4	2.33	3.90	7.07	ND	< 0.10	ND

ND is the abbreviation for non-detected.

No Pb^{2+} and Cd^{2+} ions were detected in the biofilm, while Ni^{2+} less than 0.1 ppm was detected. The presence of low concentration of Ni^{2+} was expected because of its use (in the form of $NiCl_2.6H_2O$) on preparing the trace minerals solution for acetate based AWW (Balch et al., 1979; Lovley & Phillips, 1988). Similarly, Cu^{2+} and Zn^{2+} were also used in trace minerals solution in the form of $CuSO_4.5H_2O$ and $ZnSO_4$, respectively. However, the amount of Cu^{2+} deposited was too low to affect the activity of biofilm (Shen et al. 2013). Results clearly indicated that the MFC-BOD sensor was not affected by any kind of heavy metal toxicity; therefore, in this study, toxicity was not incorporated as one of the parameters influencing the MFC-BOD sensor performance.

6.6 FISH analysis

FISH analysis was performed in order to check the presence of exo-electrogens in the biofilm. *Geobacter sulfurreducens* was assumed as the representing community of exo-electrogens in anodic biofilm. In-situ hybridization was performed with the FISH probe of *Geobacter sulfurreducens* (termed as "GEO-2"), which has a total length of 19mers sequence, and was labelled at 5' end with CY3 dye (synthesized by Supernom Pte Ltd). The FISH data confirmed that exo-electrogens were abundantly present in the anode biofilm (Fig. 6.5). The *Geobacter sulfurreducens* were shown to be homogenously dispersed throughout the biofilm.

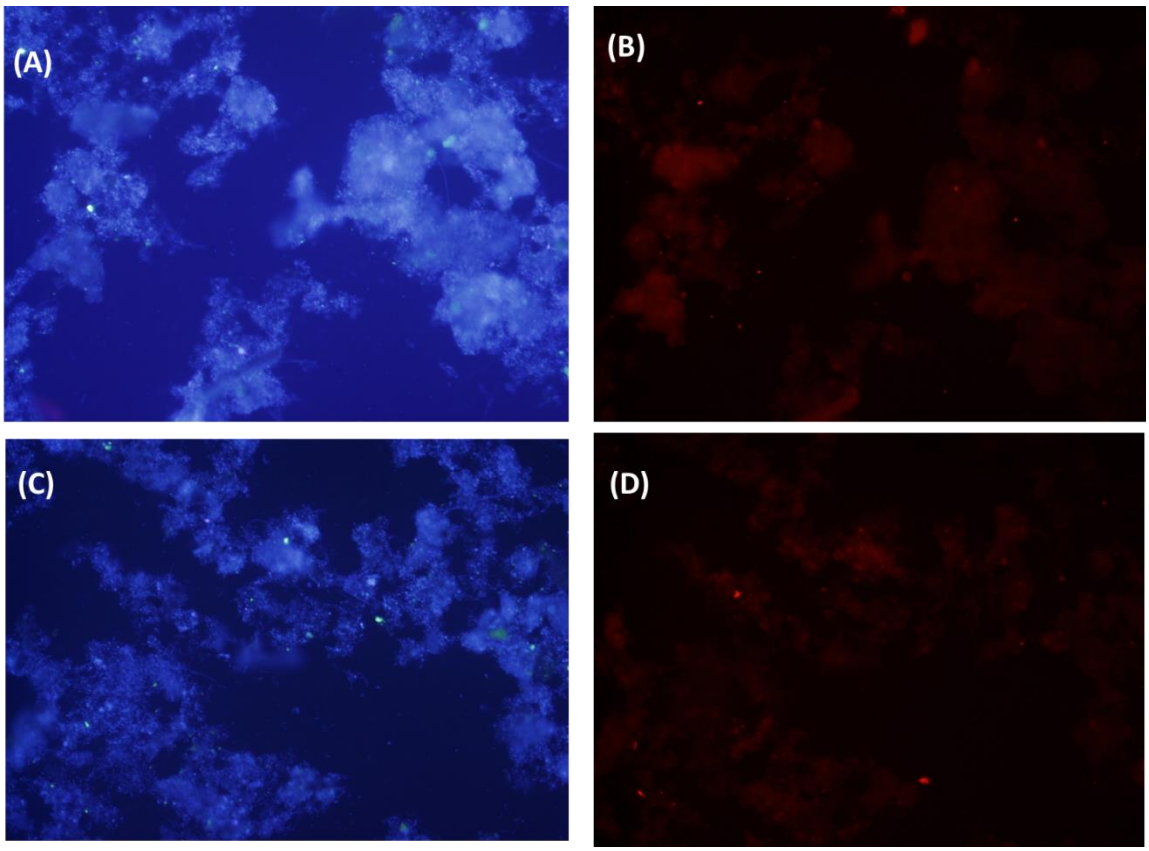

Figure 6.5: FISH images for anodic biofilm. (A) and C) shows all bacteria stained using DAPI. (B) and (D) shows *Geobacter sulfurreducens* stained using FISH probe (GEO-2, CY3).

6.7 Effect of environmental conditions

The voltage and current generation of MFC-BOD sensor is influenced by the environmental conditions such as temperature, conductivity and pH. Therefore, a correction factor (if applicable) should be incorporated to measurements done under different environmental conditions from the ones used in the calibration. In this study, the effects of different pH, conductivity and temperature on the MFC-BOD sensor were discussed. The focus of this part of the study was to estimate the change in the voltage and current generation under different environmental conditions.

6.7.1 Variation in pH

pH is one of the most important environmental factors that directly impacts the bacterial cell growth and physiology (Foster, 2000). In the case of MFC-BOD sensor, changes in the pH may affect voltage and current generation. In this study, pH of the feed was allowed to vary between 6.5 and 8.5. Figure 6.6 shows the effect of pH on voltage generation at different BOD_5 values. Three different BOD_5 values of 145 ± 6, 75 ± 6 and 30 ± 6 mg/L were applied using AWW, considering high, medium and low range of BOD_5 concentration. Increase in the voltage was observed during the pH change from 6.5 to 7.5; while voltage decreased when H^+ concentration decreased (pH 8 and 8.5). The normal pH of the feed was 7.30 ± 0.4.

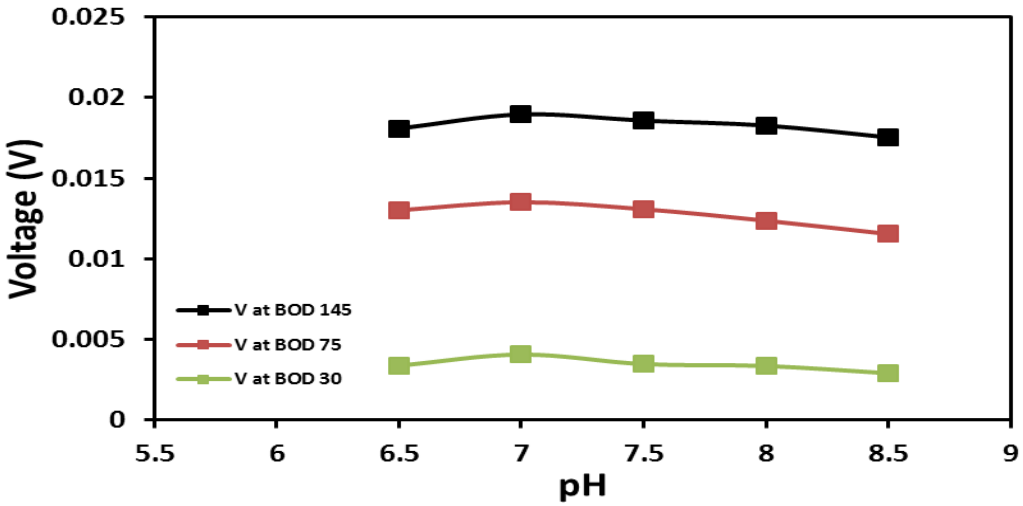

Figure 6.6: Change in the voltage generation of MFC-BOD sensor under different pH conditions and BOD_5 concentrations.

Results were consistent with those of Peixoto et al. (2011) who recorded the highest current between the pH 7-7.5, and with Gil et al. (2003) who concluded that the highest current was observed between the pH 7-8, and the decrease in current was found before and after that pH range. Low voltage generation at pH 8 and 8.5 was probably due to less proton transfer at reduced proton concentration gradient across the PEM, which further increased the internal resistance of the MFC-BOD sensor.

The internal resistance of the MFC-BOD sensor at different pH conditions was measured by the polarization curve, while the effects of pH on current and power generation were confirmed by the power-current curve. Figure 6.7 shows the P_{max} obtained at different pH values. The MFC-BOD sensor measured the highest P_{max} of 0.320 mW at a pH of 7, while it gradually decreased at a pH 7.5 (0.305 mW). The lowest P_{max} was measured at the pH of 8.5. This reconfirmed the results obtained by Peixoto et al. (2011), who found the maximum current density at pH 7. However, in other study, Jadhav et al. (2009) observed the maximum current density at pH of 6.5; although, their results were based on the batch system.

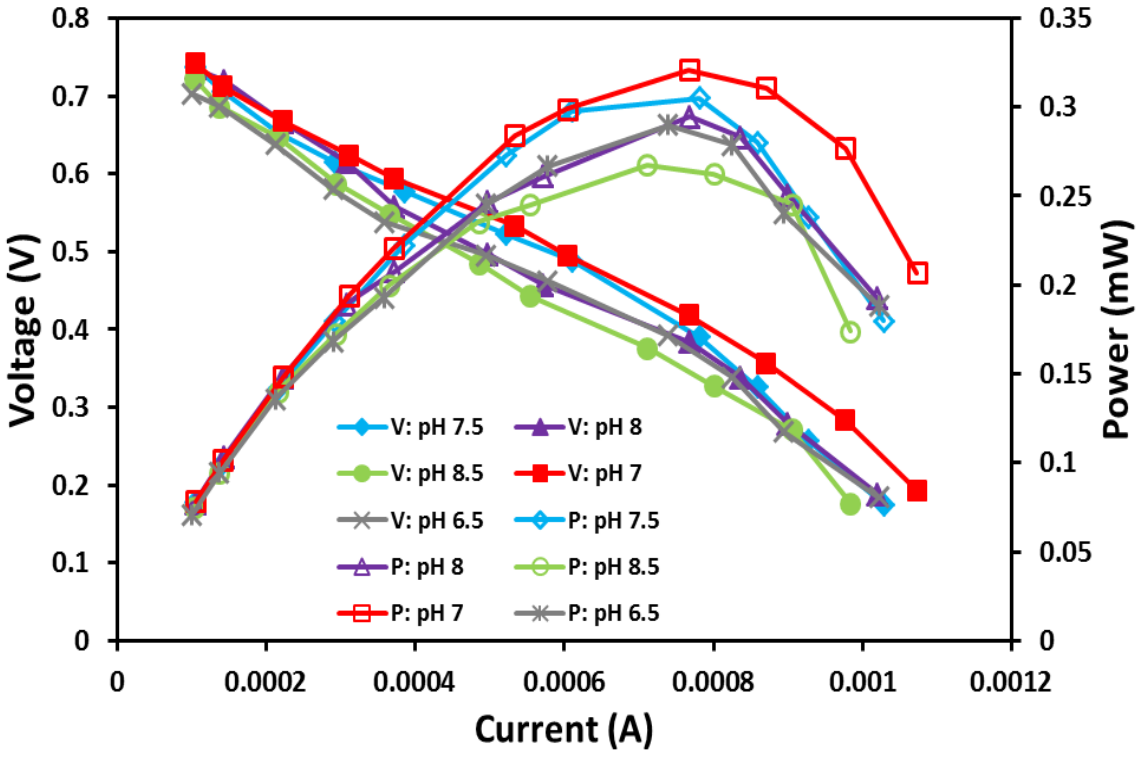

Figure 6.7: Polarization curve (closed symbols) and power-current curve (open symbols) at different pH exposure.

The effects of pH in voltage or current generation could be explained by the internal resistance. Slope of the polarization curve is referred as the internal resistance (R_{int}) of the MFC-BOD sensor, which includes ohmic resistance, activation loss and concentration polarization (Fan et al., 2008). It was clearly seen from Figure 6.7 that the change (drop or increase) in power was due to the change in the $R_{int,}$ which had the lowest value of $523 \pm 4\ \Omega$ at pH 7. The increase in pH caused an increase in the R_{int} to an average value of $571 \pm 6\ \Omega$ (at pH 8.5), and subsequently, decreased the power. The proton concentration at the anode side was decreased at higher pH (8 and 8.5) and limited proton transfer to the cathode side, which helped in increasing internal resistance of the sensor and decreasing the voltage and power generation of the MFC-BOD sensor.

6.7.2 Effect of operating temperature

The performance of the MFC-BOD sensor could be affected by the temperature as it can affect bacterial kinetics and the rate of mass transfer of protons through the liquid. The temperature of the feed was allowed to vary between four different ranges: of 20-22, 25-27, 30-32 and 34-36^{o}C, where 30-32^{o}C was measured as the ambient temperature of the laboratory and it worked as the control temperature. Figure 6.8 shows the effects of temperature in voltage and current generation at different BOD_5 concentrations. Three different BOD_5 values 145±6 mg/L, 75±6 mg/L and 30±6 mg/L were applied using AWW, considering high, medium and low range of BOD_5 concentration. A decrease in the produced voltage was seen during the lower temperature range of 20-22^{o}C, while maximum voltage generation was recorded at the highest temperature range of 34-36^{o}C. The effects of temperature were more prominent with higher BOD_5 concentration. These results were in consistent with those of Peixoto et al. (2011) who observed maximum current generation at the temperature of 35^{o}C, and with those of Liu et al. (2005) who reported higher power generation for a continuous MFC at 32^{o}C.

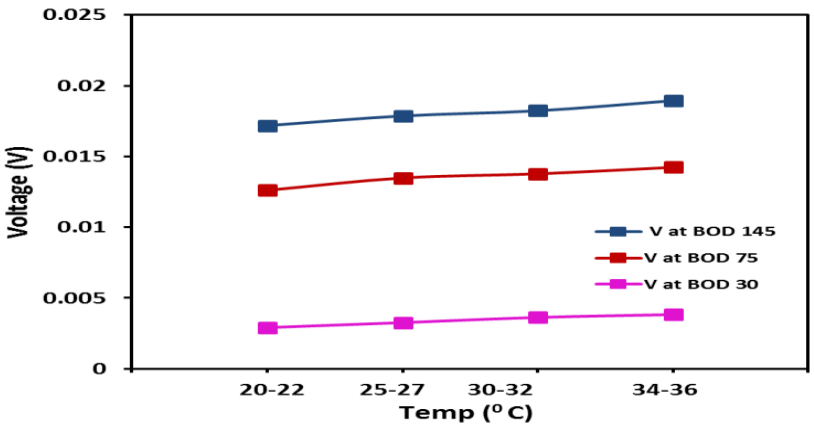

Figure 6.8: Change in the voltage generation by sensor under different temperature ranges and BOD_5 concentrations.

Figure 6.9 shows the maximum power obtained at different temperature ranges. It was observed that the open circuit voltage was almost same at every temperature range; yet, there was a significant change in the maximum power. The polarization curve explained it clearly that the power drop was not because of the E_{emf}, but due to an increase in the R_{int}, which was equaled to 572±5 Ω at the temperature range of 20-22^{o}C. The increase in R_{int} at low temperature range could be related to the slowdown of microbial metabolism, membrane permeability and an increase in the ohmic resistance due to a lower mass transfer rate in the liquid. The MFC-BOD sensor was measured with the highest P_{max} of 0.316±0.05 mW and the lowest R_{int} of 523±4 Ω at the temperature range of 34-36^{o}C, while it was lowered at the ambient temperature range of 30-32^{o}C (0.305±0.05 mW).

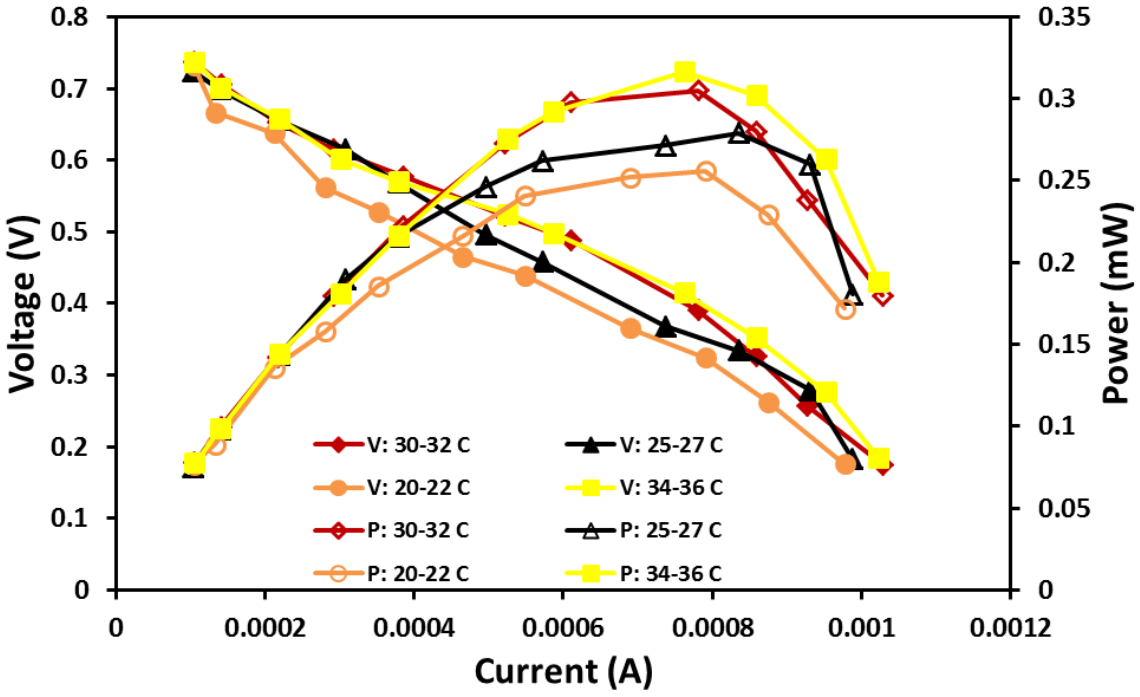

Figure 6.9: Polarization curve (closed symbols) and power-current curve (open symbols) under different operating temperature ranges

6.7.3 Effect of conductivity

An important limitation of MFC is related to the slow rate of proton transfer (Lefebvre et al., 2011). This could be improved by increasing the conductivity of the system. In the anode chamber of an MFC, increasing the conductivity might induce antagonistic effects - on the one hand increasing the conductivity of the system, but on the other hand affecting the physiology of the biofilm (Lefebvre et al., 2012). In this study, NaCl was added in order to yield different conductivity ranging from the control of 5 ms/cm to 30 mS/cm for investigating the response of MFC-BOD sensor against extreme ionic strength. Figure 6.10 shows the change in the produced voltage at different BOD_5 values with increasing conductivity. Three different BOD_5 concentrations of 145±6, 75±6 and 30±6 mg/L were applied to estimate the effects of conductivity in voltage and current generation. The current density increased with the conductivity of wastewater in the range of 5 to 20 mS/cm, from 0.0180 to 0.0192 V, respectively, at a BOD of 145±6; while voltage decreased to 0.0171 V at a conductivity of 30 mS/cm.

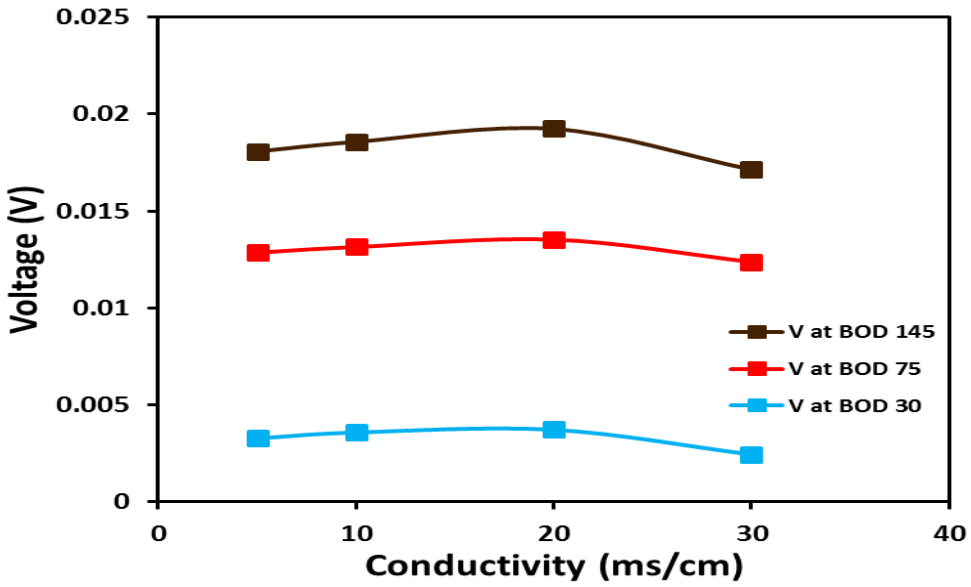

Figure 6.10: Change in the voltage generation by the MFC-BOD sensor under different conductivity and BOD_5 concentrations.

Figure 6.11 shows a comparison of the polarization curves of the MFC-BOD sensors operated with wastewater of different conductivity. The polarization behaviour was different and substantial differences were observed in both the internal resistance (represented by the slope) and the maximum power. In the absence of added conductivity (apart from the original conductivity of 5 ms/cm of AWW), the E_{emf} and R_{int} was 0.70 ± 0.1 V and 522 ± 5 Ω, respectively, resulting in a P_{max} of 0.297±0.05 mW. The E_{emf} was unaffected by the increase in conductivity (20 ms/cm), whereas the R_{int} decreased to 474 ± 3 Ω, resulting the highest P_{max} of 0.324± 0.05 mW. However, further increment in the conductivity (30 ms/cm) resulted in 14% decrease in the P_{max} (0.251± 0.05 mW) and 11% increase in the R_{int} (540 ± 5 Ω). This confirmed the trends observed with increment of conductivity by Lefebvre et al. (2011) and Liu et al. (2005).

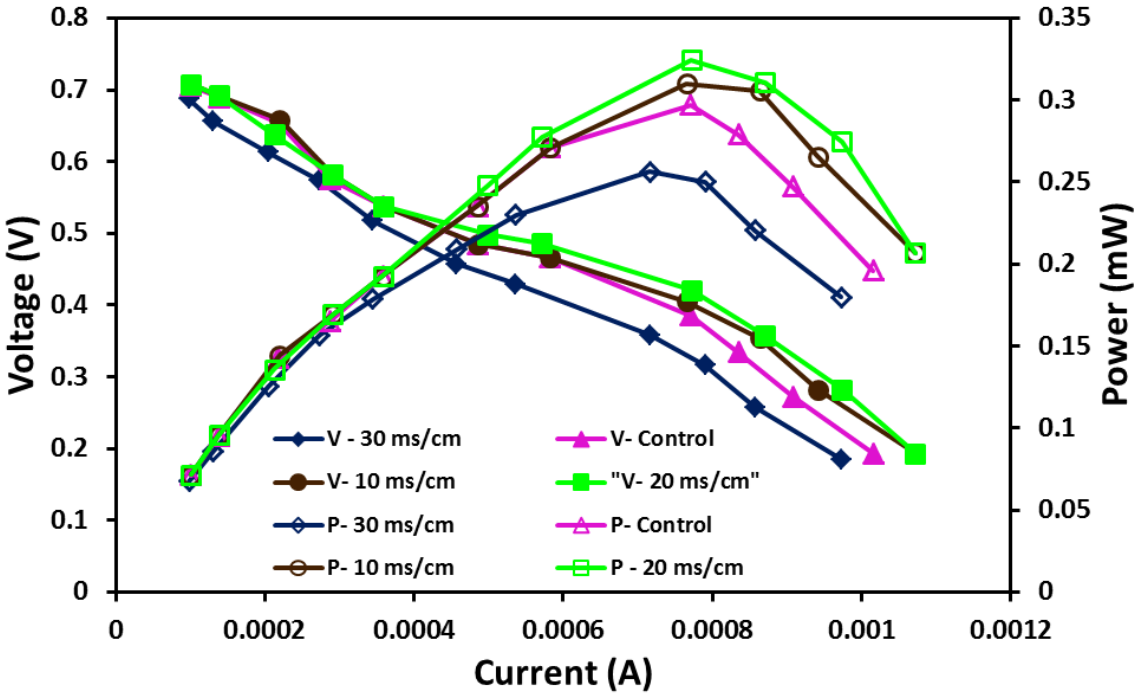

Figure 6.11: Polarization curve (closed symbols) and power-current curve (open symbols) at different conductivity.

The results showed that increasing conductivity up to 20 ms/cm enhanced the power generation, but higher conductivity had detrimental impact to the MFC-BOD sensor, indicating relatively low tolerance of anodophilic bacteria to extreme ionic strength (30 ms/cm).

6.8 Effect of anolyte recirculation

With an assumption that the recirculation of anolyte could increase the mixing (Zhang et al., 2010) and improve the performance of the MFC-BOD sensor, the effects of recirculating the anolyte were examined. The R_{int} and P_{max} of the MFC-BOD sensor were measured during the stage of recirculation by the polarization and power-current curves, respectively (Fig. 6.12). The R_{int} during the recirculation condition (500 Ω) dropped to 5% of the R_{int} under normal condition (no recirculation), resulting in a slight increase in the P_{max} (0.291 mW with recirculation and 0.283 mW without recirculation). No change in the E_{emf} at both the conditions indicated that the recirculation of anolyte could not increase the maximum voltage generation, although recirculation helped to maintain a low ohmic resistance.

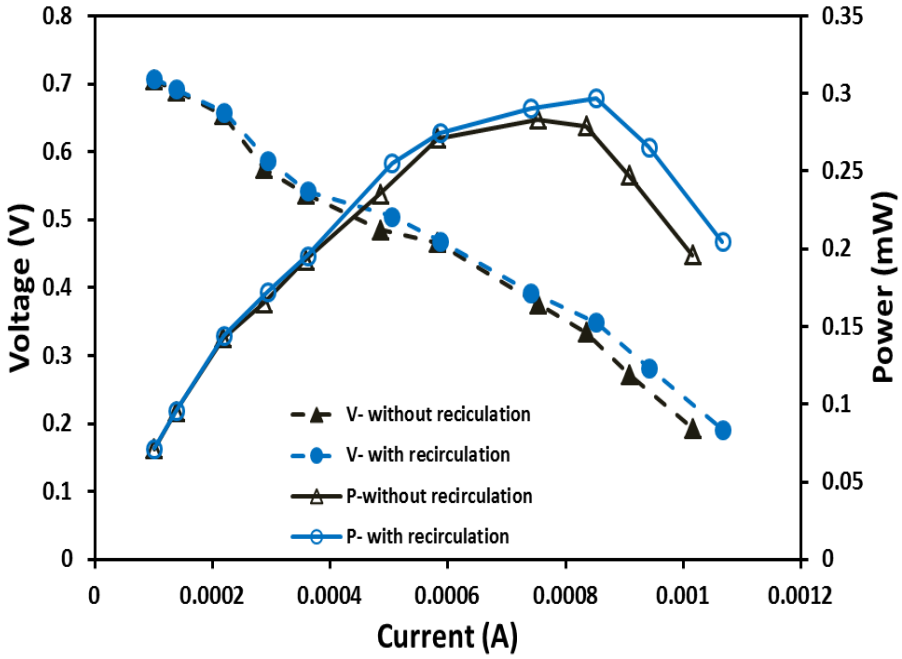

Figure 6.12: Polarization curve (closed symbols) and power-current curve (open symbols) during recirculation and no recirculation conditions.

Lowered R_{int} and improved P_{max} under the recirculation of feed motivated us to check the performance of MFC-BOD sensor by estimating its response to frequent change in BOD_5 concentration of influent during the recirculation process. The change in BOD_5 concentration of influent solution and produced voltage was measured at every hour (Fig. 6.13a). A close proximity between the changed BOD_5 and generated voltage at every hour was measured, suggesting quick response (in 1 h) of the MFC-BOD sensor against changes in the BOD_5 concentration. The probable reason for better response of the MFC-BOD sensor was the shear effects generated due to the recirculation, resulting in better diffusivity of substrate to the biofilm (Pham et al., 2008).

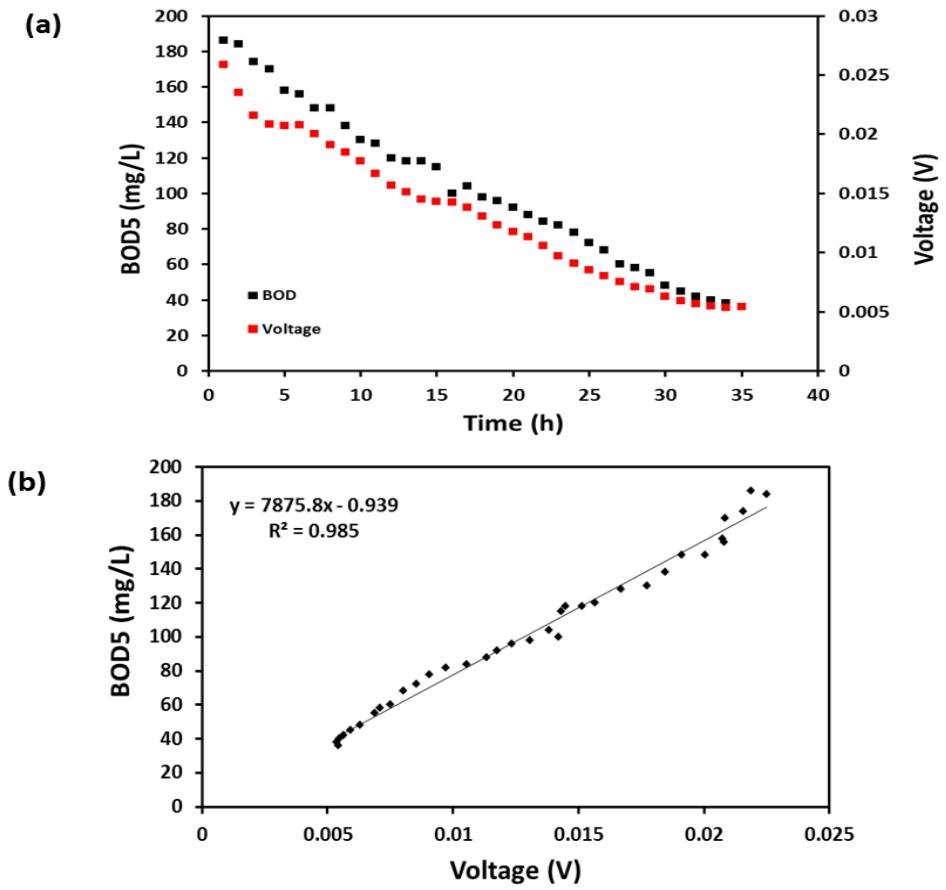

Figure 6.13: Relationship between the generated voltage and BOD_5 during the anolyte recirculation. (a) The pattern of change in BOD_5 concentration and generated voltage with time. (b) Linear relationship between the BOD_5 and generated.

The generated voltage decreased gradually over the time period of 35 h, because of reduction in BOD_5 concentration due to biodegradation by the microorganisms in the MFC-BOD sensor under recirculation mode. A linear relationship between the BOD_5 and generated voltage at every 1 h was determined (Fig. 6.13b). Several BOD_5 concentrations ranging from 190-36 mg/L were calibrated with the produced voltage. With the high regression coefficient of R^2 = 0.98, the MFC-BOD sensor showed a robust linear relationship between BOD_5 and the produced voltage. This study showed that the performance of the MFC-BOD sensor improved due to lower ohmic resistance and better diffusion of substrates to

biofilm, and indicated a suitable role of MFC-BOD sensor in the applications where influent BOD fluctuates frequently.

7. Conclusions and Recommendations

7.1 Conclusions

The purpose of this study was to demonstrate the feasibility of MFC-BOD sensor for on-line measurement of BOD in wastewater. The MFC-BOD sensor had the characteristics of quick response, high accuracy and sensitivity, simple to perform, inexpensive and long-term stability.

A single-chambered MFC was designed and constructed using MnO_2 (α, β, and γ-MnO_2) catalyst in place of expensive Pt catalyst. The performance of the MnO_2-catalyst-based-cathode MFC was investigated and compared with the Pt-catalyst-based-cathode MFC. The results showed that the β- and γ-MnO_2-catalyst-based-cathode MFCs generated comparable amount of power with that using Pt catalyst. Considering the lower cost of catalyst MnO_2 and the comparable performance, the β-MnO_2 and γ-MnO_2-based MFC were further explored as MFC-BOD sensor.

Towards the development of a potential MFC-BOD sensor, both β- and γ-MnO_2-catalyst-based-cathode MFC-BOD sensors were calibrated between the voltage and several BOD_5 concentrations. The impact of catalyst and DWW on the performance of the MFC-BOD sensor was investigated. The impact of catalyst on the performance of the MFC-BOD sensor was examined using AWW. The results showed the superiority of the β-MnO_2-MFC-BOD sensor over the γ-MnO_2-MFC-BOD sensor in terms of sensitivity and stability over time. This was supported by the improved crystallographic structure of the β-MnO_2-catalyst, which allowed better adsorption of O_2 on its surface and overall higher catalytic activity. In the case of MFC-BOD sensor, this translated into a stronger and more stable signal.

The applicability of MFC-BOD sensors was verified with real DWW and β-MnO_2-MFC-BOD sensor exhibited good performance with a regression coefficient of r^2 of 0.93 after 1.5 years. The performance of the MFC-BOD sensor dropped with DWW due to a lower mass transfer rate with DWW. The compliance of the BOD_5 values as predicted by the MFC-BOD sensors (BODp) with conventional BOD_5 was determined using 5 random samples of DWW after 1.5 years, using the calibration curves obtained at that time. The β-MnO_2-type-MFC-BOD sensors exhibited an impressive performance by establishing a close compliance between BODp and BOD_5 with slight variations of only ± 3 to 12%. Inexpensive manufacturing and maintenance cost, and reliable operational stability of the MnO_2-type-BOD-MFC sensors indicated their potential to substitute the conventional BOD_5 methods, which takes a much longer analytical time of 5 days and suffers from huge variability. However, the MFC-BOD sensor's performance was still needed to be further improved in terms of response time and sensitivity.

A sequential optimization strategy was applied to lower the response time and increase the sensitivity of the MFC-BOD sensor. This approach dealt with the concept of varying one parameter at one time, while keeping other parameters unchanged. Sequential optimization of the MFC-BOD sensor was completed in five steps – HRT optimization, volume optimization, choice of PEM, cathode catalyst and anode material. The HRT optimization was done with a view of achieving quick response time and "true" BOD measurement. Minimum BOD removal rate of 6% was obtained at a HRT of 2 min, allowing the MFC-BOD sensor to measure almost the same BOD concentration which was fed as influent. Increased electrochemical activity of microorganisms due to a lower HRT (2 min)

helped in decreasing the response time to 2-4 h for different BOD concentrations. Still with a view of checking sensor's performance at any fixed time interval, instead of waiting for the time to reach the maximum steady-state voltage, the voltage was recorded at the exact time period of 30, 60, 90 and 120 min. The rate of change in voltage with respect to the change in BOD determined the sensitivity of the MFC-BOD sensor. The voltage pattern of the MFC-BOD sensor with the anodic volume of 12.6 ml showed that MFC-BOD sensor has quick response time in both up-shift and down-shift. It was assumed that smaller volume of MFC reactor might have helped increase the electrochemical activity of biofilm due to the higher mass transfer rate. This was later confirmed by the biofilm analysis, which showed that the porous biofilm structure of the MFC-BOD sensor with a volume of 12.6 ml allowed better diffusivity of substrate and enabled higher mass transfer. A decrease in the volume of MFC-BOD sensor (from 28.3 to 12.6 ml) improved the sensitivity of sensor (± 6 to ± 4.8 %). Nafion membrane performed better than the Selemion membrane as a PEM because it enabled improved sensitivity and better linearity between the voltage and BOD_5 concentration. Higher selectivity for protons and better conductivity of the Nafion membrane made it a more suitable candidate for PEM. Higher catalytic activity of Pt, in spite of higher cost, convinced us to compare the performance of Pt-MFC-BOD sensor with β-MnO_2-MFC-BOD sensor. Pt-MFC-BOD sensor performed better with higher regression coefficient (R^2 = 0.95 at the response time of 120 min) and improved sensitivity ($\pm$ 3.4%). The comparison of graphite and the carbon cloth was the last step of the sequential optimization approach. The use of graphite as an anode material provided better conductivity and significantly improved the performance of the MFC-BOD sensor by high voltage generation, faster response

time (120 min) and better sensitivity (± 0.2%). As a result of sequential optimization, the optimized MFC-BOD sensor was determined to be with a volume of 12.6 ml, HRT of 2 min, Nafion membrane as PEM, Pt as cathode catalyst and graphite as an anode material.

The compliance of the BOD_5 values as predicted by the optimized MFC-BOD sensor (BODp) with conventional BOD_5 was determined using some random samples of DWW and the calibration curve (at a response time of 120 min) obtained by the optimized sensor. Excellent compliance between the intermediate ranges (40-110 mg/L) of BOD_5 with small standard deviation of 3-13% showed the great potential of the MFC-BOD sensor for practical applications.

The behaviour of the electrochemically-active biofilm was a key parameter of the MFC-BOD sensor. Since the characteristics of biofilm changes over time, a proportion of live and dead cells in the biofilm of different ages were estimated using flow cytometry. A decrease in the number of live cells (92 to 44%) in the period of 1 month to 1 year was observed, which was also reflected as the drop in the performance of MFC-BOD sensor over that time period. Since, the structure of biofilm also plays a significant role in the performance of MFC-BOD sensor, the thickness and density of biofilm were analysed. It was observed that MFC-BOD sensor with bigger volume could produce an anodic biofilm that was less thick, highly dense, less porous, and displayed less sensitivity to BOD concentrations. Ion chromatography showed no (or permissible) detection of heavy metal ions in the biofilm sludge and clearly indicated that the MFC-BOD sensor was not affected by any kind of heavy metal toxicity in this study.

For a wide application of MFC-BOD sensor, it was important to evaluate the performance of the sensor at different environmental conditions such as, operating temperature, anodic pH and conductivity. Certain ranges of these conditions could affect the voltage and power generation. Thus, a correction factor should be applied to measurements done under different environmental conditions from the ones used in the calibration.

7.2 Recommendations

The major limitation of using biofilm as sensing material is the lower diffusion of substrate within the every layer of biofilm, resulting in a slow response of the MFC-BOD sensor. In-depth investigation of the mass transfer rate and diffusion of substrate within the biofilm would give more information on the interpretation of the voltage output signal. The enrichment of biofilm with real wastewater instead of AWW may help microorganisms to consume more complex compunds such as proteins and carbohydrates. Besides, the role of hydraulics in the development of biofilm and performance of BOD sensor should be investigated.

For the use of MFC-BOD sensor with wastewater coming from different sources (such a pharmaceutical wastewater, industrial effluent, etc.), which may have toxicity present in the form of either heavy metals or other volatile organic compound, the effects of toxicity in the performance of MFC-BOD sensor should be included as one of the influencing parameters.

In order to allow an accurate measurement by the MFC-BOD sensor for a long period of time, the exact frequency of re-calibration of MFC-BOD sensor should be evaluated. This will help to maintain a good proportionality between BOD_5 and the recorded voltage at all times.

A detailed study on the effects of anode or cathode potential in the performance of MFC-BOD sensor is required. Use of a reference electrode and a potentiaostat enable the control of anode potential. Change in the anode potential and its effect in the response time of anodic biofilm should be investigated.

The performance of BOD sensor should be examined for the higher range of BOD concentration, especially for the concentration of influent wastewater which is coming to the treatment plant. Future study is required for decreasing the response time to few mintues and developing more compact and portable design of BOD sensor.

References

Altaş, L. (2009) Inhibitory effect of heavy metals on methane-producing anaerobic granular sludge. Journal of Hazardous Materials 162(2–3), 1551-1556.

APHA (2005) Standard Methods for the Examination for Water and Wastewater, 21st ed. APHA, Washington DC, USA.

Barbir, F. (2013) PEM Fuel Cells. Elsevier Academic Press, Amsterdam.

Beliaev, A.S., Saffarini, D.A., McLaughlin, J.L. and Hunnicutt, D. (2001) MtrC, an outer membrane decahaem c cytochrome required for metal reduction in Shewanella putrefaciens MR-1. Mol Microbiol 39(3), 722-730.

Bennetto, H.P., Delaney, G.M., Mason, J.R., Roller, S.D., Stirling, J.L. and Thurston, C.F. (1985) The sucrose fuel cell: Efficient biomass conversion using a microbial catalyst. Biotechnology Letters 7(10), 699-704.

Berney, M., Hammes, F., Bosshard, F., Weilenmann, H.U. and Egli, T. (2007) Assessment and interpretation of bacterial viability by using the LIVE/DEAD BacLight Kit in combination with flow cytometry. Appl Environ Microbiol 73(10), 3283-3290.

Blum, L.J. and Coulet, P.R. (1991) Biosensor Principles and Applications, New York.

Bond, D.R. and Lovley, D.R. (2003) Electricity Production by Geobacter sulfurreducens Attached to Electrodes. Applied and Environmental Microbiology 69(3), 1548-1555.

Bond, D.R., Holmes, D.E., Tender, L.M. and Lovley, D.R. (2002) Electrode-reducing microorganisms that harvest energy from marine sediments. Science 295(5554), 483-485.

Boulos, L., Prevost, M., Barbeau, B., Coallier, J. and Desjardins, R. (1999) LIVE/DEAD BacLight : application of a new rapid staining method for direct enumeration of viable and total bacteria in drinking water. J Microbiol Methods 37(1), 77-86.

Bourgeois, W., Burgess, J.E. and Stuetz, R.M. (2001) On-line monitoring of wastewater quality: A review. Journal of Chemical Technology and Biotechnology 76(4), 337-348.

Chae, K.J., Choi, M., Ajayi, F.F., Park, W., Chang, I.S. and Kim, I.S. (2007) Mass Transport through a Proton Exchange Membrane (Nafion) in Microbial Fuel Cells†. Energy & Fuels 22(1), 169-176.

Chan, C., Lehmann, M., Tag, K., Lung, M., Kunze, G., Riedel, K., Gruendig, B. and Renneberg, R. (1999) Measurement of biodegradable substances using the

salt-tolerant yeast Arxula adeninivorans for a microbial sensor immobilized with poly(carbamoyl) sulfonate (PCS) Part I: Construction and characterization of the microbial sensor. Biosens Bioelectron 14(2), 131-138.

Chang, I.S., Jang, J.K., Gil, G.C., Kim, M., Kim, H.J., Cho, B.W. and Kim, B.H. (2004) Continuous determination of biochemical oxygen demand using microbial fuel cell type biosensor. Biosensors & Bioelectronics 19(6), 607-613.

Chang, I.S., Moon, H., Jang, J.K. and Kim, B.H. (2005) Improvement of a microbial fuel cell performance as a BOD sensor using respiratory inhibitors. Biosensors and Bioelectronics 20(9), 1856-1859.

Chaudhuri, S.K. and Lovley, D.R. (2003) Electricity generation by direct oxidation of glucose in mediatorless microbial fuel cells. Nat Biotechnol 21(10), 1229-1232.

Chee, G.J., Nomura, Y., Ikebukuro, K. and Karube, I. (1999) Development of highly sensitive BOD sensor and its evaluation using preozonation. Analytica Chimica Acta 394(1), 65-71.

Chee, G.J., Nomura, Y., Ikebukuro, K. and Karube, I. (2000) Optical fiber biosensor for the determination of low biochemical oxygen demand. Biosens Bioelectron 15(7-8), 371-376.

Chee, G.J., Nomura, Y., Ikebukuro, K. and Karube, I. (2001) Biosensor for the evaluation of biochemical oxygen demand using photocatalytic pretreatment. Sensors and Actuators, B: Chemical 80(1), 15-20.

Chen, M., Zhang, F., Zhang, Y. and Zeng, R.J. (2013) Alkali production from bipolar membrane electrodialysis powered by microbial fuel cell and application for biogas upgrading. Applied Energy 103(0), 428-434.

Chen, S., Liu, G., Zhang, R., Qin, B. and Luo, Y. (2012) Development of the Microbial Electrolysis Desalination and Chemical-Production Cell for Desalination as Well as Acid and Alkali Productions. Environmental Science & Technology 46(4), 2467-2472.

Cheng, F.Y., Su, Y., Liang, J., Tao, Z.L. and Chen, J. (2010) MnO2-Based Nanostructures as Catalysts for Electrochemical Oxygen Reduction in Alkaline Media. Chemistry of Materials 22(3), 898-905.

Cheng, S., Liu, H. and Logan, B.E. (2006a) Increased Power Generation in a Continuous Flow MFC with Advective Flow through the Porous Anode and Reduced Electrode Spacing. Environmental Science & Technology 40(7), 2426-2432.

Cheng, S., Liu, H. and Logan, B.E. (2006b) Power densities using different cathode catalysts (Pt and CoTMPP) and polymer binders (Nafion and PTFE) in single chamber microbial fuel cells. Environmental Science and Technology 40(1), 364-369.

Chhina, H., Campbell, S. and Kesler, O. (2006) An oxidation-resistant indium tin oxide catalyst support for proton exchange membrane fuel cells. Journal of Power Sources 161(2), 893-900.

Clair, N.S.P., L. McCarty ; Gene, F. Parkin (2003) Chemistry for Environmental Engineering and Science McGraw-Hill, New York.

Clauwaert, P., Aelterman, P., Pham, T.H., De Schamphelaire, L., Carballa, M., Rabaey, K. and Verstraete, W. (2008) Minimizing losses in bio-electrochemical systems: the road to applications. Appl Microbiol Biotechnol 79(6), 901-913.

Daniels, J.S. and Pourmand, N. (2007) Label-Free Impedance Biosensors: Opportunities and Challenges. Electroanalysis 19(12), 1239-1257.

Davila, D., Esquivel, J.P., Sabate, N. and Mas, J. (2011) Silicon-based microfabricated microbial fuel cell toxicity sensor. Biosens Bioelectron 26(5), 2426-2430.

Di Lorenzo, M., Curtis, T.P., Head, I.M. and Scott, K. (2009) A single-chamber microbial fuel cell as a biosensor for wastewaters. Water Research 43(13), 3145-3154.

D'Souza, S.F. (2001) Microbial biosensors. Biosensors and Bioelectronics 16(6), 337-353.

Ekström, H., Wickman, B., Gustavsson, M., Hanarp, P., Eurenius, L., Olsson, E. and Lindbergh, G. (2007) Nanometer-thick films of titanium oxide acting as electrolyte in the polymer electrolyte fuel cell. Electrochimica Acta 52(12), 4239-4245.

Fan, Y., Sharbrough, E. and Liu, H. (2008) Quantification of the Internal Resistance Distribution of Microbial Fuel Cells. Environmental Science & Technology 42(21), 8101-8107.

Foster, J. (2000) Microbial responses to acid stress, ASM Press, Washington, DC.

Gaberlein, S., Spener, F. and Zaborosch, C. (2000) Microbial and cytoplasmic membrane-based potentiometric biosensors for direct determination of organophosphorus insecticides. Appl Microbiol Biotechnol 54(5), 652-658.

Gautschi, G. (2002) Piezoelectric sensorics: Force, strain, pressure, acceleration and acoustic emission sensors, materials and amplifiers, Springer-Verlag, Berlin.

Gil, G.C., Chang, I.S., Kim, B.H., Kim, M., Jang, J.K., Park, H.S. and Kim, H.J. (2003) Operational parameters affecting the performance of a mediator-less microbial fuel cell. Biosensors and Bioelectronics 18(4), 327-334.

Grzebyk, M. and Poźniak, G. (2005) Microbial fuel cells (MFCs) with interpolymer cation exchange membranes. Separation and Purification Technology 41(3), 321-328.

Gurung, A., Kim, J., Jung, S., Jeon, B.H., Yang, J.E. and Oh, S.E. (2012) Effects of substrate concentrations on performance of serially connected microbial fuel cells (MFCs) operated in a continuous mode. Biotechnol Lett 34(10), 1833-1839.

Han, T.-S., Kim, Y.-C., Sasaki, S., Yano, K., Ikebukuro, K., Kitayama, A., Nagamune, T. and Karube, I. (2001) Microbial sensor for trichloroethylene determination. Analytica Chimica Acta 431(2), 225-230.

Han, T.S., Sasaki, S., Yano, K., Ikebukuro, K., Kitayama, A., Nagamune, T. and Karube, I. (2002) Flow injection microbial trichloroethylene sensor. Talanta 57(2), 271-276.

Hays, S., Zhang, F. and Logan, B.E. (2011) Performance of two different types of anodes in membrane electrode assembly microbial fuel cells for power generation from domestic wastewater. Journal of Power Sources 196(20), 8293-8300.

He, Z. and Angenent, L.T. (2006) Application of bacterial biocathodes in microbial fuel cells. Electroanalysis 18(19-20), 2009-2015.

He, Z., Minteer, S.D. and Angenent, L.T. (2005) Electricity generation from artificial wastewater using an upflow microbial fuel cell. Environ Sci Technol 39(14), 5262-5267.

Heilmann, J. and Logan, B.E. (2006) Production of electricity from proteins using a microbial fuel cell. Water Environ Res 78(5), 531-537.

Hikuma, M., Suzuki, H., Yasuda, Y., Karube, I. and Suzuki, S. (1979) Amperometric estimation of BOD by using living immobilized yeasts. European journal of applied microbiology and biotechnology 8(4), 289-297.

Holmes, D.E., Bond, D.R., O'Neil, R.A., Reimers, C.E., Tender, L.R. and Lovley, D.R. (2004) Microbial communities associated with electrodes harvesting electricity from a variety of aquatic sediments. Microb Ecol 48(2), 178-190.

Holmes, D.E., Nicoll, J.S., Bond, D.R. and Lovley, D.R. (2004) Potential role of a novel psychrotolerant member of the family Geobacteraceae, Geopsychrobacter electrodiphilus gen. nov., sp. nov., in electricity production by a marine sediment fuel cell. Appl Environ Microbiol 70(10), 6023-6030.

Hu, Z., Jin, J., Abruna, H.D., Houston, P.L., Hay, A.G., Ghiorse, W.C., Shuler, M.L., Hidalgo, G. and Lion, L.W. (2007) Spatial distributions of copper in microbial biofilms by scanning electrochemical microscopy. Environ Sci Technol 41(3), 936-941.

Hyun, C.K., Tamiya, E., Takeuchi, T. and Karube, I. (1993) A novel BOD sensor based on bacterial luminescence. Biotechnol Bioeng 41(11), 1107-1111.

Ieropoulos, I., Winfield, J. and Greenman, J. (2010) Effects of flow-rate, inoculum and time on the internal resistance of microbial fuel cells. Bioresource Technology 101(10), 3520-3525.

Ieropoulos, I.A., Greenman, J., Melhuish, C. and Hart, J. (2005) Comparative study of three types of microbial fuel cell. Enzyme and Microbial Technology 37(2), 238-245.

Jadhav, G.S. and Ghangrekar, M.M. (2009) Performance of microbial fuel cell subjected to variation in pH, temperature, external load and substrate concentration. Bioresource Technology 100(2), 717-723.

Joux, F. and Lebaron, P. (2000) Use of fluorescent probes to assess physiological functions of bacteria at single-cell level. Microbes Infect 2(12), 1523-1535.

Kang, K.H., Jang, J.K., Pham, T.H., Moon, H., Chang, I.S. and Kim, B.H. (2003) A microbial fuel cell with improved cathode reaction as a low biochemical oxygen demand sensor. Biotechnology Letters 25(16), 1357-1361.

Karube, I. and Yokoyama, K. (1993) Uses of Immobilized Biological Compounds. Guilbault, G. and Mascini, M. (eds), pp. 281-287, Springer Netherlands.

Karube, I., Matsunaga, T., Mitsuda, S. and Suzuki, S. (1977a) Microbial electrode BOD sensors. Biotechnol Bioeng 19(10), 1535-1547.

Karube, I., Matsunaga, T., Tsuru, S. and Suzuki, S. (1977b) Biochemical fuel cell utilizing immobilized cells of Clostridium butyricum. Biotechnology and Bioengineering 19(11), 1727-1733.

Kaur, A., Kim, J.R., Michie, I., Dinsdale, R.M., Guwy, A.J. and Premier, G.C. (2013) Microbial fuel cell type biosensor for specific volatile fatty acids using acclimated bacterial communities. Biosensors and Bioelectronics 47(0), 50-55.

Kim, B.H., Chang, I.S., Gil, G.C., Park, H.S. and Kim, H.J. (2003) Novel BOD (biological oxygen demand) sensor using mediator-less microbial fuel cell. Biotechnology Letters 25(7), 541-545.

Kim, B.H., Park, H.S., Kim, H.J., Kim, G.T., Chang, I.S., Lee, J. and Phung, N.T. (2004) Enrichment of microbial community generating electricity using a fuel-cell-type electrochemical cell. Appl Microbiol Biotechnol 63(6), 672-681.

Kim, G.T., Webster, G., Wimpenny, J.W., Kim, B.H., Kim, H.J. and Weightman, A.J. (2006) Bacterial community structure, compartmentalization and activity in a microbial fuel cell. J Appl Microbiol 101(3), 698-710.

Kim, H.J., Park, H.S., Hyun, M.S., Chang, I.S., Kim, M. and Kim, B.H. (2002) A mediator-less microbial fuel cell using a metal reducing bacterium, Shewanella putrefaciens. Enzyme and Microbial Technology 30(2), 145-152.

Kim, M., Hyun, M.S., Gadd, G.M., Kim, G.T., Lee, S.J. and Kim, H.J. (2009) Membrane-electrode assembly enhances performance of a microbial fuel cell type biological oxygen demand sensor. Environ Technol 30(4), 329-336.

Kim, M., Park, H.S., Jin, G.J., Cho, W.H., Lee, D.K., Hyun, M.S., Choi, C.H. and Kim, H.J. (2006) A novel combined biomonitoring system for BOD measurement and toxicity detection using microbial fuel cells, pp. 1247-1248.

Kim, M., Sik Hyun, M., Gadd, G.M. and Joo Kim, H. (2007) A novel biomonitoring system using microbial fuel cells. J Environ Monit 9(12), 1323-1328.

Kim, M., Youn, S.M., Shin, S.H., Jang, J.G., Han, S.H., Hyun, M.S., Gadd, G.M. and Kim, H.J. (2003b) Practical field application of a novel BOD monitoring system. Journal of Environmental Monitoring 5(4), 640-643.

Kim, M.N. and Kwon, H.S. (1999) Biochemical oxygen demand sensor using Serratia marcescens LSY 4. Biosens Bioelectron 14(1), 1-7.

Kumlanghan, A., Liu, J., Thavarungkul, P., Kanatharana, P. and Mattiasson, B. (2007) Microbial fuel cell-based biosensor for fast analysis of biodegradable organic matter. Biosensors and Bioelectronics 22(12), 2939-2944.

Kwok, W.K., Picioreanu, C., Ong, S.L., van Loosdrecht, M.C., Ng, W.J. and Heijnen, J.J. (1998) Influence of biomass production and detachment forces on biofilm structures in a biofilm airlift suspension reactor. Biotechnol Bioeng 58(4), 400-407.

Larminie, J. and Dicks, A. (2003) Fuel Cell Systems Explained, New York.

Le, X.T. (2013) Contribution to the study of properties of Selemion AMV anion exchange membranes in acidic media. Electrochimica Acta 108(0), 232-240.

Lee, J., Phung, N.T., Chang, I.S., Kim, B.H. and Sung, H.C. (2003) Use of acetate for enrichment of electrochemically active microorganisms and their 16S rDNA analyses. FEMS Microbiol Lett 223(2), 185-191.

Lefebvre, O., Al-Mamun, A. and Ng, H.Y. (2008) A microbial fuel cell equipped with a biocathode for organic removal and denitrification. Water Science and Technology 58(4), 881-885.

Lefebvre, O., Ooi, W.K., Tang, Z., Abdullah-Al-Mamun, M., Chua, D.H.C. and Ng, H.Y. (2009) Optimization of a Pt-free cathode suitable for practical applications of microbial fuel cells. Bioresource Technology 100(20), 4907-4910.

Lefebvre, O., Shen, Y., Tan, Z., Uzabiaga, A., Chang, I.S. and Ng, H.Y. (2011a) A comparison of membranes and enrichment strategies for microbial fuel cells. Bioresource Technology 102(10), 6291-6294.

Lefebvre, O., Tan, Z., Kharkwal, S. and Ng, H.Y. (2012) Effect of increasing anodic NaCl concentration on microbial fuel cell performance. Bioresource Technology 112(0), 336-340.

Lefebvre, O., Uzabiaga, A., Chang, I., Kim, B.-H. and Ng, H. (2011) Microbial fuel cells for energy self-sufficient domestic wastewater treatment—a review and discussion from energetic consideration. Applied Microbiology and Biotechnology 89(2), 259-270.

Li, X., Hu, B.X., Suib, S., Lei, Y. and Li, B.K. (2010) Manganese dioxide as a new cathode catalyst in microbial fuel cells. Journal of Power Sources 195(9), 2586-2591.

Li, Y.R. and Chu, J. (1991) Study of BOD microbial sensors for waste water treatment control. Appl Biochem Biotechnol 28-29, 855-863.

Lima, F.H.B., Calegaro, M.L. and Ticianelli, E.A. (2006) Investigations of the catalytic properties of manganese oxides for the oxygen reduction reaction in alkaline media. Journal of Electroanalytical Chemistry 590(2), 152-160.

Liu, C., Zhao, H., Gao, S., Jia, J., Zhao, L., Yong, D. and Dong, S. (2013) A reagent-free tubular biofilm reactor for on-line determination of biochemical oxygen demand. Biosensors and Bioelectronics 45(1), 213-218.

Liu, H. and Logan, B. (2004) Electricity generation using an air-cathode single chamber microbial fuel cell (MFC) in the absence of a proton exchange membrane. ACS National Meeting Book of Abstracts 228(1).

Liu, H., Cheng, S. and Logan, B.E. (2005) Power Generation in Fed-Batch Microbial Fuel Cells as a Function of Ionic Strength, Temperature, and Reactor Configuration. Environmental Science & Technology 39(14), 5488-5493.

Liu, H., Cheng, S. and Logan, B.E. (2005a) Production of electricity from acetate or butyrate using a single-chamber microbial fuel cell. Environmental Science and Technology 39(2), 658-662.

Liu, J. and Mattiasson, B. (2002) Microbial BOD sensors for wastewater analysis. Water Research 36(15), 3786-3802.

Liu, J., Björnsson, L. and Mattiasson, B. (2000) Immobilised activated sludge based biosensor for biochemical oxygen demand measurement. Biosensors and Bioelectronics 14(12), 883-893.

Liu, Z.D., Lian, J., Du, Z.W. and Li, H.R. (2006) [Construction of sugar-based microbial fuel cells by dissimilatory metal reduction bacteria]. Sheng Wu Gong Cheng Xue Bao 22(1), 131-137.

Logan, B., Cheng, S., Watson, V. and Estadt, G. (2007) Graphite fiber brush anodes for increased power production in air-cathode microbial fuel cells. Environmental Science and Technology 41(9), 3341-3346.

Logan, B.E. (2008) Microbial Fuel Cells, John Wiley & Sons, New York.

Logan, B.E. and Regan, J.M. (2006) Electricity-producing bacterial communities in microbial fuel cells. Trends in Microbiology 14(12), 512-518.

Logan, B.E., Hamelers, B., Rozendal, R., Schröder, U., Keller, J., Freguia, S., Aelterman, P., Verstraete, W. and Rabaey, K. (2006) Microbial fuel cells: Methodology and technology. Environmental Science and Technology 40(17), 5181-5192.

Logan, B.E., Murano, C., Scott, K., Gray, N.D. and Head, I.M. (2005) Electricity generation from cysteine in a microbial fuel cell. Water Research 39(5), 942-952.

Lu, M., Kharkwal, S., Ng, H.Y. and Li, S.F.Y. (2011) Carbon nanotube supported MnO 2 catalysts for oxygen reduction reaction and their applications in microbial fuel cells. Biosensors and Bioelectronics 26(12), 4728-4732.

Lu, M., Guo, L., Kharkwal, S., Wu, H.n., Ng, H.Y. and Li, S.F.Y. (2013) Manganese–polypyrrole–carbon nanotube, a new oxygen reduction catalyst for air-cathode microbial fuel cells. Journal of Power Sources 221(0), 381-386.

Lyon, D.Y., Buret, F., Vogel, T.M. and Monier, J.M. (2010) Is resistance futile? Changing external resistance does not improve microbial fuel cell performance. Bioelectrochemistry 78(1), 2-7.

Madigan, M.T.M., J.M.; Parker, J. (1997) Brock biology of microorganisms, Prentice-Hall International Inc., Englewood Cliffs, NJ.

Mai-Prochnow, A., Evans, F., Dalisay-Saludes, D., Stelzer, S., Egan, S., James, S., Webb, J.S. and Kjelleberg, S. (2004) Biofilm development and cell death in the marine bacterium Pseudoalteromonas tunicata. Appl Environ Microbiol 70(6), 3232-3238.

Maiyalagan, T. and Viswanathan, B. (2008) Catalytic activity of platinum/tungsten oxide nanorod electrodes towards electro-oxidation of methanol. Journal of Power Sources 175(2), 789-793.

Marty, J.L., Olive, D. and Asano, Y. (1997) Measurement of BOD: Correlation Between 5-Day BOD and Commercial BOD Biosensor Values. Environ Technol 18(3), 333-337.

Matsunaga, T., Karube, I. and Suzuki, S. (1980) A specific microbial sensor for formic acid. European journal of applied microbiology and biotechnology 10(3), 235-243.

Menicucci, J., Beyenal, H., Marsili, E., Veluchamy, R.A., Demir, G. and Lewandowski, Z. (2006) Procedure for determining maximum sustainable power generated by microbial fuel cells. Environ Sci Technol 40(3), 1062-1068.

Mikkelsen, S.R. and Corton, E. (2004) Bioanalytical Chemistry, John Wiley and Sons, New Jeresy.

Min, B., Cheng, S. and Logan, B.E. (2005) Electricity generation using membrane and salt bridge microbial fuel cells. Water Research 39(9), 1675-1686.

Moon, H., Chang, I.S., Kang, K.H., Jang, J.K. and Kim, B.H. (2004) Improving the dynamic response of a mediator-less microbial fuel cell as a biochemical oxygen demand (BOD) sensor. Biotechnology Letters 26(22), 1717-1721.

Mulchandani, A. Kim, R. (1998) Enzyme and Microbial Biosensors: Techniques and Protocols, Humana Press, Totowa, NJ.

Myers, J.M. and Myers, C.R. (2001) Role for outer membrane cytochromes OmcA and OmcB of Shewanella putrefaciens MR-1 in reduction of manganese dioxide. Appl Environ Microbiol 67(1), 260-269.

Nevin, K.P., Kim, B.C., Glaven, R.H., Johnson, J.P., Woodard, T.L., Methe, B.A., Didonato, R.J., Covalla, S.F., Franks, A.E., Liu, A. and Lovley, D.R. (2009) Anode biofilm transcriptomics reveals outer surface components essential for high density current production in Geobacter sulfurreducens fuel cells. PLoS One 4(5), e5628.

Niessen, J., Schröder, U. and Scholz, F. (2004b) Exploiting complex carbohydrates for microbial electricity generation – a bacterial fuel cell operating on starch. Electrochemistry Communications 6(9), 955-958.

Niessen, J., Schröder, U., Rosenbaum, M. and Scholz, F. (2004a) Fluorinated polyanilines as superior materials for electrocatalytic anodes in bacterial fuel cells. Electrochemistry Communications 6(6), 571-575.

O'Hayre, R.,.Cha, S.W., Colella, W., Prinz, F.B. (2005) Fuel Cell Fundamentals, John Wiley & Sons, New York.

Obuchowska, A. (2008) Quantitation of bacteria through adsorption of intracellular biomolecules on carbon paste and screen-printed carbon electrodes and voltammetry of redox-active probes. Anal Bioanal Chem 390(5), 1361-1371.

Oh, S.E. and Logan, B.E. (2006) Proton exchange membrane and electrode surface areas as factors that affect power generation in microbial fuel cells. Applied Microbiology and Biotechnology 70(2), 162-169.

Ohki, A., Shinohara, K., Ito, O., Naka, K., Maeda, S., Sato, T., Akano, H., Kato, N. and Kawamura, Y. (1994) A Bod Sensor Using Klebsiella Oxytoca AS1. International Journal of Environmental Analytical Chemistry 56(4), 261-269.

Palchetti, I. and Mascini, M. (2008) Electroanalytical biosensors and their potential for food pathogen and toxin detection. Anal Bioanal Chem 391(2), 455-471.

Pandit, S., Sengupta, A., Kale, S. and Das, D. (2011) Performance of electron acceptors in catholyte of a two-chambered microbial fuel cell using anion exchange membrane. Bioresource Technology 102(3), 2736-2744.
Pant, D., Van Bogaert, G., Diels, L. and Vanbroekhoven, K. (2010) A review of the substrates used in microbial fuel cells (MFCs) for sustainable energy production. Bioresource Technology 101(6), 1533-1543.

Park, D.H. and Zeikus, J.G. (1999) Utilization of electrically reduced neutral red by Actinobacillus succinogenes: Physiological function of neutral red in membrane-driven fumarate reduction and energy conservation. Journal of Bacteriology 181(8), 2403-2410.

Park, D.H. and Zeikus, J.G. (2000) Electricity generation in microbial fuel cells using neutral red as an electronophore. Applied and Environmental Microbiology 66(4), 1292-1297.

Park, D.H., Kim, B.H., Moore, B., Hill, H.A.O., Song, M.K. and Rhee, H.W. (1997) Electrode reaction of Desulfovibrio desulfuricans modified with organic conductive compounds. Biotechnology Techniques 11(3), 145-148.

Park, H.S., Kim, B.H., Kim, H.S., Kim, H.J., Kim, G.T., Kim, M., Chang, I.S., Park, Y.K. and Chang, H.I. (2001) A novel electrochemically active and Fe(III)-reducing bacterium phylogenetically related to Clostridium butyricum isolated from a microbial fuel cell. Anaerobe 7(6), 297-306.

Pasco, N.F., Weld, R.J., Hay, J.M. and Gooneratne, R. (2011) Development and applications of whole cell biosensors for ecotoxicity testing. Anal Bioanal Chem 400(4), 931-945.

Patil, S., Harnisch, F. and Schroder, U. (2010) Toxicity response of electroactive microbial biofilms--a decisive feature for potential biosensor and power source applications. Chemphyschem 11(13), 2834-2837.

Peixoto, L., Min, B., Martins, G., Brito, A.G., Kroff, P., Parpot, P., Angelidaki, I. and Nogueira, R. (2011) In situ microbial fuel cell-based biosensor for organic carbon. Bioelectrochemistry 81(2), 99-103.

Pham, C.A., Jung, S.J., Phung, N.T., Lee, J., Chang, I.S., Kim, B.H., Yi, H. and Chun, J. (2003) A novel electrochemically active and Fe(III)-reducing bacterium phylogenetically related to Aeromonas hydrophila, isolated from a microbial fuel cell. FEMS Microbiol Lett 223(1), 129-134.

Pham, H.T., Boon, N., Aelterman, P., Clauwaert, P., De Schamphelaire, L., van Oostveldt, P., Verbeken, K., Rabaey, K. and Verstraete, W. (2008) High shear enrichment improves the performance of the anodophilic microbial consortium in a microbial fuel cell. Microb Biotechnol 1(6), 487-496.
Pham, T.H., Jang, J.K., Moon, H.S., Chang, I.S. and kim, B.H. (2005) Improved performance of microbial fuel cell using membrane-electrode assembly. Journal of Microbiology and Biotechnology 15(2), 438-441.

Porter, J., Deere, D., Hardman, M., Edwards, C. and Pickup, R. (1997) Go with the flow – use of flow cytometry in environmental microbiology. FEMS Microbiology Ecology 24(2), 93-101.

Rabaey, K. and Verstraete, W. (2005) Microbial fuel cells: novel biotechnology for energy generation. Trends in Biotechnology 23(6), 291-298.

Rabaey, K., Boon, N., Hofte, M. and Verstraete, W. (2005a) Microbial phenazine production enhances electron transfer in biofuel cells. Environ Sci Technol 39(9), 3401-3408.

Rabaey, K., Boon, N., Siciliano, S.D., Verhaege, M. and Verstraete, W. (2004) Biofuel cells select for microbial consortia that self-mediate electron transfer. Appl Environ Microbiol 70(9), 5373-5382.

Rabaey, K., Bützer, S., Brown, S., Keller, J. and Rozendal, R.A. (2010) High Current Generation Coupled to Caustic Production Using a Lamellar Bioelectrochemical System. Environmental Science & Technology 44(11), 4315-4321.

Rabaey, K., Clauwaert, P., Aelterman, P. and Verstraete, W. (2005b) Tubular microbial fuel cells for efficient electricity generation. Environ Sci Technol 39(20), 8077-8082.

Rabaey, K., Read, S.T., Clauwaert, P., Freguia, S., Bond, P.L., Blackall, L.L. and Keller, J. (2008) Cathodic oxygen reduction catalyzed by bacteria in microbial fuel cells. ISME J 2(5), 519-527.

Reshetilov, A.N., Trotsenko, J.A., Morozova, N.O., Iliasov, P.V. and Ashin, V.V. (2001) Characteristics of Gluconobacter oxydans B-1280 and Pichia methanolica MN4 cell based biosensors for detection of ethanol. Process Biochemistry 36(10), 1015-1020.

Reynolds, D.M. and Ahmad, S.R. (1997) Rapid and direct determination of wastewater BOD values using a fluorescence technique. Water Research 31(8), 2012-2018.

Rezaei, F., Richard, T.L., Brennan, R.A. and Logan, B.E. (2007) Substrate-Enhanced Microbial Fuel Cells for Improved Remote Power Generation from Sediment-Based Systems. Environmental Science & Technology 41(11), 4053-4058.

Rhoads, A., Beyenal, H. and Lewandowski, Z. (2005) Microbial fuel cell using anaerobic respiration as an anodic reaction and biomineralized manganese as a cathodic reactant. Environ Sci Technol 39(12), 4666-4671.

Riedel, K. (1998) Enzyme and Microbial Biosensors. Mulchandani, A. and Rogers, K. (eds), pp. 199-223, Humana Press.

Riedel, K., Lange, K.P., Stein, H.J., Kühn, M., Ott, P. and Scheller, F. (1990) A microbial sensor for BOD. Water Research 24(7), 883-887.

Riedel, K., Renneberg, R., Kühn, M. and Scheller, F. (1988) A fast estimation of biochemical oxygen demand using microbial sensors. Applied Microbiology and Biotechnology 28(3), 316-318.

Ringeisen, B.R., Henderson, E., Wu, P.K., Pietron, J., Ray, R., Little, B., Biffinger, J.C. and Jones-Meehan, J.M. (2006) High power density from a miniature microbial fuel cell using Shewanella oneidensis DSP10. Environ Sci Technol 40(8), 2629-2634.

Rismani-Yazdi, H., Christy, A.D., Dehority, B.A. and Tuovinen, O.H. (2005) Bioconversion of cellulose into electricity using rumen microorganisms as biocatalysts in a microbial fuel cell.

Roche, I. and Scott, K. (2009) Carbon-supported manganese oxide nanoparticles as electrocatalysts for oxygen reduction reaction (orr) in neutral solution. Journal of Applied Electrochemistry 39(2), 197-204.

Roche, I., Katuri, K. and Scott, K. (2010) A microbial fuel cell using manganese oxide oxygen reduction catalysts. Journal of Applied Electrochemistry 40(1), 13-21.

Rozendal, R.A., Hamelers, H.V.M., Molenkamp, R.J. and Buisman, C.J.N. (2007) Performance of single chamber biocatalyzed electrolysis with different types of ion exchange membranes. Water Research 41(9), 1984-1994.

Sangeetha, S., Sugandhi, G., Murugesan, M., Murali Madhav, V., Berchmans, S., Rajasekar, R., Rajasekar, S., Jeyakumar, D. and Prabhakar Rao, G. (1996) Torulopsis candida based sensor for the estimation of biochemical oxygen demand and its evaluation. Electroanalysis 8(7), 698-701.

Schreiter, P.P., Gillor, O., Post, A., Belkin, S., Schmid, R.D. and Bachmann, T.T. (2001) Monitoring of phosphorus bioavailability in water by an immobilized luminescent cyanobacterial reporter strain. Biosens Bioelectron 16(9-12), 811-818.

Sevda, S., Dominguez-Benetton, X., Vanbroekhoven, K., Sreekrishnan, T.R. and Pant, D. (2013) Characterization and comparison of the performance of two different separator types in air-cathode microbial fuel cell treating synthetic wastewater. Chemical Engineering Journal 228, 1-1.

Shabani, A., Zourob, M., Allain, B., Marquette, C.A., Lawrence, M.F. and Mandeville, R. (2008) Bacteriophage-modified microarrays for the direct impedimetric detection of bacteria. Anal Chem 80(24), 9475-9482.

Shao, Y., Liu, J., Wang, Y. and Lin, Y. (2009) Novel catalyst support materials for PEM fuel cells: current status and future prospects. Journal of Materials Chemistry 19(1), 46-59.

Shen, Y., Wang, M., Chang, I.S. and Ng, H.Y. (2013) Effect of shear rate on the response of microbial fuel cell toxicity sensor to Cu(II). Bioresour Technol 136, 707-710.

Shen, Y.J., Lefebvre, O., Tan, Z. and Ng, H.Y. (2012) Microbial fuel-cell-based toxicity sensor for fast monitoring of acidic toxicity. Water Sci Technol 65(7), 1223-1228.

Sone, Y., Ekdunge, P. and Simonsson, D. (1996) Proton conductivity of nafion 117 as measured by a four-electrode AC impedance method. Journal of the Electrochemical Society 143(4), 1254-1259.

Stein, N.E., Hamelers, H.V.M. and Buisman, C.N.J. (2012a) Influence of membrane type, current and potential on the response to chemical toxicants of a microbial fuel cell based biosensor. Sensors and Actuators B: Chemical 163(1), 1-7.

Stein, N.E., Hamelers, H.V.M. and Buisman, C.N.J. (2012b) The effect of different control mechanisms on the sensitivity and recovery time of a microbial fuel cell based biosensor. Sensors and Actuators B: Chemical 171–172(0), 816-821.

Stocks, S.M. (2004) Mechanism and use of the commercially available viability stain, BacLight. Cytometry A 61(2), 189-195.

Sun, M., Sheng, G.-P., Zhang, L., Xia, C.-R., Mu, Z.-X., Liu, X.-W., Wang, H.-L., Yu, H.-Q., Qi, R., Yu, T. and Yang, M. (2008) An MEC-MFC-Coupled System for Biohydrogen Production from Acetate. Environmental Science & Technology 42(21), 8095-8100.

Susmel, S., Guilbault, G.G. and O'Sullivan, C.K. (2003) Demonstration of labeless detection of food pathogens using electrochemical redox probe and screen printed gold electrodes. Biosens Bioelectron 18(7), 881-889.

Sverige, S.-S.i. (1979) Water analysis-Determination of biochemical oxygen demand,BOD, of water—dilution method (Svensk Standard SS 02 81 43 E), The Swedish Standards Institution, Stockholm.

Tag, K., Lehmann, M., Chan, C., Renneberg, R., Riedel, K. and Kunze, G. (2000) Measurement of biodegradable substances with a mycelia-sensor based on the salt tolerant yeast Arxula adeninivorans LS3. Sensors and Actuators B: Chemical 67(1–2), 142-148.

Tan, T.C. and Wu, C. (1999) BOD sensors using multi-species living or thermally killed cells of a BODSEED microbial culture. Sensors and Actuators, B: Chemical 54(3), 252-260.

Tan, T.C., Li, F. and Neoh, K.G. (1993) Measurement of BOD by initial rate of response of a microbial sensor. Sensors and Actuators B: Chemical 10(2), 137-142.

Tender, L.M., Reimers, C.E., Stecher, H.A., 3rd, Holmes, D.E., Bond, D.R., Lowy, D.A., Pilobello, K., Fertig, S.J. and Lovley, D.R. (2002) Harnessing microbially generated power on the seafloor. Nat Biotechnol 20(8), 821-825.

Ter Heijne, A., Hamelers, H.V., De Wilde, V., Rozendal, R.A. and Buisman, C.J. (2006) A bipolar membrane combined with ferric iron reduction as an efficient cathode system in microbial fuel cells. Environ Sci Technol 40(17), 5200-5205.

Ter Heijne, A., Hamelers, H.V.M., Saakes, M. and Buisman, C.J.N. (2008) Performance of non-porous graphite and titanium-based anodes in microbial fuel cells. Electrochimica Acta 53(18), 5697-5703.
Thévenot, D.R., Toth, K., Durst, R.A. and Wilson, G.S. (2001) Electrochemical biosensors: recommended definitions and classification. Biosensors and Bioelectronics 16(1–2), 121-131.

Thurston, C.F., Bennetto, H.P. and Delaney, G.M. (1985) Glucose metabolism in a microbial fuel cell. Stoichiometry of product formation in a thionine-mediated Proteus vulgaris fuel cell and its relation to coulombic yields. Journal of General Microbiology 131(6), 1393-1401.

Thygesen, A., Poulsen, F.W., Min, B., Angelidaki, I. and Thomsen, A.B. (2009) The effect of different substrates and humic acid on power generation in microbial fuel cell operation. Bioresource Technology 100(3), 1186-1191.

Tibazarwa, C., Corbisier, P., Mench, M., Bossus, A., Solda, P., Mergeay, M., Wyns, L. and van der Lelie, D. (2001) A microbial biosensor to predict bioavailable nickel in soil and its transfer to plants. Environ Pollut 113(1), 19-26.

Torres, C.I., Lee, H.S. and Rittmann, B.E. (2008) Carbonate species as OH- carriers for decreasing the pH gradient between cathode and anode in biological fuel cells. Environ Sci Technol 42(23), 8773-8777.

Turner, A.P.F., Karube, I., Wilson, G.S. (1992) Biosensors: Fundamentals and Applications, Mir Publishers, Moscow.

Vanrolleghem, P.A. and Lee, D.S. (2003) On-line monitoring equipment for wastewater treatment processes: state of the art. Water Sci Technol 47(2), 1-34.

Verma, N. and Singh, M. (2003) A disposable microbial based biosensor for quality control in milk. Biosens Bioelectron 18(10), 1219-1224.

Virdis, B., Rabaey, K., Rozendal, R.A., Yuan, Z.G. and Keller, J. (2010) Simultaneous nitrification, denitrification and carbon removal in microbial fuel cells. Water Research 44(9), 2970-2980.

Wei, Z., Huang, W., Zhang, S. and Tan, J. (2000) Carbon-based air electrodes carrying MnO2 in zinc–air batteries. Journal of Power Sources 91(2), 83-85.

Xing, D., Cheng, S., Logan, B.E. and Regan, J.M. (2010) Isolation of the exoelectrogenic denitrifying bacterium Comamonas denitrificans based on dilution to extinction. Appl Microbiol Biotechnol 85(5), 1575-1587.

Yang, Z., Sasaki, S., Karube, I. and Suzuki, H. (1997) Fabrication of oxygen electrode arrays and their incorporation into sensors for measuring biochemical oxygen demand. Analytica Chimica Acta 357(1–2), 41-49.

Yang, Z., Suzuki, H., Sasaki, S. and Karube, I. (1996) Disposable sensor for biochemical oxygen demand. Appl Microbiol Biotechnol 46(1), 10-14.

You, S.J., Zhao, Q.L., Zhang, J.N., Jiang, J.Q. and Zhao, S.Q. (2006) A microbial fuel cell using permanganate as the cathodic electron acceptor. Journal of Power Sources 162(2), 1409-1415.

Zhang, D., Chi, D., Okajima, T. and Ohsaka, T. (2007) Catalytic activity of dual catalysts system based on nano-manganese oxide and cobalt octacyanophthalocyanine toward four-electron reduction of oxygen in alkaline media. Electrochimica Acta 52(17), 5400-5406.

Zhang, E., Xu, W., Diao, G. and Shuang, C. (2006) Electricity generation from acetate and glucose by sedimentary bacterium attached to electrode in microbial-anode fuel cells. Journal of Power Sources 161(2), 820-825.

Zhang, F., Ge, Z., Grimaud, J., Hurst, J. and He, Z. (2013) Improving electricity production in tubular microbial fuel cells through optimizing the anolyte flow with spiral spacers. Bioresource Technology 134, 251-256.

Zhang, L.X., Liu, C.S., Zhuang, L., Li, W.S., Zhou, S.G. and Zhang, J.T. (2009a) Manganese dioxide as an alternative cathodic catalyst to platinum in microbial fuel cells. Biosensors & Bioelectronics 24(9), 2825-2829.

Zhang, Y. and Angelidaki, I. (2011) Submersible microbial fuel cell sensor for monitoring microbial activity and BOD in groundwater: Focusing on impact of anodic biofilm on sensor applicability. Biotechnol Bioeng.

Zhao, F., Harnisch, F., Schröder, U., Scholz, F., Bogdanoff, P. and Herrmann, I. (2005) Application of pyrolysed iron(II) phthalocyanine and CoTMPP based oxygen reduction catalysts as cathode materials in microbial fuel cells. Electrochemistry Communications 7(12), 1405-1410.

Zhou, M., Wang, H., Hassett, D.J. and Gu, T. (2013) Recent advances in microbial fuel cells (MFCs) and microbial electrolysis cells (MECs) for wastewater treatment, bioenergy and bioproducts. Journal of Chemical Technology & Biotechnology 88(4), 508-518.